Sílvia Raquel das Neves Pinão

DEVELOPMENT OF MEMBRANES CONTAINING A CONTROLLED DRUG RELEASE SYSTEM FOR OPHTHALMOLOGICAL APPLICATIONS

Master's thesis in Chemical Engineering, specialization in Biosystems, supervised by Doctor António Jorge Rebelo Ferreira Guiomar and Doctor Patrícia de Jesus Pinto Alves, and submitted to the Department of Chemical Engineering, Faculty of Science and Technology, University of Coimbra.

September, 2016

· U C ·

UNIVERSIDADE DE COIMBRA

Sílvia Raquel das Neves Pinão

DEVELOPMENT OF MEMBRANES CONTAINING A CONTROLLED DRUG RELEASE SYSTEM FOR OPHTHALMOLOGICAL APPLICATIONS

Supervisors
Doctor António Jorge Rebelo Ferreira Guiomar
Doctor Patrícia De Jesus Pinto Alves

Institutions
Department of Chemical Engineering
Department of Life Sciences
Faculty of Science and Technology
University of Coimbra

Coimbra, 2016

· U   C ·

UNIVERSIDADE DE COIMBRA

"The only thing worse than being blind is having sight but no vision."

Helen Keller

Acknowledgements

Abstract

The effectiveness of drug administration strongly depends on attainment of an effective drug concentration in the area to be treated, for a sufficient period of time. Nowadays, the most used drug administration method for many eye diseases is delivery through eye drops, although it is very inefficient and can lead to negative side effects. The use of soft contact lenses as drug delivery systems appeared as a promising alternative, due to the prolonged contact with the eye surface, high degree of comfort and biocompatibility.

In this work, membranes for controlled release of an antibiotic (moxifloxacin, MFX) were developed. They were based on chitosan and polyacrylates, employing solvent evaporation and bulk polymerization methods, respectively. Three of the developed membranes were selected for further study and loading of MFX: a chitosan-based membrane, which also contained gelatin, crosslinked with glyoxal and plasticized with poly(vinyl alcohol) and poly(ethylene glycol) (CBM 16), and two acrylate-based membranes, one prepared from methyl methacrylate (MMA), octadecyl methacrylate (ODMA) and 2-ethylhexyl acrylate (EHA) (ABM 4) and, the other, prepared from MMA, ODMA, EHA and methacrylic acid (MAA) (ABM 5). It was also studied the influence of a modification by gamma radiation-grafting of the ABM 4 membrane in three different ways: (i) grafting with 2-hydroxyethyl methacrylate (HEMA) employing a 25 KGy radiation dose (ABM 4.1), (ii) grafting with *N*,*N*-dimethylaminoethyl methacrylate (DMAEMA) employing 15 and 25 KGy radiation doses (ABM 4.2 and ABM 4.4, respectively), and (iii) grafting with DMAEMA in the presence of MFX, employing a radiation dose of 15 kGy, with and without subsequent loading of MFX by soaking (ABM 4.3).

The swelling capacity, water contact angle, infrared vibrational spectra and cytotoxicity of these membranes were determined. The results showed that ABM 5 was the membrane most similar to commercial SCLs.

MFX was introduced in the most promising membranes by occlusion (O) and soaking (S), in order to prepare drug release systems. The drug release results showed that membranes ABM 4 and ABM 5 loaded by occlusion (ABM 4 – O; ABM 5 – O), were the membranes that showed the highest drug release time (3 days). Relatively to the gamma radiation-grafted membranes loaded by soaking, the best result was obtained

with ABM 4.4 - S, with 2 days of drug release and the modification by grafting improved the drug release duration when the drug was loaded by soaking, but worsened it when the drug was loaded by occlusion.

KEYWORDS: Controlled release; Contact lens; Moxifloxacin; Chitosan; Polyacrylates.

Resumo

A eficácia da administração de um fármaco depende muito da sua concentração no local a ser tratado, durante um período de tempo adequado. Hoje em dia, o método de administração de fármacos mais utilizado para muitas doenças oculares é a aplicação de colírios, embora este método seja muito ineficiente e pode levar a efeitos secundários indesejáveis. O uso de lentes de contacto como sistemas de libertação de fármacos é uma alternativa promissora, devido ao contacto prolongado com a superfície do olho, ao alto grau de conforto e à biocompatibilidade.

Neste trabalho, foram desenvolvidas membranas para serem usadas como sistemas de libertação controlada de um antibiótico (moxifloxacina, MFX), partindo de quitosano e de poliacrilatos e utilizando os métodos de evaporação do solvente e de polimerização na massa, respectivamente. Três das membranas desenvolvidas foram seleccionadas para os estudos subsequentes e para carregamento de MFX: uma membrana à base de quitosano, contendo, também, gelatina, reticulada com glioxal e plastificada com poli(álcool vinílico) e poli(etileno glicol) (CBM 16) e duas membranas à base de poliacrilatos, uma preparada a partir de metacrilato de metilo (MMA), metacrilato de octadecilo (ODMA) e acrilato de 2-etil-hexilo (EHA) (ABM 4) e outra preparada a partir de MMA, ODMA, EHA e ácido metacrílico (MAA) (ABM 5). Também foi estudada a influência de uma modificação da membrana ABM 4 de três maneiras diferentes, por copolimerização enxerto utilizando radiação gama: (i) enxerto com metacrilato de 2-hidroxietilo (HEMA) empregando uma dose de radiação de 25 kGy (ABM 4.1); (ii) enxerto com metacrilato de *N*,*N*-dimetilaminoetilo (DMAEMA), empregando doses de radiação 25 e 15 kGy (ABM 4.2 e ABM 4.4, respectivamente) e (iii) enxerto com DMAEMA na presença de MFX, empregando uma dose de radiação de 15 kGy, com e sem um carregamento subsequente por *soaking* numa solução de MFX (ABM 4.3).

Foi determinada a capacidade de inchaço, o ângulo de contacto com a água, os espectros vibracionais no infravermelho e a citotoxicidade das membranas. Os resultados mostraram que a membrana ABM 5 foi a que apresentou características mais semelhantes às de lentes de contacto comerciais.

Introduziu-se MFX nas membranas mais promissoras quer por oclusão (O), quer por imersão (*soaking*; S), de modo a preparar sistemas de libertação controlada. Os

resultados da libertação de MFX permitiram concluir que as membranas ABM 4 e ABM 5 carregadas por oclusão (ABM 4 – O; ABM 5 – O), foram as que apresentaram um maior tempo de libertação de fármaco (3 dias). Relativamente às membranas modificadas por enxerto empregando radiação gama e carregadas por imersão, concluiu-se que a membrana com o melhor resultado foi a ABM 4.4 - S, com 2 dias de libertação de fármaco e que a modificação por enxerto melhorou a libertação de fármaco quando este foi introduzido por imersão, mas piorou-a quando o fármaco foi introduzido por oclusão.

PALAVRAS-CHAVE: Libertação controlada; Lentes de contacto; Moxifloxacina; Quitosano; Poliacrilatos.

Contents

List of Figures

List of Tables

List of abbreviations

ABM	Acrylate-Based Membranes
ABM – O	Acrylate-Based Membranes load by Occlusion
ABM – S	Acrylate-Based Membranes load by Soaking
ATR	Attenuated Total Reflectance
ATS	Artificial tear solution
Au	Gold
Brij®35	Poly (ethylene glycol) dodecyl ether
CBM	Chitosan-Based Membranes
CBM – O	Chitosan-Based Membranes load by Occlusion
CBM – S	Chitosan-Based Membranes load by Soaking
CDI	N-Cyclohexyl-N'-(2-morpholinoethyl)carbodiimide metho-p-toluenesulfonate
Co	Cobalt
Cs	Cesium
CS	Chitosan
Cts	Counts
DDS	Drug delivery system
DMAEMA	N,N-dimethylaminoethyl methacrylate
DMSO	Dimethyl sulfoxide
EHA	2-ethylhexyl acrylate
EWC	Equilibrium Water Content
FT-IR	Fourrier Transform Infrared spectroscopy
GL	Glyoxal
HEMA	2-hydroxyethyl methacrylate
Ir	Iridium
MAA	Methacrylic acid
MFX	Moxifloxacin
MMA	Methyl methacrylate
MTS	3-(4,5-dimethyl-2-yl)-5-(3-carboxymethoxyphenyl)-2-(4-sulfophenyl)-2H-tetrazolium
ODMA	Octadecyl methacrylate
PB	Benzoyl peroxide
PEG	Poly (ethylene glycol)
PVA	Poly (vinyl alcohol)
Ra	Radium
SC	Swelling Capacity
SCL	Soft contact lens
TEC	Triethyl citrate
T_g	Glass transition temperature
UV	Ultraviolet
UV-VIS	Ultraviolet-Visible

Objectives and Report Overview

Context

Medication is applied to the surface of the eye to treat it in conditions such as infections, conjunctivitis, blepharitis, and dry eye syndrome, or to provide intraocular treatment through the cornea for diseases such as glaucoma or uveitis [1]. The effectiveness of this type of drug administration strongly depends on attainment of an effective drug concentration in the infected area for a sufficient period of time [2].

Nowadays, the most used drug administration method for many eye diseases is delivery through eye drops. There are practical reasons for the widespread use of eye drops, such as the favorable cost, the greater simplicity of formulation development and production and the good acceptance by patients. This type of administration covers 90% of the treatments used to deliver drugs to the eye, although it is very inefficient and can lead to side effects. Approximately 90-95% of the drug applied as drops is lost across conjunctiva or drained by the effect of blinking and lacrimal fluid renewal, and a fraction of the dose lost through the conjunctiva and the nasolacrimal conduct is absorbed into the bloodstream. In addition to drug wastage, the entry of certain drugs in the bloodstream leads to undesirable side effects [3]. Application of ophthalmic drugs as drops results in rapid variation in the drug delivery rates to the cornea, which limits the efficacy of therapeutic systems. In order to keep the drug concentration within the therapeutic limits, the administration of the drop has to be frequently repeated, providing pulse-type concentration profiles. The need to put eye drops frequently can often lead to a possible reduction in the compliance rate of patients to treatments [2].

During the past decades, new approaches and strategies have been developed with the aim of controlling essential parameters able to improve the treatment performance, such as the rate, period of time and targeting of delivery, employing the so called drug delivery systems (DDSs) [4]. The use of soft contact lenses (SCLs) for therapeutic purposes is well-established in ophthalmological clinical practice, in which they are used to correct refractive errors, protect the eye, relieve pain and maintain hydration of the surface eye. The use of SCLs as DDSs appeared as a promising alternative, due to the high degree of comfort, biocompatibility and prolonged contact with the eye surface. SCLs are already prescribed for postoperative use, in which they

protect the cornea during the process of cell growth and adhesion leading to wound healing, and against irritants such as sutures [3]. They have been prescribed for use in combination with eye drops, in order to prolong the residence time of drug in the cornea. Alternatively, drugs can be loaded into the SCLs which, when in place, release the drug. However, in spite of more than 50 years of research and of the great interest at the academic, clinical and industrial levels, no ophthalmologic lens preloaded with drug is commercially available.

This report is organized in 4 main chapters. Chapter 1 gives a theoretical framework on the subject regarding anatomic and physiological consideration on drug bioavailability, gives an overview in the main polymers used in controlled drug delivery systems and drug release mechanisms. It is also discussed the importance of the drug immobilization methods and it is described the materials used in the membranes developed in this work, with respective reactions. It is approached the mathematical models used to describe the drug release kinetics and finally it is described the membranes characterization techniques used. In Chapter 2 is made a practical framework with the materials and methods used in the membranes preparation. It is presented a detailed description of the experimental procedures for the membranes development, its characterization techniques and motivations for its implementation. In Chapter 3 are presented the formulation selection, characterization results and discussion according to the application. Finally, in Chapter 4 it is summarized the conclusions of the experimental work and some recommendations to develop in the future.

Scope of the work

This work focuses on developing membranes loaded with the antibiotic moxifloxacin (MFX) for pre- and post-operative contact lenses, in order to achieve sustained drug release and improved drug bioavailability, for pre- and post-operative prophylaxis of ocular infections. To do so, MFX was loaded into chitosan-based and acrylate-based membranes, prepared by solvent evaporation and bulk polymerization, respectively. It was made *in vitro* drug release and the MFX-loaded membranes with best results were characterized. It was also studied the drug release kinetics and the biocompatibility of the best membrane.

Chapter 1

1 Introduction

1.1 Anatomy and Physiology of the Eye

Eyes are the organs of vision. They collect light from the surrounding environment and convert it into an electrochemical impulse. These impulses go to the brain where they are interpreted and create notion of shapes, colors and dimensions of objects. The eyeball has approximately 24 mm of anteroposteior diameter and is 12 mm wide [5].

The process of vision begins with the light coming in the eye through the cornea. The cornea is an external clear layer at the front of the eye. After it, there is a progression to the pupil where the intensity of light is regulated. The light reaches then the crystalline lens that focuses it in the retina. The retina converts the image into a set of electrochemical impulses and transmits these signals to the brain through complex neural pathways (Figure 1-1). Each eye transmits a slightly different inverted image, which is combined and corrected when its signals reach the brain.
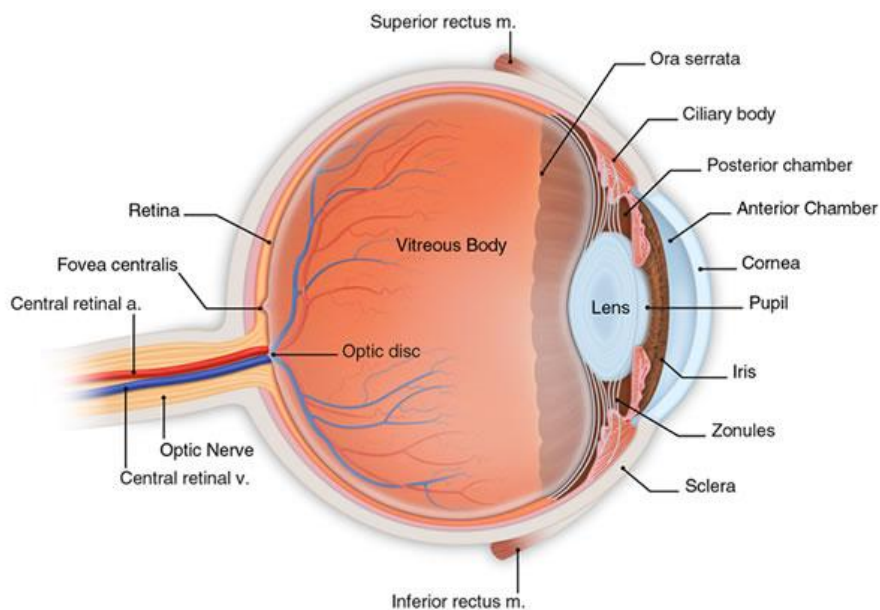
Figure 1-1 - Schematic cross section of the eye anatomy [6].

Another structure associated with the eye is the lacrimal apparatus. It is the physiological system containing the structures for tear production and drainage. The lacrimal apparatus works to keep the eye moist, free of dust and other irritating particles. It includes the lacrimal gland, which secretes tears at a constant stream and washes down over small openings located in the inner corner of the eye. [7].

1.2   Drug bioavailability and Physiological Considerations

The eye is, anatomically and physiologically, a complex and incomparable structure with some defensive structure machineries. The physiology ensures that strange entities do not enter the eye. The eye prevents the entry of noxious entities through mechanisms such as lacrimation, reflex blinking, rapid tear turnover drainage (residence time approximately 2 to 5 minutes [8]) and the fact that most of the instilled volume is lost through the pre-corneal area due to low permeability and metabolic barriers. These mechanisms give rise to a low bioavailability of applied drugs [9].

The main routes to ocular therapeutics administration are local and systemic (Figure 1-2). The local route includes eye drops, eye ointments, ocular inserts, drug-impregnated contact lens, subconjunctival injection, subtenon injection, retrobulbar injections and injections into the eye, which can be intracameral and intravitreal [10].Topical medication is used to treat surface and intraocular conditions. Topical administration can be through several types of dosage forms, including solutions, emulsions, suspensions, ointments, soluble gels, solid hydrophilic inserts, drug-impregnated contact lenses, rate-controlled release systems. Periocular injections may be underneath the conjunctiva or beneath the tenon's capsule. Through periocular injections, the drug passes the sclera and into the eye by simple diffusion.

Systemic route includes drug administration through oral route and by injections. The main barriers affecting the entrance of drug inside the eye by systemic route are the blood aqueous barrier and the blood retinal barrier. There are two other factors that are worth mention: the solubility of drug molecules and their molecular size [10]. This means that smaller drug molecules attain much higher concentration in aqueous humour compared to higher drug molecules. This route has the disadvantage of unwanted exposure of the body to high drug doses, which can bring systemic side effects and toxicity [11].
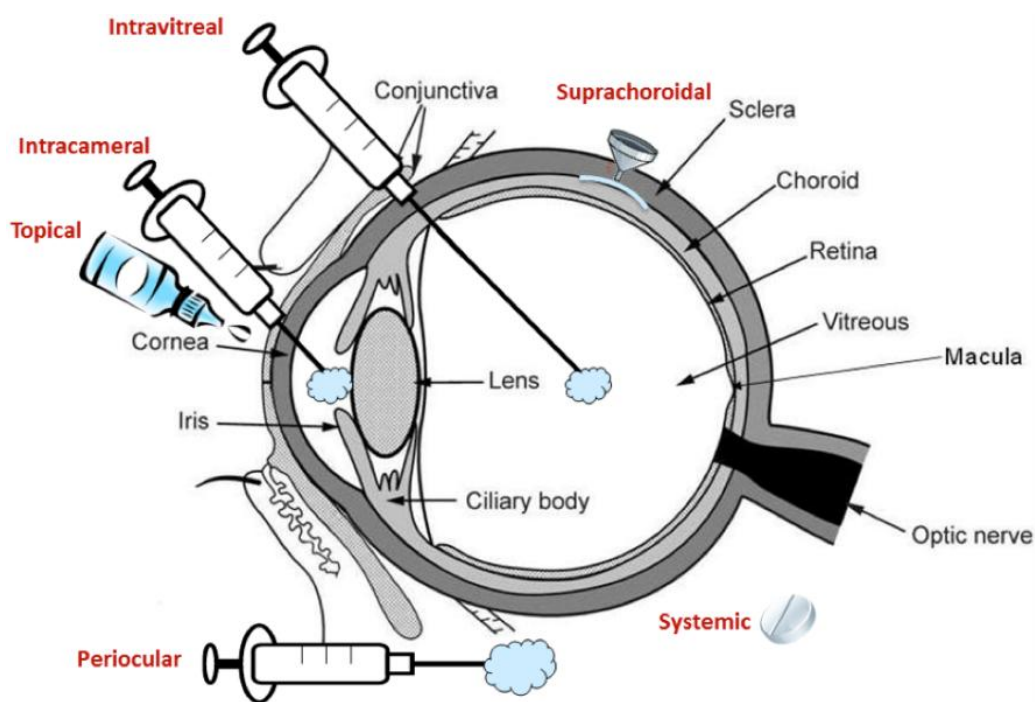
Figure 1-2 - Possible drug delivery routes scheme [12].

1.3 Controlled Drug Release Systems

There are several advantages of local drug administration in relation to systemic administration: (i) the drug acts only in the organ/tissue desirable, (ii) the doses to be used are much smaller, (iii) avoidance of the hepatic metabolism and (iv) reduced side effects. In the conventional drug administration route, drug concentration exhibits pulse profiles that decrease in short time (Figure 1-3). To keep the drug concentration in the therapeutic levels, the administration is repeated frequently. If drug concentration exceeds the therapeutic level it can be toxic and, below the minimum concentration, it would not have the desired therapeutic effect. The difference between these two levels is known as the therapeutic index. In Figure 1-3, it is shown the drug concentration in plasma for a single and several applications through a conventional application route and by a controlled release system. With a single application, the only way to increase therapeutic time is increasing the drug dose. However, the plasma drug concentration would exceed the toxic level. Thence, the need for development of a controlled release device able to keep the drug concentration in plasma steady for a long period of time without reach toxic levels [13].
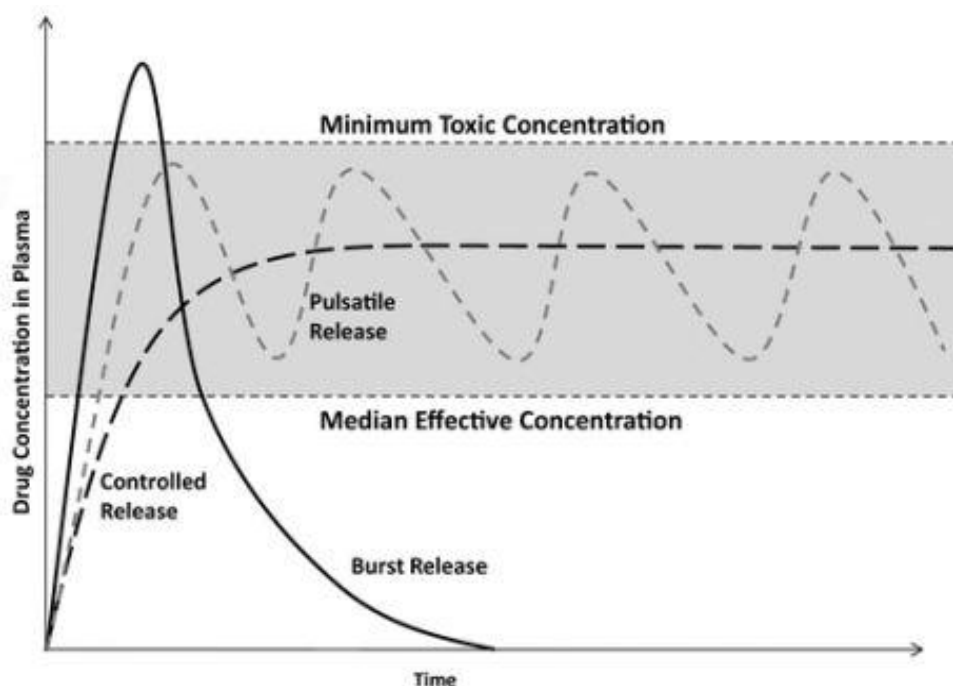
Figure 1-3 - Plasmatic profile of a drug admistered through three distinct modes: pulsatile release, controlled release and brust release [13].

The main motivation for drug delivery through controlled release systems is the possibility of administering an optimal amount of drug for a desired time period, avoiding oscillations of the amount of drug in the body during the treatment. Thus, increased bioavailability is assured, reduction of side effects is warranted and the desired therapeutic effect is enhanced [14]. In order to achieve the therapeutic purpose, selection of the most suitable administration route is of unquestionable importance. DDSs enable the delivery of an active compound in a controlled manner (time period and release rate) and within the therapeutic index [4]. It can be produced with natural or synthetic polymers; they can show biodegradability, depending on the polymer used. In Table 1.1 are listed some of the most widely used and investigated polymers in this field.

Table 1.1 - Overview in polymers used in DDSs [4].

DDS Polymers	

Natural Polymers	1. Proteins
	    • Collagen
	    • Gelatin
	    • Albumin
	2. Polysaccharides
	    • Chitosan
	    • Alginic Acid
	    • Dextran

Synthetic Polymers	Biodegradable
	3. Polyesters
	    • Poly(lactic acid)
	    • Poly(lactic-co-glycolic acid)
	4. Poly(ortho esters)
	5. Poly(alkyl cyanoacrylates)
	Non-Biodegradable
	6. Acrylic polymers
	    • Poly(methyl methacrylate)
	    • Poly(hydroxyethyl methacrylate)

Artificial Polymers	7. Cellulose Derivatives
	    • Ethyl cellulose
	    • Hydroxypropyl methylcellulose

The polymeric materials selected for a DDS must be biocompatible, i.e., interact favorably with the human body, be non-toxic and non-allergenic, should be easy to prepare, of low cost, chemically stable, of easy excretion, comfortable to the patients, biodegradable (if required) and not causing chemical or physical alteration of the drug [4]. Their hydrophobic/hydrophilic character is also an important feature, since they are going to contact a hydrophilic medium (the tears). Additionally, the polymeric matrix should be capable of releasing drugs by reproducible and predictable kinetics.

Controlled-release polymeric systems can be classified according to the mechanism which controls the release of the therapeutic agent (Figure 1-4).
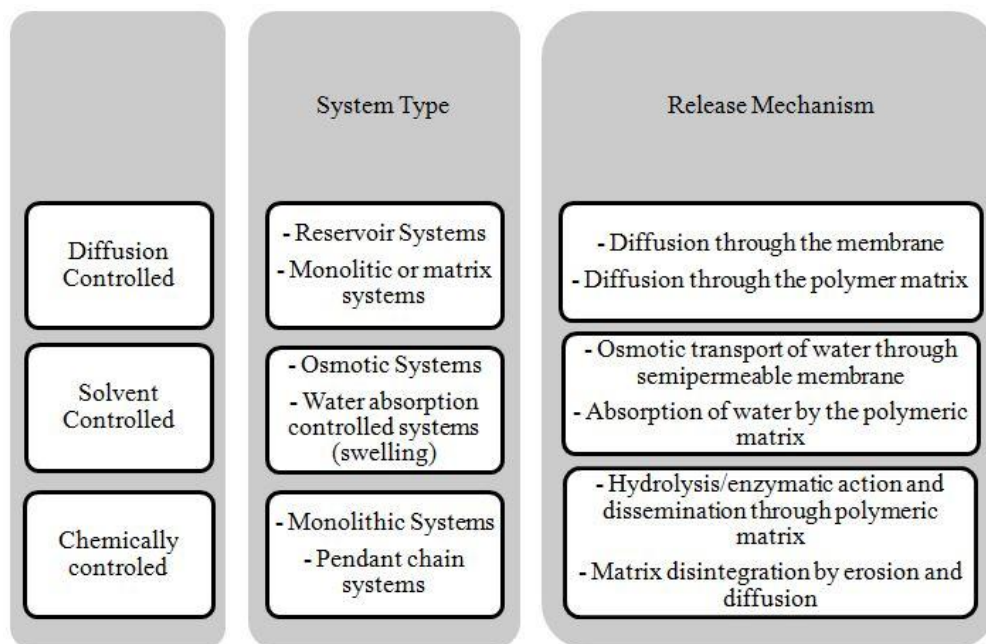
Figure 1-4 - Controlled release systems and their release mechanisms [15].

Release systems controlled by diffusion are divided into two types: reservoir systems and matrix systems. A DDS reservoir consists of a device comprising a drug core, in liquid or solid form, surrounded by a non-biodegradable polymeric membrane, through which the drug diffuses slowly. Generally, these devices assume a spherical, cylindrical or disc geometry. The diffusion rate is determined by drug properties and by the characteristics of the polymer membrane. In a matrix device, the drug is uniformly dispersed or dissolved in a polymer matrix and the release rate of the drug is controlled by diffusion through the matrix.

DDSs activated by the solvent are divided into two types: controlled release driven by osmotic pressure and controlled release driven by the water absorption (swelling). The simplest DDS controlled by osmotic pressure is an enclosure of a semi-permeable polymer membrane, which is permeable only to solvent molecules, with an orifice (exit port). Within the reservoir is a drug in solid form and a saturated solution of drug. The osmotic pressure formed due to the difference in drug concentration between outside and inside of the semi-permeable membrane, causes a flow of fluid from outside to inside the device, forcing the movement of drug to the outside, through the orifice in the membrane.

In the DDSs controlled by water absorption, the drug is dispersed or dissolved in a polymer matrix comprising a crosslinked hydrophilic polymer (hydrogel). These matrices

have the ability to absorb a large amount of water, swelling without dissolving, and the drug release rate is essentially controlled by the water absorption rate of the polymer matrix.

Chemically controlled release systems comprise all the formulations where the drug diffusion is controlled by disintegration of the polymer matrix. In monolithic systems, the drug initially dispersed in a polymer matrix is released once the polymer begins to erode or degrade. For pendant chain systems, the drug molecules are covalently attached to the principal polymer chain through easily degradable linkages. Thus, as the polymer comes into contact with water or other agents (such as hydrolytic enzymes), the drug is released at a controlled rate.

Some DDSs do not fit well into any of these categories. In many cases, the release of the drug is determined by a combination of several possible mechanisms [16].

1.4   Soft Contact Lenses

The soft contact lens is an optical device which is placed over the cornea and remains on the surface of the eye throughout blinking [17]. SCLs must be transparent, mechanically stable, provide oxygen permeability and be water wettable, to guarantee comfort and safety during usage [18]. The bioavailability of ophthalmologic drugs can be improved by employing an SCL [19]. When SCLs are used with eye drops, they prolong the contact time of the eye drops at the ocular surface and slow down the clearance of the drug. Different materials can be applied during the development of contact lenses and can be combined with strategies of drug immobilization, providing successful tools for ocular drug delivery systems [17].

1.4.1   Drug Immobilization in Soft Contact Lenses

There are papers published from the 1960s, soon after the introduction of soft contact lenses, postulating the application of contact lenses as drug delivery devices [20]. Traditionally, loading of drugs into SCLs is achieved by soaking or absorption, which can be achieved by immersion of the SCL in a drug solution of known concentration, for a few hours. This allows the contact lens to absorb the solution containing the drug and

release the drug by simple diffusion, when placed on the eye. Although this approach is more efficient than drug administration by eye drops, there are some limitations [21]: this type of drug release system cannot provide a slow and sustained drug release, since the entire drug incorporated into the matrix by absorption is usually released within a few hours and the amount of drug that can be incorporated in the lens is limited by the equilibrium solubility of the drug in the lens material [22].

Another drug loading method is occlusion. This method consists on trapping the drug within the polymer by dissolving the drug in the mixture reaction containing the monomers, allowing the drug to be retained within the polymeric matrix formed. This method has some advantages, such as the use of small amounts of drug, it is a simple method and allows the immobilization of a wide variety of drugs. However, there is the possibility of drug degradation by the presence of free radicals during polymerization or by the polymerization temperature, and drug release can be very fast or slow, depending on the resulting polymer porosity [23].

The therapeutic benefit may also be limited by the drug capacity of the lenses. The loading capacity of the drug is related with the swelling degree of the lenses or the equilibrium solubility of the drug in the polymeric matrix. This is a particular concern when working with hydrophilic drugs and hydrophobic SCLs, which are not a receptive environment for hydrophilic drug molecules.

Other approaches to the use of SCLs as drug delivery devices include the creation of drug diffusion barriers by surface modification of the SCLs [24]. Polymer surface modification can be divided into three categories: (i) Physical methods, which include the use of plasma, which contains reactive species such as free radicals, electrons, ions and excited molecules, and the use of electromagnetic radiation, such as visible light, UV, gamma rays and lasers; (ii) Chemical treatment, which involves chemical reactions at the surface by which molecules possessing functional groups such as carboxyl, amine, alcohol are covalently attached to the surface; and (iii) Biological methods, which include physical adsorption, chemical conjugation, crosslinking, and other methods of immobilization of enzymes, peptides, polysaccharides, and nucleic acids [25] [26]. In addition to being a barrier for drug release, the surface treatment must maintain a stable tear film layer, allow low levels of bacterial adhesion, minimize the accumulation of deposits or substances from tear and not to be irritant [27].

Other strategies developed with the aim of loading drugs into SCLs are the use of supercritical solvent-soaked lenses, molecular imprinted polymeric hydrogels, which

create a contact lens with a high affinity and selectivity for a given drug, and the development of various nanoparticulate-based DDSs, such as nanoparticles, nanoemulsions, nanosuspensions and liposomes [19].

1.5 Drug Used: Moxifloxacin

Moxifloxacin is an antibiotic which belongs to a class of drugs called quinolone antibiotics [28], more specifically to the fourth-generation fluoroquinolones against ocular pathogens [29]. In the form of eye drops, is used for treating bacterial ocular infections. It has excellent pharmacokinetics[a] and tissue penetration. It can be delivered via intravenous, oral or topical routes, and is particularly suitable as monotherapy for infections that are likely to be polymicrobial [30]. Table 1.2 shows some properties of MFX where MIC is minimum inhibitory concentration, the lowest concentration that prevents visible growth of a bacteria. MFX's antibacterial spectrum includes Gram-positive organisms such as *S. aureus* and *Streptococci*. It is also active against several other species but it relatively poor activity against *Pseudomonas spp* [30]. MFX differs from other fluoroquinolones by greater activity against Gram positive bacteria and anaerobes.

Table 1.2 - Physicochemical characteristics of moxifloxacin hydrochloride (MFX). MIC: minimum inhibitory concentration.

Chemical Formula	$C_{21}H_{25}ClFN_3O_4$
Structural Formula	
Molecular weight	437.89 g/mol
Solubility [31]	Soluble in water (24 mg/ml), DMSO (88 mg/ml at 25° C) and ethanol (<1 mg/ml at 25° C)
Spectrophotometry (λ_{max}) [32]	290 nm
MIC_{50}[a] in aqueous solution [33]	0.05 μg/mL
MIC_{90}[b] in aqueous solution [33]	2.2 μg/mL
Thermal stability [34] [35]	$\approx 250\ ℃$
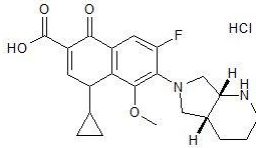
[a] MIC_{50} is the concentration that inhibits 50% of isolates tested.
[b] MIC_{90} is the concentration that inhibits 90% of isolates tested.

---

[a] It concerns the absorption, tissue distribution, biotransformation and elimination of drugs and determines the intensity of a drug's effect [56].

MFX acts by inhibiting enzymes responsible for replication, translation, repair and recombination of bacterial DNA. It is known that there are four bacterial DNA topoisomerases that, in various forms, are actively involved in the DNA synthesis process. Quinolones bind, in the presence of DNA, to topoisomerase II (DNA gyrase) and IV, by changing the conformation of these proteins and cleaving the DNA chain. Changes in the structure of these enzymes confer resistance to quinolones [36].

Eye infections are a common cause of conjunctivitis. In conjunctivitis, the eye becomes inflamed, the white of the eye may appear red and the eyelids may be swollen. Initially, only one eye can be affected, but often spreads to both eyes. For more severe infections, or infections that not disappear on their own, eye drops of an antibiotic such as moxifloxacin are administered (0.5% MFX) or a pill is taken once a day (400-800 mg MFX) during 7-8 days [37]. Studies evaluating the penetration of moxifloxacin into the aqueous chambers by topical or oral routes of administration report the following concentration levels [33]: (i) topical dosing protocols used in pre- and post-cataract and refractive surgeries, with dosing frequencies of 4 times a day, report concentration levels ranging from 0.38 ± 0.32 µg/mL to 2.28 ± 1.23 µg/mL; and (ii) oral route concentrations, ranged from 0.21 ± 0.21 µg/mL to 2.33 ± 0.85 µg/mL.

1.6   Chitosan-Based Membranes

This section presents the reagents used for the production of the chitosan-based membranes prepared, including plasticizers such as PEG 300, PVA and TEC and crosslinking agents such as GL and CDI, and the main reactions occurring.

1.6.1   Chitosan

Chitosan (CS) is a polysaccharide composed of units of β-(1→4)-*N*-acetyl-D-glucosamine and β-(1→4)-glucosamine. It is obtained by the alkaline deacetylation of chitin (Figure 1-5), a natural polysaccharide which can be found on the shells of marine crustaceans and insects, being the most abundant biopolymer in nature after cellulose.
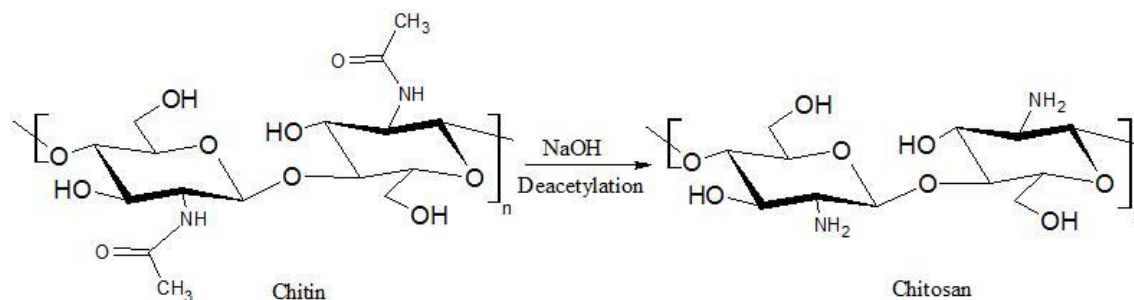
Figure 1-5 - Deacetylation reaction of the polysaccharide chitin to chitosan [4].

CS has an unusual combination of chemical and biological properties, such as reactive amine groups, low toxicity, biocompatibility, biodegradability, hemostatic activity, anti-microbial activity against bacteria and fungi and acceleration of tissue regeneration. For these reasons, it is widely used in biomedical and pharmaceutical applications, namely in DDS [4]. Chitosan is also used as a functional monomer or supporting matrix because of its low cost and high content of amino and hydroxyl functional groups. However, it is insoluble in water and in organic solvents, which may cause technical difficulties in handling and limit its application. However, it is soluble in dilute acidic solutions (pH < 5), due to protonation of its amine groups.

Chitosan has been combined with other natural and synthetic polymers. Among them, chitosan/gelatin composite films, prepared by solvent evaporation, allowed an increase in water absorption and in oxygen and solute permeability. Chitosan/gelatin composite films are more permeable, transparent, flexible and biocompatible films and have potential to be used as a contact lens material [18] and were used in this work.

1.6.2 Gelatin

Gelatin is a protein obtained by the partial hydrolysis of collagen (Figure 1-6). In aqueous solution, gelatin undergoes a sol-gel transition, forming a gel which has a mainly disordered structure with regions of local order. When temperature is lower than 35 ℃, its melting point, this order is lost and a viscous solution containing the polymer in a random spatial distribution is formed [38]. It is used in the biomedical area given its non-immunogenic, biodegradable and biocompatible character. Due to its high solubility in water and poor mechanical properties, it is necessary to crosslink it [4].
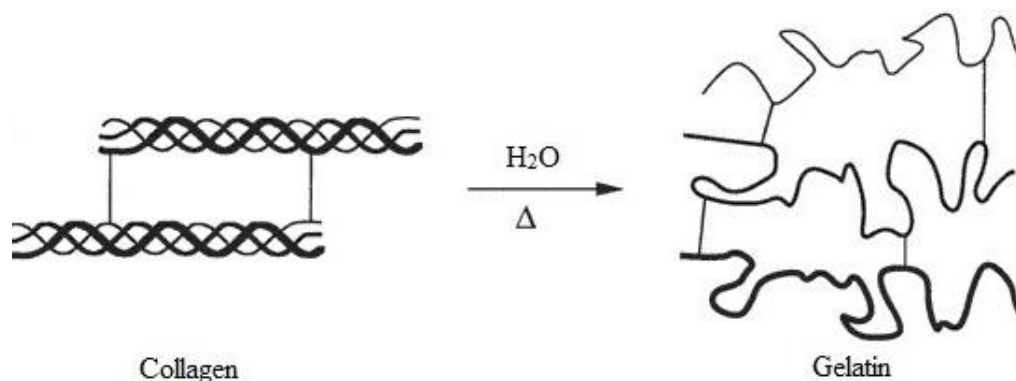
Collagen   Gelatin

Figure 1-6 - Schematic representation of the hydrolysis of collagen to form gelatin [39].

1.6.3 Plasticizers

The main role of plasticizers is to improve the mechanical properties of polymers by increasing flexibility and decreasing tensile strength. The effectiveness of the plasticizer depends on its chemical structure, compatibility and miscibility with the polymer and its molecular weight and concentration. Consequently, different polymers require different plasticizers [40]. We have used poly(ethylene glycol) (PEG) has a gelatin plasticizer. Cao *et al.* [41] studied the influence of different plasticizers on the mechanical properties of gelatin membranes. It was concluded that poly(ethylene glycol) (PEG) of low molecular weight exhibited a better plasticizing effect and resulted in membranes with better visual properties. It is believed that polar groups (-OH) present at both extremities of the PEG chains develop polymer-PEG hydrogen bonds, replacing the polymer-polymer interactions. Low molecular weight PEGs would be more efficient as plasticizers since they exhibit a larger number of hydroxyl groups per mole than high molecular weight PEGs.

Poly(vinyl alcohol) (PVA) is a polymer with good biocompatibility, high elasticity and hydrophilic characteristics. There are many reports concerning which relate that PVA has been blended with CS [42].

Triethyl citrate is a hydrophobic plasticizer used in the production of films extruded through PVA increasing flexibility and reducing tensile strength and temperature of glass transition. It has been used in the pharmaceutical industry for the production of biodegradable materials, which do not present toxicity [43].

1.6.4 Crosslinkers

The molecules employed in this study to crosslink the CS/gelatin films were a water-soluble carbodiimide (CDI) and glyoxal (GL). These are molecules which are reactive towards carboxylic groups (CDI) and hydroxyl and amine groups (GL). CDIs convert carboxylic groups in a form which can react with nucleophiles such as amine groups, forming amide bonds. For gelatin, they are as efficient as the most common crosslinker of gelatin (glutaraldehyde), with the advantage of increasing mechanical stiffness and degradation resistance without being cytotoxic [44].

GL is a bifunctional coupling agent with two highly reactive aldehyde groups. When employed at an acidic pH, it is an efficient crosslinker of polymers bearing hydroxyl groups, due to its capacity of forming acetals. Numerous studies have reported the improvement of the mechanical properties of chitosan through GL crosslinking for various biomedical applications [45]. At an alkaline pH, GL will react with amine groups.

1.7 Reactions Involved in the Preparation of Chitosan-Based Membranes

CS-based membranes were prepared using CS and gelatin in the presence of lactic acid and of a CDI. As shown in Figure 1-7, the reaction between a CDI and the components of this formulation starts with the activation of carboxylic groups of lactic acid or gelatin, in which CDI reacts with a carboxylic group, forming an unstable, reactive *O*-acylisourea ester.
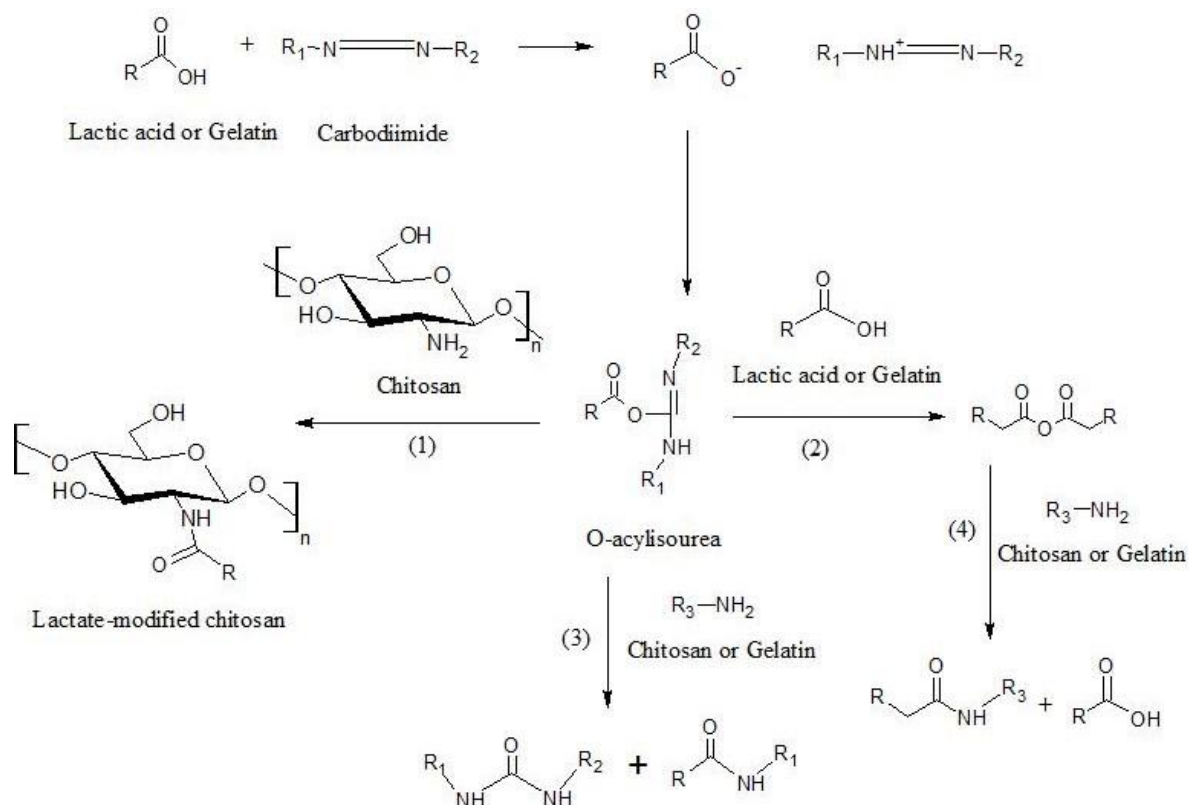
Figure 1-7 - Reactions with chitosan and gelatin after formation of the O-acylisourea intermediate [46] [47].

This *O*-acylisourea reacts with amine groups of CS (1) or gelatin (2) and an amide bond and a urea product is formed (3). A lactate-modified CS results, due to reaction between the CDI-activated lactate and CS, as well as a lactate-modified gelatin, due to reaction between the CDI-activated lactate and gelatin. The *O*-acylisourea can also react with the carboxyl group of lactic acid to form an anhydride (2) which will then react with amine groups from CS or from gelatin (4), to form amide bonds. In summary, crosslinking will occur by amide bond formation between carboxylic groups of gelatin and amine groups of both CS and gelatin. Additionally, some units of *β*-(1→4)-*N*-acetyl-D-glucosamine in chitosan will be covalently modified by lactic acid at their amine group, as well as aspartate and lysine residues in gelatin.

GL is a crosslinking agent which can react either with hydroxyl or amine groups, depending on the pH of the reaction medium (Figure 1-8, illustrated for the case of CS) [45]. In this work, GL was reacted at an acidic pH, at which it would react with hydroxyl groups in PEG, CS and/or gelatin.
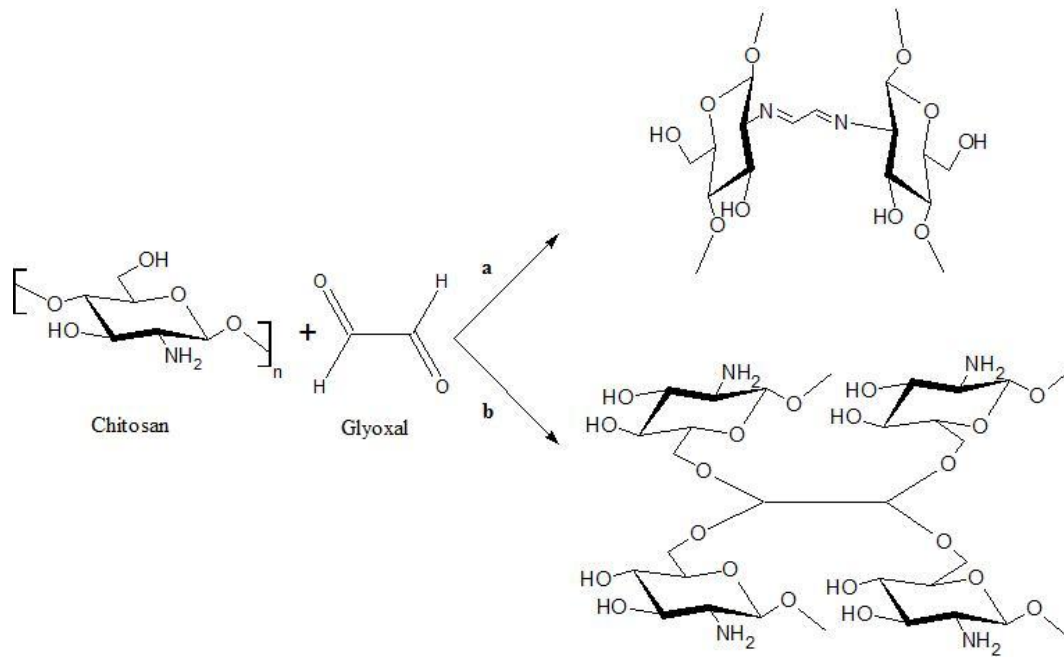
Figure 1-8 - Chitosan crosslinking reaction with glyoxal. a) Glyoxal reaction with amine groups of chitosan. b) glyoxal reaction with hydroxyl groups of chitosan [45].

1.8 Acrylate-Based Membranes

Table 1.3 shows the monomers used to prepare the acrylate-based membranes used in this work.

Table 1.3 - Monomers used to prepare the acrylate-based membranes employed.

Monomers	Initials	Structure
Methyl methacrylate	MMA	$CH_2 = C$ with $COOCH_3$ and CH_3
Octadecyl methacrylate	ODMA	$CH_2 = C$ with $COO(CH_2)_{16}CH_3$ and CH_3
2-Ethylhexyl acrylate	EHA	$CH_2 = C$ with $COO(CH_2)_4CH_3$, C_2H_5 and H
Hydroxyethyl methacrylate	HEMA	$CH_2 = C$ with $COO(CH_2)_2OH$ and CH_3
Methacrylic acid	MAA	$CH_2 = C$ with $COOH$ and CH_3

The methyl methacrylate (MMA) is a biocompatible and biostable monomer, which gives rise to a very transparent polymer, poly(methyl methacrylate) (PMMA). PMMA is non-biodegradable and does not absorb water, being dimensionally stable. It was the first acrylic polymer to be used in a biomedical application and nowadays, it is still used in the fabrication of SCLs [4]. However, it does not allow oxygen to pass through; it is uncomfortable and, as such, can cause adverse effects in the eye.

Another monomer used is octadecyl methacrylate (ODMA). It is a water-insoluble, low volatility, monofunctional methacrylate monomer with a long, hydrophobic side chain and it has been employed to impart flexibility, improved impact strength and low shrinkage [48].

The poly(2-ethylhexyl acrylate) (PEHA) is a polymer with very good film forming properties and good low temperature flexibility, due to the presence of a branched and somewhat long alkyl pendant group. It shows also low volume shrinkage [49].

It was also used poly(2-hydroxyethyl methacrylate) (PHEMA). It is a flexible hydrogel which can enhance the oxygen permeability of a copolymer. It was among the first polymers used in the preparation of SCLs, which showed good comfort and could be worn for longer [50].

Lastly, polymers such as poly(methacrylic acid) (PMAA) have been added to soft lens polymer formulations. It is known that adding ionized groups (negatively charged) such as carboxylates (-COOH) within the polymer matrix can increase the water content of the formulation. Therefore, the higher the amount of MAA, the higher the water content and consequently, higher oxygen permeability. Otherwise, there are some disadvantages in using MAA, such as a significant level of protein adsorption on the lens surface and within the lens matrix and dimensional instability when the lens is heat-disinfected [51].

1.8.1 Polymerization Reactions

Chain-growth polymerization describes a method where monomers are added one by one to an active site on the growing chain. It occurs in three sequential steps: initiation, propagation and termination. The most common type of chain-growth polymerization is by free radical. Free radicals are often created by division of a molecule

– the initiator – into two fragments. They are highly reactive species, due to the presence of an unpaired electron. In this work, benzoyl peroxide was the initiator used, which was converted to free radical species by heat. The decomposition of this initiator to give species with free radicals is shown in Figure 1-9. There are secondary reactions of combination and decomposition of radical species resulting from the split of benzoyl peroxide, which are not represented.
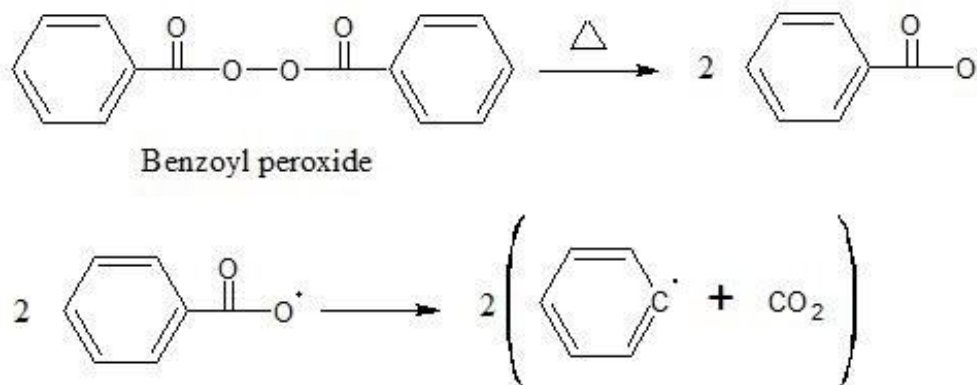
Figure 1-9 - Decomposition of benzoyl peroxide.

In the next phase – initiation −, the free radical species adds to the monomer, breaking the monomer's double bond by stealing an electron, leaving one of the carbon atoms of the double bond with an unpaired electron, which is a free radical. In the propagation phase, the formed activated monomer molecule attacks the double bond of another monomer molecule and becomes covalently attached to it, transferring its radical to the other monomer species, which is now able to react with another monomer molecule. When this step is repeated successively, a polymer chain is obtained (Figure 1-10).
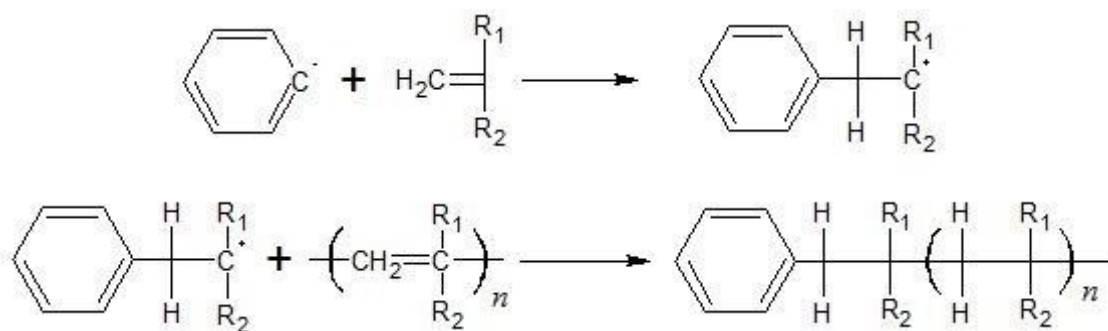
Figure 1-10 - Chain initiation and propagation by chain-growth polymerization.

Note that, when more than one monomer is used, the monomer units be organized in several ways, giving rise to random (a), alternating (b), block (c) and graft (d) copolymers (Figure 1-11).

a) $+$ABBACDDCABCCBA$+_n$

b) $+$ABCDABCDABCDAB$+_n$

c) $+$AAABBBCCCDDDAA$+_n$

d) $+$AABACDDCABDBCA$+_n$
E
E
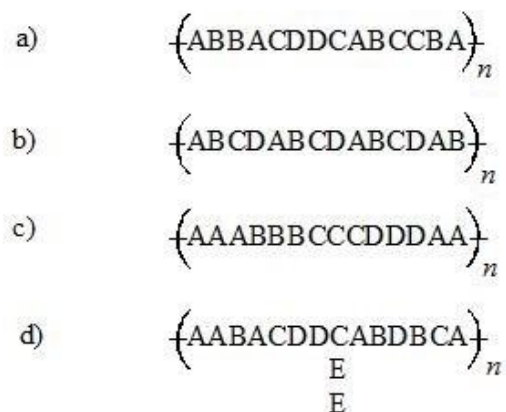
Figure 1-11 - Arrangement of monomers in the copolymerization.

The final phase – termination – may occur in two different ways: combination and disproportionation. Termination by combination occurs when two growing polymer chains react with each other by their free radicals, forming a C−C single bond (Figure 1-12 a). Termination by disproportionation happens when a free radical of a growing polymer chain steals an hydrogen atom from the carbon radical of another growing chain, resulting a carbon-carbon double in the hydrogen-accepting chain (Figure 1-12 b).
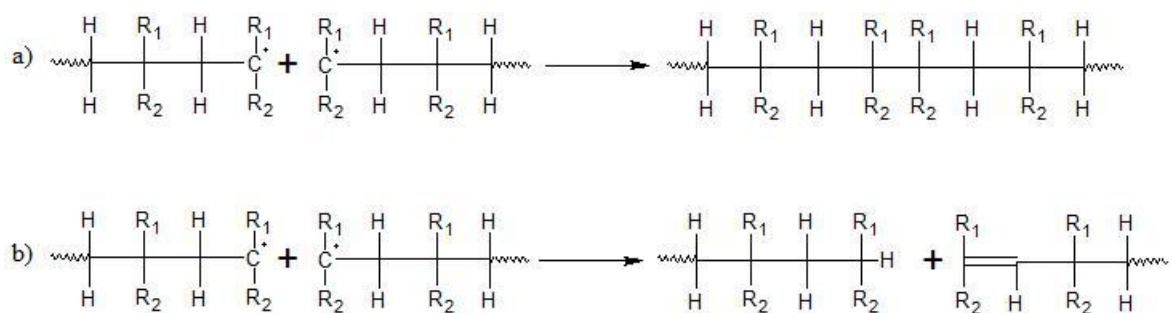
Figure 1-12 - Chain termination by combination (a) and disproportionation (b).

1.9   Acrylate-Based Membrane Grafting with Gamma Radiation

Gamma radiation is a form of ionizing radiation of low wavelength and high energy, having a high penetration power and being able to abstract electrons from matter. The source of gamma rays can be Co^{60}, Au^{198}, Ir^{192}, Cs^{137}, Ra^{226} [52], but the most suitable is Co^{60}, which has a relatively higher energy and fairly long half-life. Currently, all industrial radiation processing facilities employ Co^{60} as the gamma radiation source [53]. Gamma radiation is able to form free radicals when interacting with organic molecules. When used with monomers, it can initiate free radical chain-growth polymerization occurs. As the environment which received gamma radiation becomes sterile, the final material is sterile. For this reason, this polymerization initiation method is increasingly used in biomedical applications.

1.9.1   Grafting of Acrylate-Based Membranes Employing Gamma Radiation

Graft polymerization can be used for surface modification, in which the surface is the polymer which is being grafted with another polymer. In this work, two monomers were used to graft the prepared membranes: 2-hydroxyethyl methacrylate (HEMA) and *N*,*N*-dimethylaminoethyl methacrylate (DMAEMA). For surface grafting, the surface can be irradiated either in the presence or absence of the monomer. In this work, irradiation in the presence of the monomer was employed. The incident radiation breaks chemical bonds in the material to be grafted, forming free radicals. These reactive surface groups are then exposed to the monomer. The C=C double bonds of the monomer reacts with the free radicals at the surface and propagates as a free radical chain reaction, resulting polymer chains attached to the surface of the grafted polymer. The HEMA and DMAEMA surface reactions are represented in Figure 1-13 [15].
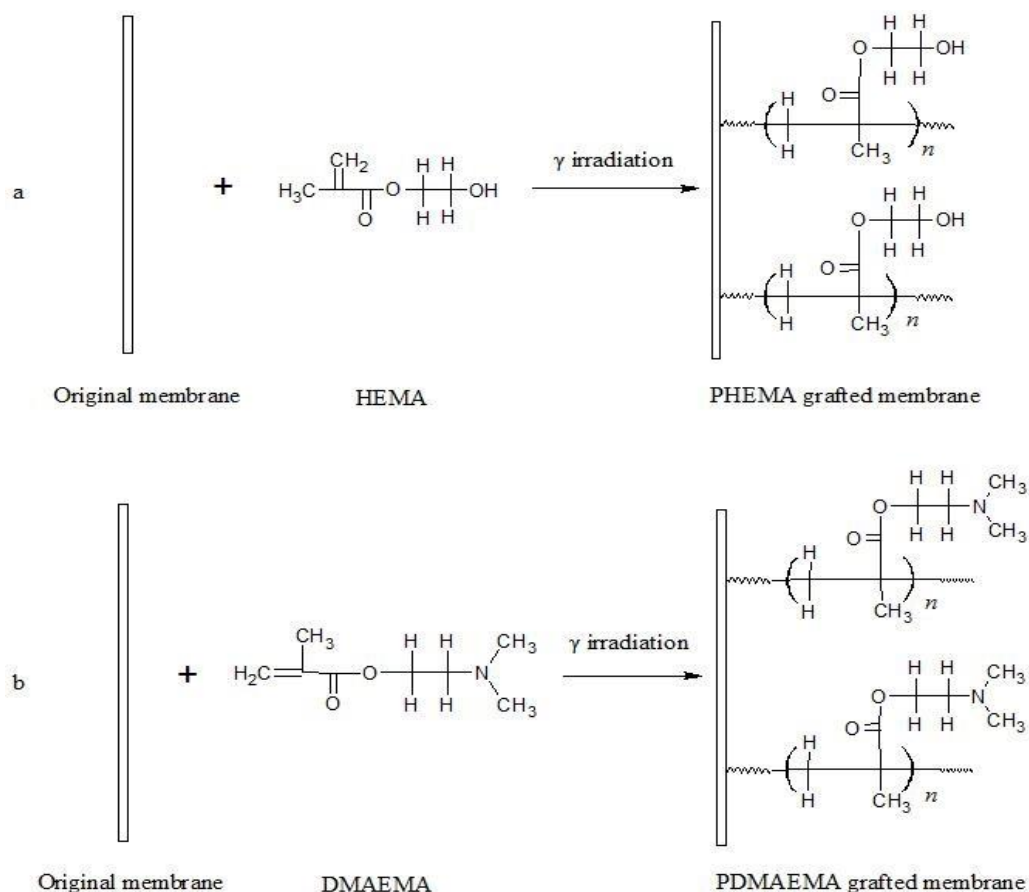
Figure 1-13 - Schematic representative of surface grafting with (a) HEMA and (b) DMAEMA, employing gamma radiation[50].

1.10 Analysis of the Drug Release Kinetics Employing Mathematical Models

Diffusion is a mass transfer process due to a concentration gradient. In the case of this work, it is the transfer of a drug from the site where it has a higher concentration (interior of the polymeric matrix) to the site of lower concentration (artificial tear solution). In the evaluation of the diffusion of MFX, the existing concepts developed for the processes of water absorption by polymers can be applied. Alfrey, Gurnee and Lloyd proposed 3 categories to classify the transport of a penetrant through a polymer, depending on the limiting kinetic step in the absorption rate [54]:

- Case I: Simple Fickian diffusion; occurs when the diffusion rate of the solvent is lower than the relaxation rate of the polymer matrix;
- Case II: Transport controlled by relaxation; occurs when the diffusion is faster compared to the relaxation of the polymer matrix;

- Non-fickian diffusion or anomalous diffusion; occurs when the diffusion rates and the relaxation rates are similar.

To determine the mechanism that determines the entry or the release of a molecule in this cases, it can be used Equation 1, proposed by Korsmeyer and Peppas. It describes the release of a drug having regard to its diffusion and the relaxation of the polymer network,

$$\frac{M_t}{M_\infty} = kt^n \qquad \qquad \text{Equation 1}$$

where M_t is the mass of drug released at time t, M_∞ is the mass of drug released at the equilibrium, k is a kinetic structural/geometric constant characteristic of the system (Equation 2) and n is the diffusional exponent, whose value depends on the absorption mechanism and indicates the release kinetic order [55] [56]. This expression is only valid for the first 60% of cumulative release, $0 \leq M_t/M_\infty \leq 0.6$ [57].

$$k = 4 \left(D/_{\pi l^2} \right)^{1/2} \qquad \qquad \text{Equation 2}$$

Equation 2 provides the value of the diffusion coefficient (D) that also depends on the membrane thickness (l) and Table 1.4 shows the relationship between the value of n, the respective release mechanism and the empirical models for a planar matrix system, which was the geometry used in this work.

Table 1.4 - Drug transport mechanisms and diffusional exponents by Korsmeyer-Peppas model for a planar polymeric matrix [58] [59].

Diffusional exponent, n	Transport mechanism	Time dependence
$n < 0.5$	Quasi-Fickian diffusion	-
$n = 0.5$	Simple Fickian diffusion (Case I transport)	$t^{-0.5}$
$0.5 < n < 1$	Anomalous transport	t^{n-1}
$n = 1$	Case II transport	Time independent
$n > 1$	Super Case II transport	t^{n-1}

Quasi-Fickian diffusion occurs when the drug diffusion rate is much lower than the rate of polymer relaxation. The Fickian diffusion is characterized by a low rate of diffusion of the drug to the exterior of the matrix relative to the speed of the relaxation of the polymer, induced by water absorption. Therefore, the main mechanism that controls the release is diffusion. Simple Fickian diffusion is characterized by $n = 0.5$ in the Korsmeyer-Peppas model, which corresponds to the Higuichi model (presented next). In non-Fickian processes, the chains do not have enough mobility to allow rapid entry of the solvent that would allow the drug release from the matrix and then the relaxation of the chains may be slower than the diffusion of the drug. Non-Fickian processes have been classified into three types, depending on the drug diffusion relative speeds. For anomalous transport, the drug diffusion rate and relaxation of the polymer are of the same order of magnitude. In the Case II the drug diffusion rate is greater than the relaxation of the polymer matrix, adjusting to the kinetic model of order zero, by having a constant release over time. Finally, Super case II transport is characterized by a delay in drug release from the start and acceleration at the end of the release before reaching a *plateau*.

To determine n and D values, a linearization of the model developed by Korsmeyer and Peppas is made by plotting $\log M_t/M_\infty$ (until 0.6) versus $\log t$ (Figure 1-14). The slope of the trend line is n and the intercept is k, a value required to determine D by Equation 2.
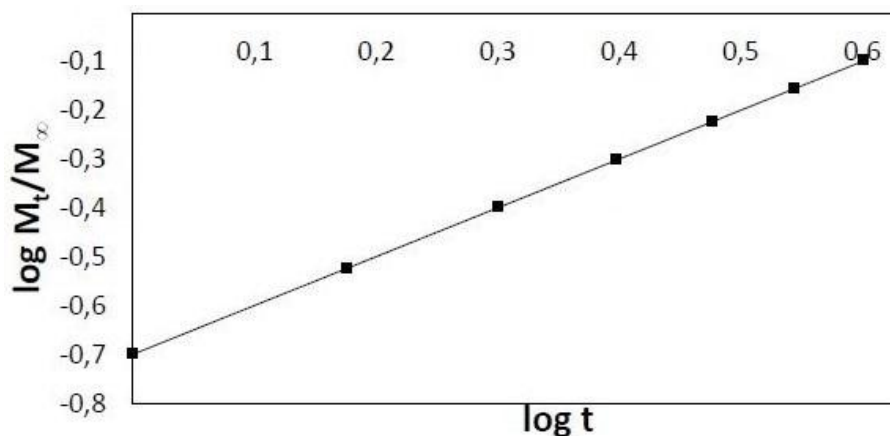
Figure 1-14 - Graphical representation of the model of Korsmeyer and Peppas.

There are several other mathematical models that have been used for a better understanding of the release profiles. For this work, models that describe the drug release from planar, solid, non-eroding matrices, whose release is controlled by diffusion, were

selected [60]. Thus, in addition to the Korsmeyer-Peppas model presented above, the most suitable models are the kinetic models of zero order, first order and the Higuchi model.

The zero order release kinetics represents pharmaceutical forms that release drug slowly and do not suffer degradation [58]. It can be defined by Korsmeyer and Peppas model with $n = 1$ (Case II), as shown in Equation 3,

$$W_0 - W_t = kt \hspace{4cm} \text{Equation 3}$$

where W_0 is the initial amount of drug in the pharmaceutical form, W_t the amount of drug at instant t and k is the release zero order constant. Equation 2 can be simplified by dividing it by W_0 (Equation 4),

$$f_t = 1 - \frac{W_t}{W_0} = kt \hspace{4cm} \text{Equation 4}$$

being f_t the fraction o drug released at time t. It is obtained a curve of the type $f(t) = a + bt$, as shown in Figure 1-15. The pharmaceutical forms which follow the profile release the same amount of drug per unit time, being one of the best ways to controlled release.
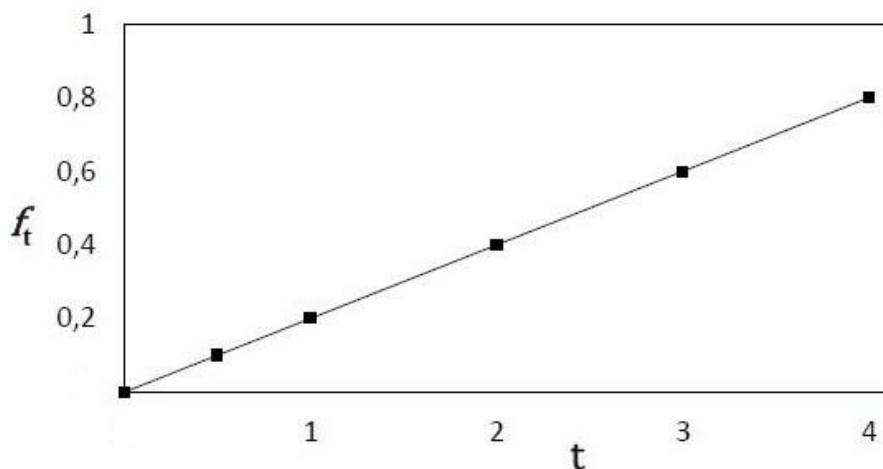
Figure 1-15 - Graphical model of order zero representation.

The first order kinetics describes systems where the release rate depends on the concentration of drug, as described in Equation 5,

$$\log C_\mathrm{t} = \log C_0 + \frac{kt}{2.303}$$

Equation 5

where C_t is the amount of drug released at time t, C_0 is the initial amount of drug in the solution and k is the release constant of first order. Figure 1-16 shows the decimal logarithm of the amount released *versus* time, with a slope of $-k/2.303$. The pharmaceutical forms which follow the profile are, for example, porous matrices with hydrophilic drugs.
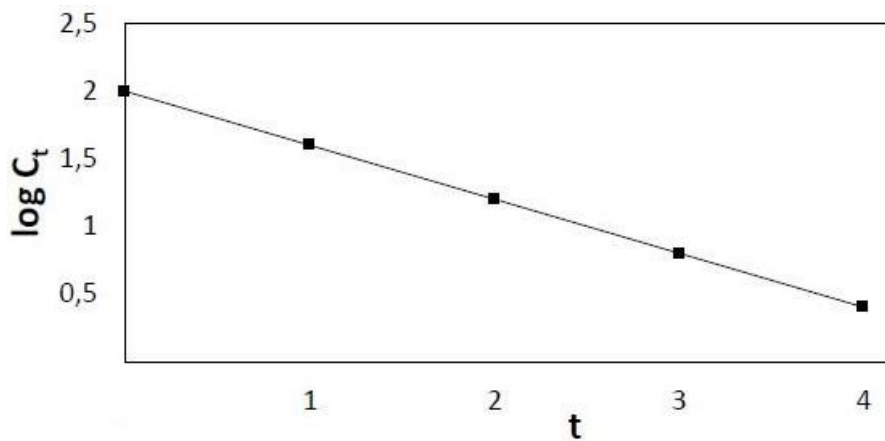
Figure 1-16 - Graphical representation of the first order model.

Higuchi has developed a model for drug release based on the assumption that the polymeric matrices have no structural change in the presence of water. As mentioned for the Korsmeyer-Peppas model, when $n = 0.5$, that model is equivalent to Higuchi's model, which describes a drug release as a diffusion process based on Fick's first law, dependent on the square root of time. Higuchi model is represented by Equation 6,

$$f_\mathrm{t} = K_\mathrm{H} t^{1/2}$$

Equation 6

where f_t is the amount of drug dissolved in time t and K_H is the dissolution constant Higuchi. It is obtained a curve of the type $f(t) = a + bt^{0.5}$, as shown in Figure 1-17.
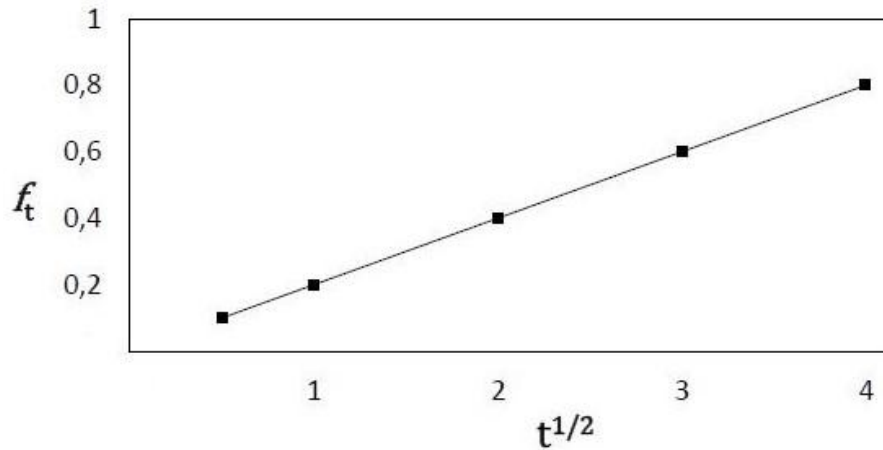
Figure 1-17 - Graphical representation of the Higuchi model.

Researchers have used various criteria for selecting which model exhibits the best fit to the release curve. Among them, one can find Akaike Information Criterion (AIC), the Bayesian information criterion (BIC) [61] and the criterion of adjusting the curves in points using the coefficient of determination, R^2. For the R^2, there is a criterion that sets 0.99 as the limit value [62] and a criterion which indicates that the model with higher R^2 is accepted [60]. In this work, it is assumed that the adjustment border for R^2 is 0.95 due to the irregularity of the profiles. This criterion means that the model will fit 95% of the data points.

1.11 Characterization Techniques

1.11.1 Swelling Capacity

The water content of soft contact lenses allows oxygen to pass through the lenses and keeps the cornea healthy during contact lens wear. However, lenses with higher water content tend to be too fragile and manufacturers tend to make them thicker [63]. The equilibrium water content (EWC) of SCLs is defined as the maximum quantity of water that a membrane is able to retain when immersed in water, after reaching a state of equilibrium and is calculated from Equation 7,

$$\textbf{EWC \%} = \frac{w_{t_\infty} - w_0}{w_{t_\infty}} \times \textbf{100} \qquad \text{Equation 7}$$

where w_{t_∞} is the hydrated sample weight in the equilibrium and w_0 is the dry mass of the membrane.

As the water absorption of the polymer is directly related to its bulk hydrophobicity, it is an important evaluation parameter. Naturally, a hydrophilic polymer absorbs more water than a hydrophobic one. The water content of commercial SCLs can range from approximately 38 to 85% (w/w) [64]. Table 1.5 shows some SCLs currently available in the market with respective water content.

Table 1.5 - Water content of commercial SCLs currently available [27]

Commercial name	Focus® Night&Day TM	PureVision TM	Acuvue® Advance TM	Acuvue® Oasys™	O2Optix TM	Biofinity TM
Water content (%)	24	36	47	38	33	48

1.11.2 Contact Angle Goniometry

The water contact angle, which is a measure of wettability of a surface, has been used to try to predict contact lens on-eye wettability. Failure to achieve a stable ocular tear film layer can reduce comfort and affect visual performance and it is required for drug delivery from SCLs. The wettability is quantified by measuring the contact angle (θ) at an interface where there is contact between the three phases interacting (solid, liquid and vapour) (Figure 1-18). The degree of wetting is determined by a balance between liquid-solid adhesive forces and liquid cohesive forces acting on the membrane surface.
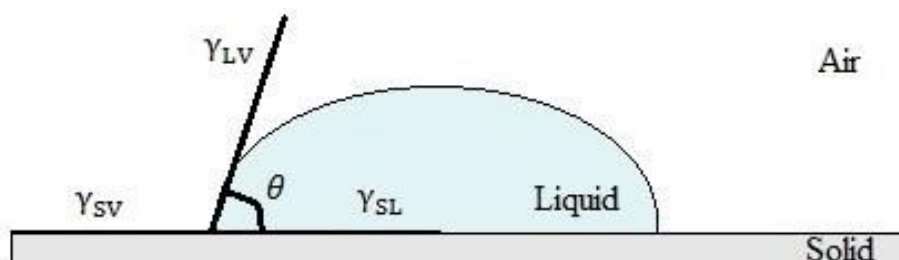
Figure 1-18 - Contact angle between the solid surface and a liquid drop.

The equilibrium between solid, liquid and vapor phases is defined by the Young equation showed in Equation 8,

$$\gamma_{SV} = \gamma_{SL} + \gamma_{LV} \cos \theta \qquad\qquad \text{Equation 8}$$

where γ_{SV}, γ_{SL} and γ_{LV} correspond respectively to the superficial tensions of the solid-vapor, solid-liquid and liquid-vapor interfaces and θ is the contact angle.

There are several techniques to measure the contact angle. The most used are the sessile drop and the captive bubble techniques. As the SCLs are used in hydrated form on the eyes, the method used to measure the contact angle of hydrated surfaces is captive bubble method. In this method, the membrane is submerged in water and an air bubble is released from beneath the sample from a needle immersed in the water, and it is allowed to rise and attach to the sample's surface (Figure 1-19). The contact angle is then measured between the membrane surface and the tangent line passing through one of the two three-phase contact points (left and right contact angles, when viewing a cross-section of the bubble on the surface; Figure 1-19) [65].
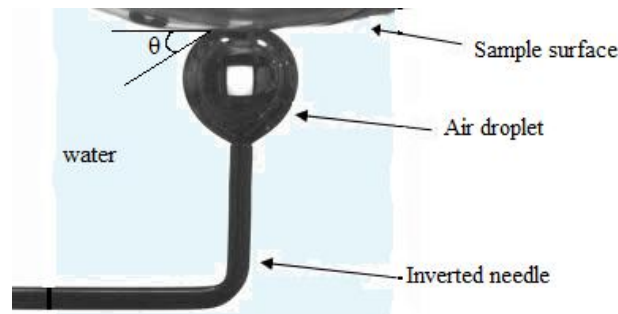
Figure 1-19 - Representation of measurement of the contact angle (θ) of an SCL by the captive bubble technique [67].

Table 1.6 shows some contact lenses available on the market with their respective water contact angle values.

Table 1.6 - Contact angle of silicone SCLs currently available on the market for captive bubble technique [68] [69]

Commercial name	Acuvue Oasys	PureVision™	Air Optrix Night and Day	O₂ Optrix
Contact angle (º)	32.4	30.1	25	44.3

1.11.3 Sample Transmittance

Transmittance is an important property of the SCL, mainly to accomplish good visual performance but also for protection from ultraviolet (UV) light. The amount of light transmitted by a sample is determined by comparing the initial intensity of incident light (I_0) and the transmitted light intensity, after passing through the lens (I). Percent transmittance, T (%), is defined in Equation 9.

$$T(\%) = \frac{I}{I_0} \times 100 \qquad\qquad \text{Equation 9}$$

Because the intensity of the transmitted light (I) is never greater than the intensity of the incident light (I_0), transmittance (T) is always less than 100%. Table 1.7 shows UV and visible transmittance of SCLs available on the market.

Table 1.7 - UV and Visible transmittance in some SCL available on the market [70].

Commercial name	1 Day Acuvue	Surevue	2 Week Acuvue	Vistavue
UV transmittance (%)	0.4 to 82.8	0.3 to 89.0	0.4 to 91.3	0.4 to 88.4
Visible transmittance (%)	83 to 90			

1.11.4 Fourier Transform Infrared Spectroscopy

Fourier Transform Infrared spectroscopy (FTIR) is based in the fact that chemical bonds, when excited with infrared radiation, vibrate at particular wavenumber. Thereby, a vibration frequency can be associated with a specific type of chemical bond. FTIR can be combined with the Attenuated Total Reflectance (ATR) sampling tool to enable study of samples directly in the solid or liquid state without further preparation. It works by directing an infrared beam through an ATR crystal in contact with the sample. The crystal reflects the beam in its internal surface and, at each reflection point, the beam penetrates a few micrometers beyond the crystal and into the sample. FT-IR/ATR was employed with the objective of identifying and determining the molecular composition of each membrane and, when surface modification was employed, to detect the presence of the coating.

1.11.5 Citotoxicity study

Biocompatibility is defined as the capacity of a material to perform its function in the body without causing adverse responses that damage the tissue and/or surrounding organs. The cytotoxicity of a material is one of the aspects of biocompatibility which must be evaluated [71]. The cytotoxicity of the synthesized materials was evaluated employing a novel tetrazolium compound (3-(4,5-dimethyl-2-yl)-5-(3-carboxymethoxyphenyl)-2-(4-sulfophenyl)-2H-tetrazolium, inner salt; MTS), which evaluates cell viability after contact with the test material. Metabolism in viable cells produces reducing compounds (NADH or NADPH), which are able to reduce MTS into a soluble formazan product; when dead, cells lose the ability to reduce tetrazolium when dead. Consequently, the absorbance of the colored formazan product is proportional to the number of viable cells. The citoxicity evaluation was performed according to ISO 10993-5, which considers a cytotoxic effect when more than 30% of viable cells are dead after contacting the test sample [72].

Chapter 2

2 Materials and Methods

2.1 Materials

The reagents used to prepare the chitosan-based membranes were the following: low molecular weight (190 – 310) chitosan (CS) 75 - 85% deacetylated, lactic acid (90%), triethyl citrate (TEC) (99%), poly(ethylene glycol dodecyl ether) and (Brij®35) acquired from Acrós Organics, Belgium; porcine gelatin type A and poly(ethylene glycol) (PEG) provided by Aldrich, United Kingdom (MW: 300); poly(vinyl alcohol) (PVA; 98%; MW: 9500), obtained from Sigma-Aldrich, USA; branched and linear poly(lactic acid) (PLA; MW: 856.8 and 630.6, respectively), synthesized in the laboratory; *N*-cyclohexyl-*N'*-(2-morpholinoethyl)carbodiimide metho-*p*-toluenesulfonate (CMC $\geq$ 97%) from Fluka, Germany and glyoxal (40%) obtained from BASF, Germany.

For acrylic-based membranes, the following reagents were used: methyl methacrylate (MMA), hydroxyethyl methacrylate (HEMA), lactic acid and the initiator benzoyl peroxide (BP; 75%) from Acrós Organics, Belgium; ethylhexyl acrylate (EHA), octadecyl methacrylate (ODMA) and methacrylic acid (MAA) provided from Sigma-Aldrich, USA. The membranes with surface modification was developed using hydroxyethyl methacrylate (HEMA) and *N,N*-dimethylaminoethyl methacrylate (DMAEMA) from Aldrich, United Kingdom.

The release medium, which pretends simulate the ionic strength of tear fluid and have some of the salts present in tear fluid, was prepared with calcium chloride ($CaCl_2$) ($\geq$ 99,5%) from Fluka, Germany; sodium bicarbonate ($NaHCO_3$) acquired from Fisher Scientific, England; potassium chloride (KCl) obtained from Merck, Germany and sodium chloride (NaCl) ($\geq$ 99%), from Sigma-Aldrich, USA.

The drug used was moxifloxacin hydrochloride (MFX) acquired from Carbosynth, UK.

The materials used in the biocompatibility tests were CellTiter 96® Aqueous One Solution Reagent (MTS) purchased from Promega (Madison, USA), Fetal bovine serum

(FBS) (free from any antibiotic) purchased from Biochrom AG (Berlin, Germany), amphotericin B, Eagle's Minimum Essential Medium (MEM), trypsin were purchased from Sigma–Aldrich (Sintra, Portugal).

2.2 Methods

2.2.1 Preparation of Chitosan-Based Membranes

The composition of the CS-based membranes prepared can be seen on Table 2.1. They were prepared employing phase inversion by solvent evaporation.

Table 2.1 - Composition of the CS-based membranes prepared.

Composition	CBM 1	CBM 2	CBM 3	CBM 4	CBM 5	CBM 6	CBM 7	CBM 8
Chitosan (%; w/v)	2	2	2	2	2	2	2	0.5
Lactic acid (%; v/v)	1	1	1	1	1	1	1	1
PVA (%; w/v)	2	2	-	2	2	-	-	2
PLA branched (%, w/v)	2	-	-	2	-	-	-	-
PLA linear (%; w/v)	-	2	-	-	-	-	-	-
CMC (%; w/v)	0.1	0.1	-	-	0.1	0.1	0.1	0.1
Gelatin (%; w/v)	-	-	-	-	1	1	1	0.5
Brij®35 (%; w/v)	-	-	-	-	-	-	2	-
TEC (%; w/v)	-	-	-	-	-	2	-	-
Glyoxal (%; v/v)	0.1	0.1	-	0.05	-	-	-	-
Composition	CBM 9	CBM 10	CBM 11	CBM 12	CBM 13	CBM 14	CBM 15	CBM 16
Chitosan (%; w/v)	0.5	0.5	0.5	0.5	0.5	2	2	2
Lactic acid (%; v/v)	1	1	1	1	1	1	1	1
PVA (%; w/v)	1	-	2	1	-	2	2	2
CMC (%; w/v)	0.1	0.1	0.2	0.2	0.2	1	0.5	0.5
Gelatin (%; w/v)	0.5	0.5	0.5	0.5	0.5	2	2	2
PEG 300 (%; v/v)	1	2	-	1	2	2	2	2
Glyoxal (%; v/v)	-	-	0.4	0.4	0.4	1	1	0.2

For that, chitosan was dissolved in a 1% (w/v) aqueous lactic acid solution at different concentrations, under magnetic stirring. All the other reagents were added after dissolution of the chitosan, being the last reagent added glyoxal. For membrane 5, wherein the gelatin is part of the formulation, it was necessary first to dissolve gelatin at 50 ºC with magnetic stirring. Subsequently, the mixture with about 20 mL was placed in a Petri dish of 7 cm in diameter. It was allowed to evaporate at 40 ºC for about 2 days and

a week. The resulting membrane was removed from the Petri dish with the aid of forceps and cut into circles of 14 mm diameter (diameter of the SCLs available in the market). When membrane removal was difficult, the membrane was hydrated before removal, to become more malleable.

2.2.2 Preparation of Acrylate-Based Membranes

The method used in the synthesis of acrylate-based membranes was bulk copolymerization, which is a reaction which occurs in the presence of the monomers but in the absence of a solvent, by adding a soluble initiator to the monomers. Table 2.2 shows the composition of the acrylate-based membranes prepared.

Table 2.2 - Composition of the acrylate-based membranes prepared.

Composition (%)	ABM 1	ABM 2	ABM 3	ABM 4	ABM 4.1	ABM 4.2	ABM 4.3	ABM 4.4	ABM 5
MMA [#]	60	80	70	50	50	50	50	50	25
ODMA [#]	40	-	-	25	25	25	25	25	25
EHA [#]	-	20	-	25	25	25	25	25	25
HEMA [#]	-	-	30	-	-	-	-	-	-
MAA [#]	-	-	-	-	-	-	-	-	25
Lactic acid [# b]	-	-	-	10	10	10	10	10	10
Surface treatment	-	-	-	-	Grafting of HEMA (dose: 25 KGy)	Grafting of DMAEMA (dose :25 KGy)	Grafting of DMAEMA (dose: 15 KGy + drug)	Grafting of DMAEMA (dose: 15 KGy)	-
Benzoyl peroxide*	0.5	0.5	0.5	0.5	0.5	0.5	0.5	0.5	0.5

[#] Percentage with regard to the mass of monomers.
* Percentage with regard to the mol of monomers
[b] Applied only in occlusion drug impregnation.

To prepare the membranes, the monomers were mixed and the initiator (benzoyl peroxide, BP) was added and stirred until dissolved. The prepared solution was injected with a syringe between two glass plates covered with teflon sheets and with a silicone spacer with 0.5 mm thick. The two covered glass plates were maintained together with the aid of adhesive tape and four binder clips (Figure 2-1). After injection of the reaction mixture in the mold, it was placed in an oven at 40 ℃ and its temperature was gradually increased until reaching 80 ℃. After 3 hours at 80 ℃, they were removed from the oven and separated from the plates.
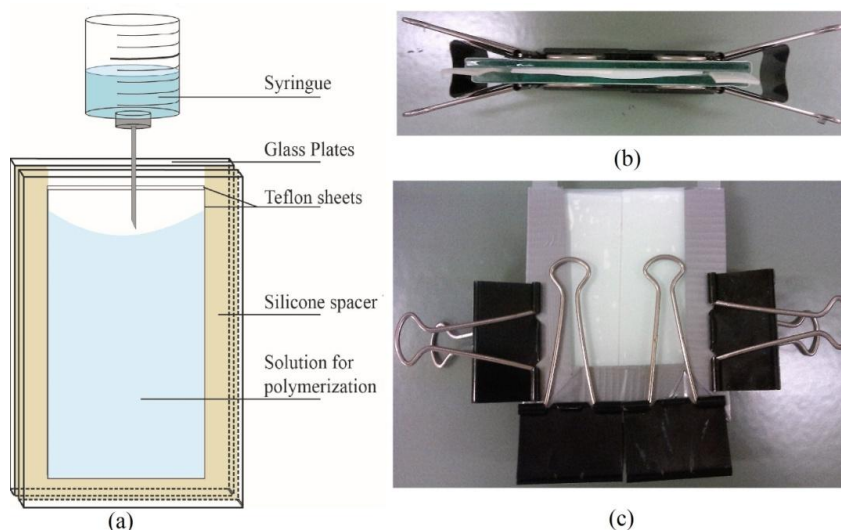
Figure 2-1 - Scheme of the mold used for preparation of acrylate-based membranes (a) and top (b) and side (c) views of the mold employed.

2.2.3   Surface Modification by Gamma Radiation Grafting

Four samples of membrane 4 with 1 cm^2 each were submitted to surface modification by grafting, employing gamma radiation. For that, the membrane 4.1 was introduced in a glass vial containing 5 mL of a 0.41 M HEMA solution in methanol and membrane 4.2 was placed in another vial containing 5 mL of 0.41 M DMAEMA aqueous solution. The monomer solutions were previously bubbled with N_2, for 3 min. The irradiation was made with a Co^{60} source located at Instituto Superior Técnico – Campus Tecnológico e Nuclear, in Sacavém. Each vial received a dose rate of 1.5 KGy/h for 16h40m, which resulted in an absorbed dose of 25 KGy.

Membranes 4.3 and 4.4 were introduced in a glass vial containing 5 mL of a 0.4 M DMAEMA aqueous solution. The monomer solutions were previously bubbled with N_2, for 3 min. The irradiation was also made with a Co^{60} source at a dose rate of 1.5 KGy/h for 10 h, which resulted in an absorbed dose of 15 KGy. Figure 2-2 shows the vials with the respective membranes after irradiation.

After the irradiation, unreacted monomers were removed by washing the membranes with 5 mL of water for 1 h employing magnetic stirring.

Figure 2-2 - Vials with the membranes after irradiation.

2.2.4 Drug Loading

To load drug into the membranes, two approaches were followed: occlusion and soaking. In occlusion, the drug was added to the monomers solution before the polymerization. For that, 1 mg of MFX was added per mL of monomers solution. In drug loading by soaking, the prepared membranes were immersed in 5 mL of a 5 mg MFX per mL of ATS for 16 hours, under shaking at 37 ºC and at 100 rpm.

In the case of the surface modification by gamma radiation grafting, membranes, were only loaded by soaking after the irradiation under the same conditions mentioned above for the case of loading by soaking. In addition, membrane 4.3 was also irradiated in the presence of MFX (1 mg/mL in the monomer solution) and it was studied by two different ways: with and without subsequent loading of MFX by soaking.

2.2.5 Drug Release Studies

In order to have a release medium which had some similarity with the tear fluid, a solution which aims to simulate the salt content, ionic strength and pH of tear fluid was employed [73]. This solution, which was referred to as "artificial tear solution" (ATS), has a pH of 7.4 and its composition is represented on Table 2.3.

Table 2.3 - Composition of the artificial tear solution (ATS) [73].

Salt	NaCl	KCl	CaCl$_2$	NaHCO$_3$
Concentration (g/L)	6.7	1.0	0.08	2.0

The release studies were carried out at the physiological temperature of 37 ℃, under shaking (100 rpm), employing a Thermoshake RO 500 incubator (Thermoshake Gerhardt, Germany). They were conducted in 5 mL of ATS placed in 15 mL Falcon tubes, in triplicate, placed in an incubator at 37 ℃ and employing shaking at 100 rpm. In the case of modified surface membranes, only one sample was studied because there was not enough material. For quantification of the released drug, 5 µL aliquots were withdrawn and subsequently replaced with fresh ATS at pre-determined times. This procedure was also carried out with membranes without drug (blanks) in order to discount residues that could leach out of the polymer matrix and absorb at the same wavelength used to quantify MFX. The obtained drug release profiles represent the cumulative mass of drug released per sample mass *versus* time.

2.2.6 Drug Quantification Method

The quantification of the drug released was carried out by measuring the transmittance at 290 nm of the collected aliquots, employing a modular UV-VIS spectrophotometer (Scan Sci, Portugal) and a quartz cell (*Labbox*, Spain). The conversion of transmittance into concentration was done using a calibration curve prepared from a series of MFX solutions of known concentration (range: 0.5 to 7 µg/mL) employing an equation of the type $y = ax^2 + bx + c$, where y is the intensity in cts and x is the concentration of the released drug in µg/mL.

2.3 Membranes Characterization

2.3.1 Swelling Capacity

The water swelling capacity of the membranes was determined gravimetrically. The membrane samples were dried in a vacuum oven at room temperature until reaching a constant weight. This value was the dry mass (w_0). Thereafter, each sample was immersed in ATS, at room temperature. At set time periods, samples were withdrawn from the solution; the excess surface water was removed with moistened filter paper and was weighted (w_t). The samples were returned to the solution until a constant weight was

attained. The swelling capacity (SC) at the end of each period was calculated from Equation 10.

$$SC\ (\%) = \frac{w_t - w_0}{w_t} \times 100$$ 　　　　　Equation 10

When a constant SC value was attained, w_{t_∞}, the equilibrium water content (EWC) was calculated by Equation 7.

2.3.2 Contact Angle Goniometry

The measurement of the contact angle was made by the captive bubble method employing an OCA-20 contact angle goniometer from Dataphysics (Germany). Through an optical microscope with a goniometer on which the bubble is viewed in profile, the SCA-20 software automatically calculates the contact angle on both sides of the bubble by the Young-Laplace method. The obtained angle is the average of the right and left contact angles of the bubble.

The captive bubble method consists in placing an air bubble with 5 µL in contact with the surface of a sample whose surface is in contact with water (Figure 2-3).

(1) Membrane Support
(2) Glass Cell
(3) Curved Needle
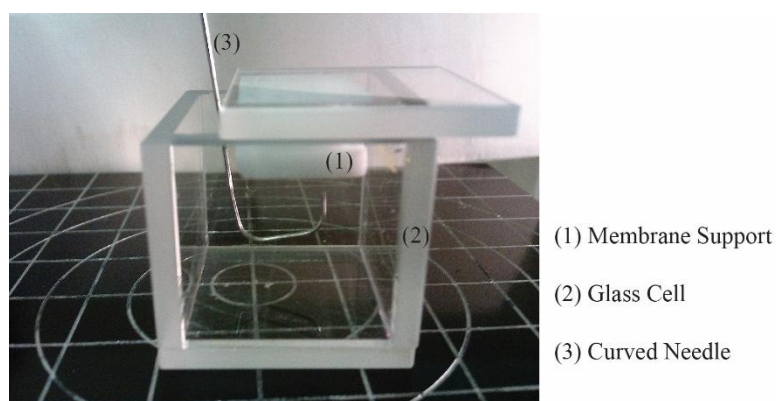
Figure 2-3 - Photograph of the assembly employed in the captive bubble method.

For that, the sample surface to be analyzed was placed, with the aid of adhesive tape, in contact with the surface of water located inside a glass cell (GC 10 glass cell,

Dataphysics, Germany), which contained a curved needle attached to an empty syringe. Bubbles were formed at the tip of the needle and released so that they attached to the immersed sample surface.

In each sample, measurements were made for 5 air bubbles and, for each membrane, 3 samples were evaluated (triplicate).

2.3.3 Membrane Transmittance

Membrane transmittance was determined in the wavelength range 200-800 nm, using a spectrophotometer UV/VIS V-530 (Jasco, USA). A hydrated sample from each membrane was cut and pasted over a quartz cuvette, making use of the surface tension between the surface of the cuvette and the membrane.

2.3.4 ATR-FTIR Characterization

The ATR-FTIR spectra of dry membranes were recorded in a Jasco 4200 FTIR spectrometer (Jasco, Japan), equipped with a Golden Gate Single Reflection Diamond ATR (Specac, England). Spectra were obtained by recording 128 scans at room temperature, with a resolution of 4 cm^{-1}.

2.3.5 Cytotoxicity evaluation

2.3.5.1 Proliferation of corneal endothelial cells in the presence of the most promising membranes

Before performing the test itself in the presence of the membranes, it is necessary to cultivate the corneal endothelial cells (CEC), harvested from rabbit eyes. Thus, harvested cells were grown in Eagle's minimum essential medium (MEM) supplemented with 10% fetal bovine serum (FBS) and growth factors (epidermal, fibroblast and nerve growth factors). Subsequently, to assess cell behavior in the presence of the membranes samples were placed in a 96-well plate properly sterilized with UV radiation exposure for at least 30 minutes. CEC were seeded at a density of 2×10^4 cells/well. Cell growth was

monitored using an Olympus CX41 inverted light microscope (Tokyo, Japan) equipped with an Olympus SP-500 UZ digital camera for 1, 3 and 7 days.

2.3.5.2 **Characterization of the cytotoxicity of the SCLs**

The cytotoxicity tests were performed in the Faculty of Health Sciences, University of Beira Interior, in Covilhã. To do so, CEC were seeded at the same initial density in the presence of the material, in 96-well plates, with 200 µL of MEM and incubated at 37 ℃, in a 5% CO_2 humidified atmosphere. After the incubation period (1, 3 and 7 days), cell viability was evaluated using an MTS assay. Thus, the culture medium was replaced in each sample by 100 µL of fresh medium and 20µL of MTS, followed by their incubation for 4 hours at 37 ℃, in a 5% CO_2 atmosphere. To determine the absorbance of each well was used a microplate reader (Biorad xMark microplate spectrophotometer), at 492 nm. Wells containing the cells culture medium without materials were used as negative control (K^-). For positive control, it was added ethanol (96%) to the wells containing cells (K^+).

Chapter 3

3 Results and Discussion

3.1 Chitosan-Based Membranes Prepared

Chitosan-based membranes were prepared with several different concentrations and reagents. In order to prepare a drug controlled release system, the formulation was adjusted to achieve the main requirements. Figure 3-1 shows photographs of the prepared membranes.

CBM 1: 2% CS + 2% PVA + 2% PLA branched + 0,1% CMC + 0,1% Glyoxal	CBM 2: 2% CS + 2% PVA + 2% PLA linear + 0,1% CMC + 0,1% Glyoxal	CBM 3: 2% CS	CBM 4: 2% CS + 2% PVA + 2% PLA branched + 0,05% Glyoxal
CBM 5: 2% CS + 2% PVA + 0,1% CMC + 1% Gelatin	CBM 6: 2% CS + 0,1% CMC + 1% Gelatin + 2% TEC	CBM 7: 2% CS + 0,1% CMC + 1% Gelatin + 2% Brij® 35	CBM 8: 0,5% CS + 2% PVA + 0,1% CMC + 0,5% Gelatin
CBM 9: 0,5% CS + 1% PVA + 0,1% CMC + 0,5% Gelatin + 1% PEG 300	CBM 10: 0,5% CS + 0,1% CMC + 0,5% Gelatin + 2% PEG 300	CBM 11: 0,5% CS + 2% PVA + 0,2% CMC + 0,5% Gelatin + 0,5% Glyoxal	CBM 12: 0,5% CS + 1% PVA + 0,2% CMC + 0,5% Gelatin + 1% PEG 300 + 0,4% Glyoxal
CBM 13: 0,5% CS + 0,2% CMC + 0,5% Gelatin + 2% PEG 300 + 0,4% Glyoxal	CBM 14: 2% CS + 2% PVA + 1% CMC + 2% Gelatin + 2% PEG 300 + 1% Glyoxal	CBM 15: 2% CS + 2% PVA + 0.5% CMC + 2% Gelatin + 2% PEG 300 + 1% Glyoxal	CBM 16: 2% CS + 2% PVA + 1% CMC + 2% Gelatin + 2% PEG 300 + 0,2% Glyoxal

Figure 3-1 - Appearance of the chitosan-based membranes prepared.

As shown in Figure 3-1, chitosan-based membranes have a yellow coloration due to the color of the chitosan powder, which was yellow. It is found that, with the use of PEG 300 and PVA, one was able to obtain a transparent and colorless membrane (CBM 12). This may be due to some interaction between the plasticizers and glyoxal with the pigment that makes chitosan yellow. When the amount of chitosan increased to 2% (w/v), the membrane became again yellow, maybe due to its greater thickness, but remained transparent. It is also noted that the evaporation time of the solvent was higher when gelatin was added to the formulation. This fact is probably due to the multiple hydrogen bonds formed between gelatin and water.

3.2   Formulation Selection

The first requirement that the membranes have to fulfill to be used as contact lens is not dissolve in the tear film. As such, they were placed in water for 4 days. Other convenient features are transparency and malleability. Table 3.1 presents the characteristics of the prepared membranes relatively to their solubility in water, transparency and malleability.

Table 3.1 - Solubility in water, transparency and malleability results of the chitosan-based membranes. Membranes compositions are shown in Table 2.1.

Membrane	CBM 1	CBM 2	CBM 3	CBM 4	CBM 5	CBM 6	CBM 7	CBM 8
Dissolve in water?	**No**	**No**	Yes	**No**	Yes	Yes	Yes	Yes
Is it transparent?	No	No	No	No	No	No	No	No
Is it malleable?	No	**Yes**	**Yes**	**Yes**	No	No	No	**Yes**
Membrane	CBM 9	CBM 10	CBM 11	CBM 12	CBM 13	CBM 14	CBM 15	CBM 16
Dissolve in water?	Yes	Yes	**No**	**No**	**No**	**No**	**No**	**No**
Is it transparent?	**Yes**	No	No	**Yes**	No	**Yes**	**Yes**	**Yes**
Is it malleable?	**Yes**	**Yes**	**Yes**	**Yes**	**Yes**	**Yes**	No	**Yes**

The membranes that dissolved in water were excluded. As expected, all membranes crosslinked with glyoxal didn't dissolve in water. The crosslinking is a process that occurs when polymeric chains are linked by covalent bonds, forming connections between linear chains. As such, polymer chains which are covalently attached to each other through a crosslinker cannot be completely separated by the solvent molecules and will not dissolve. Crosslinking also results in the formation of stiffer membranes.

Transparency was improved by adding gelatin to the formulation and a plasticizer appropriate for gelatin membranes. The PVA/PEG 300 ratio had to be optimized to obtain a transparent membrane. Through CBM 8, CBM 9 and CBM 10, it was concluded that the best ratio of plasticizers was 50% each.

Regarding the malleability, it is controlled by two main factors: the concentration of the crosslinking agent and the plasticizer used. It was concluded that the best membrane to meet all these requirements was CBM 16 (2% CS + 2% PVA + 1% CMC + 2% Gelatin + 2% PEG 300 + 0.2% Glyoxal). The CBM 12 (0.5% CS + 1% PVA + 0.2% CMC + 0.5% Gelatin + 1% PEG 300 + 0.4% Glyoxal) was not chosen because, after a first drug release evaluation, it was found that released the drug in minutes and then it was increased the CS and Gelatin composition as well as the crosslinkers. The CBM 14 (2% CS + 2% PVA + 1% CMC + 2% Gelatin + 2% PEG 300 + 1% Glyoxal) become brittle after placed in water, probably due to the output of PVA, which is an external plasticizer and then it was increased the amount of CMC.

3.3   Acrylic-based Membranes Prepared

Acrylic-based membranes were prepared with different monomers and proportions. Figure 3-2 shows photographs of the prepared membranes.

| ABM 1: 60% MMA + 40% ODMA | ABM 2: 80% MMA + 20% EHA | ABM 3: 70% MMA + 30% HEMA | ABM 4: 50% MMA + 25% ODMA + 25% EHA | ABM 5: 25% MMA + 25% ODMA + 25% EHA + 25% MAA |
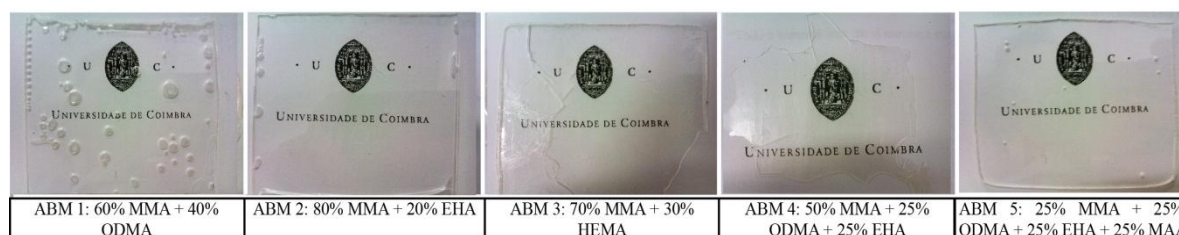
Figure 3-2 - Appearance of the acrylic-based membranes prepared.

As can be seen in membrane ABM 1, bubbles were present. This is due to release of CO_2 during initiator decomposition, in the first stage of polymerization. For this reason, a heating ramp step was implemented to help release CO_2 before viscosity increase, which succeeded in avoiding the presence of bubbles (as visible in ABM 2 to ABM 5, Figure 3-2).

3.4   Formulation Selection

As the Chitosan-based membranes, acrylate-based membranes have to meet the same criteria. They were also placed in water for 4 days. Table 3.2 presents the results relative to their solubility in water, transparency and malleability.

Table 3.2 - Solubility in water, transparency and malleability in water of the acrylate-based membranes. Membranes compositions are shown in Table 2.2.

Membrane	ABM 1	ABM 2	ABM 3	ABM 4	ABM 5
Dissolve in water?	No	No	No	No	No
Is it transparent?	Yes	Yes	Yes	Yes	Yes
Is it malleable?	No	No	No	Yes	Yes

As show in Table 3.2, none of the membranes dissolved in water due the fact that the monomers gave rise to polymers which are not water-soluble. All the membranes were, maybe due the fact that the most abundant polymer in the formulations was PMMA, which is a transparent polymer. ABM 4 (50% MMA + 25% ODMA + 25% EHA) and ABM 5 (25% MMA + 25% ODMA + 25% EHA + 25% MAA) were the best membranes in relation to malleability. This is likely to be due to the long aliphatic, flexible chain of ODMA, which gives rise to more flexible membranes. On the contrary, MMA, a monomer with a short lateral chain, gives rise to more rigid membranes.

3.5   Characterization of Selected Membranes

3.5.1   Swelling Capacity

By the analysis of the swelling capacity, it is possible to evaluate the bulk hydrophilicity of polymers. Figure 3-3 shows the time profiles of the swelling capacity of the membranes and Table 3.3 shows the results of de equilibrium water content (EWC (%)) of each membrane.

Results and Discussion
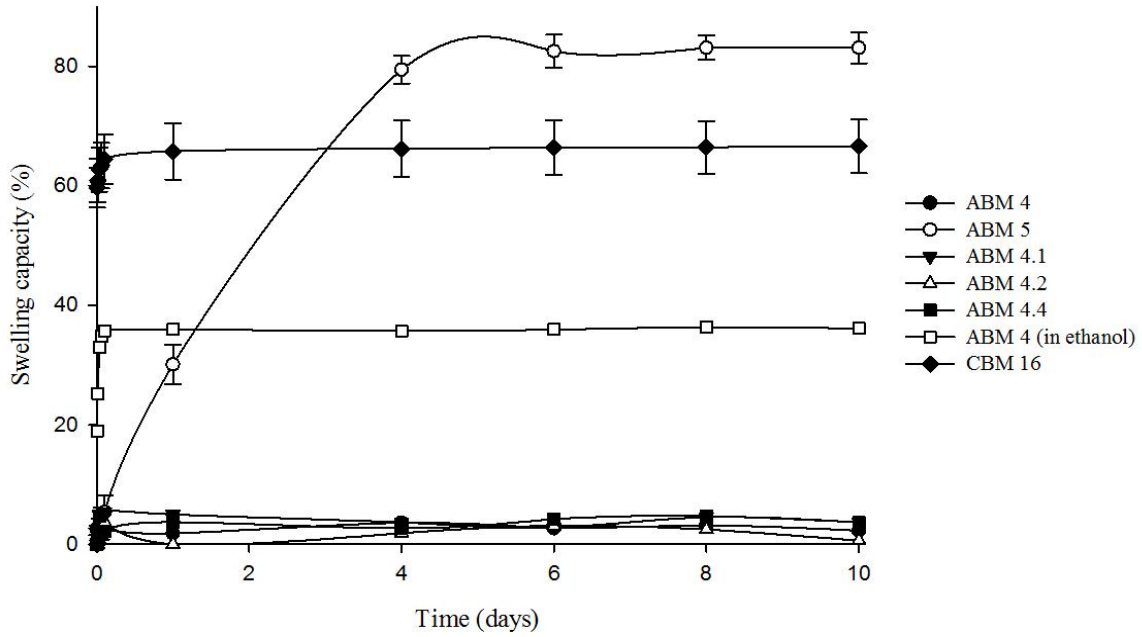
Figure 3-3 - Comparison of the swelling capacity time profiles of ABM and CBM when placed in ATS (error: standard deviation; $n = 3$ to ABM 4, ABM 5 and CBM 16 and $n = 1$ to ABM 4.1, ABM 4.2 and ABM 4.4). The membranes with a modified surface are ABM 4.1, ABM 4.2, ABM 4.4.

In all the samples, except ABM 5, there is a rapid absorption of water, reaching equilibrium in 20 minutes. ABM 5 reaches equilibrium 6 days after the beginning of the study.

Table 3.3 - Equilibrium water content (EWC) of the best ABM and CBM membranes in ATS (error: standard deviation; $n = 3$ to ABM 4, ABM 5 and CBM 16 and $n = 1$ to ABM 4.1, ABM 4.2 and ABM 4.4).

Membrane	Composition	EWC (%)
ABM 4	50% MMA + 25% ODMA + 25% EHA	3 ± 0.2
ABM 4.1	ABM 4 + HEMA coating irradiated with 25 kGy	3
ABM 4.2	ABM 4 + DMAEMA coating irradiated with 25 kGy	3
ABM 4.4	ABM 4 + DMAEMA coating irradiated with 15 kGy	4
ABM 5	25% MMA + 25% ODMA + 25% EHA + 25% MAA	82 ± 3
CBM 16	2% CS + 2% PVA + 1% CMC + 2% Gelatin + 2% PEG 300 + 0.2% Glyoxal	66 ± 4

As showed in Table 3.3, ABM 4, ABM 4.1, ABM 4.2 and ABM 4.4 have similar and very low EWC values, an indication of bulk hydrophobicity. Probably, this hydrophobicity is due to the hydrophobicity of the monomers employed and low mobility of the chains in the matrix, which prevents the swelling of the polymer. Thus, it can be concluded that the membrane ABM 4.4 have higher EWC than the other membranes with

surface modification because the introduction of the hydrophilic DMAEMA co-monomer, enhanced hydrophilicity of resultant hydrogel matrix caused an increase in the equilibrium swelling capacity. [74] It is found that membrane 4.2, also grafted with DMAEMA, have the same EWC than membrane 4.1 grafted with HEMA. This fact is probably due to the greater grafting at the surface which causes the ATS to have greater difficulty in crossing the modified surface of ABM 4.2

As expected, the membrane with MAA (ABM 5) and gelatin (CBM 16) show very large EWC values due to their capacity to form hydrogen bonds with water molecules through their carboxyl (MAA) and carboxyl, hydroxyl and amine groups (gelatin). CBM 16 also has chitosan with amine and hydroxyl groups and PVA with hydroxyl groups which may provide hydrophilicity to the membrane.

As, by definition, hydrogels usually contain water at least 10% of their total weight [75], it is concluded that ABM 5 and CBM 16 are hydrogels. As mentioned in section 1.13.1, the water content of contact lenses can range from approximately 38 to 85%. It can be concluded that membranes ABM 5 and CBM 16 satisfy this requirement.

3.5.2 Contact angle goniometry

This technique allows an evaluation of the surface hydrophilicity of materials. Table 3.4 shows the contact angles obtained by the captive bubble method.

Table 3.4 - Average and standard deviation values of the contact angles obtained by the bubble captive method (error: standard deviation; $n = 1$, with 15 drops measured in each sample).

Membrane	Composition	Contact angle (°)
ABM 4	50% MMA + 25% ODMA + 25% EHA	32 ± 2
ABM 4.1	ABM 4 + HEMA coating irradiated with 25 kGy	36 ± 4
ABM 4.2	ABM 4 + DMAEMA coating irradiated with 25 kGy	31 ± 1
ABM 4.4	ABM 4 + DMAEMA coating irradiated with 15 kGy	27 ± 2
ABM 5	25% MMA + 25% ODMA + 25% EHA + 25% MAA	35 ± 2
CBM 16	2% CS + 2% PVA + 1% CMC + 2% Gelatin + 2% PEG 300 + 0.2% Glyoxal	31 ± 2

All contact angle values are in agreement with the values of contact angles of the lenses available on the market. Through analysis of Table 3.4 it can be observed that the ABM 4.4 surface is the most hydrophilic, followed by ABM 4.2 and CBM 16. As concluded in the Section 3.5.1, the DMAEMA is a hydrophilic monomer and introducing

hydrophilic DMAEMA enhance its hydrophilicity. The ABM 4.2 is less hydrophilic due the higher grafting that decreases the space of the polymeric network in the membrane's surface. Once the DMAEMA is only in the surface, the difference in hydrophilicity for surface modified membranes is more marked in the analysis of contact angles than the EWC. The CBM 16 has carboxyl, hydroxyl and amine groups that provide hydrophilic properties.

3.5.3 Sample transmittance

The transmittance (%) profiles of the visible (400 – 800 nm) and ultraviolet (UV) (200 – 400 nm) spectrum are shown in Figure 3-4. From these profiles, the quantitative values of the transmittance of the membranes can be determined by calculating the mean absorbance across the range of the visible and UV.
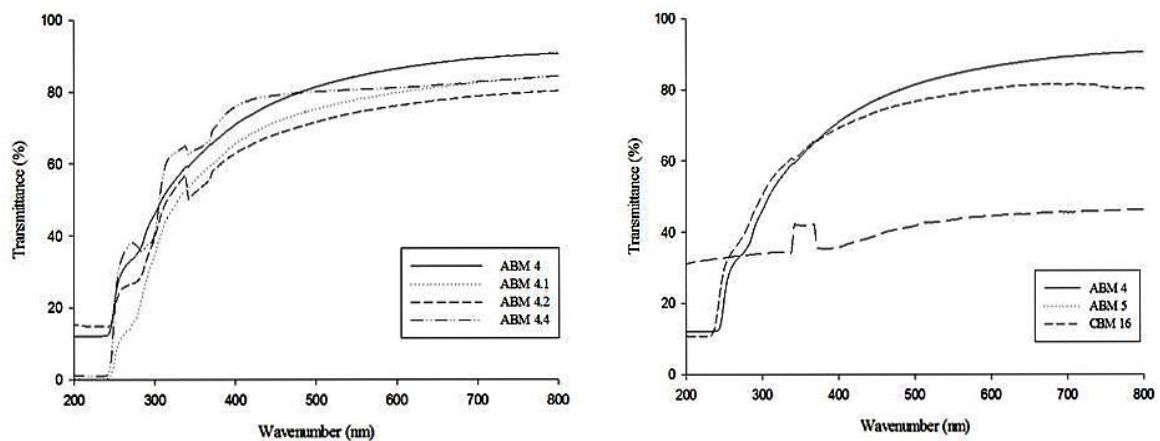
Figure 3-4 - Transmittance spectrum of the best membranes developed between 200 and 800 nm.

All transmittance spectra were similar except for the chitosan membrane profile. The spectra of the acrylic-based membranes show a slight drop off beginning at 800 nm and ending at 250 nm. Chitosan-based membrane has poor transmittance range, with all the spectra range below 40%. It is also observed in the Figure 3-4 that in some profiles there is a small peak at 350 nm. This is probably due to the changing of the lamp that emits radiation in visible for the lamp that emits ultraviolet radiation.

Table 3.5 - Average and standard deviation values for visible transmittance and range values of UV spectrum of the best ABM and CBM membranes (error: standard deviation; $n = 1$).

Membrane	Composition	Visible T (%)	UV T (%) [c]
ABM 4	50% MMA + 25% ODMA + 25% EHA	81 ± 13	12 to 71
ABM 4.1	ABM 4 + HEMA coating irradiated with 25 kGy	75 ± 13	0.4 to 66
ABM 4.2	ABM 4 + DMAEMA coating irradiated with 25 kGy	72 ± 12	15 to 63
ABM 4.4	ABM 4 + DMAEMA coating irradiated with 15 kGy	80 ± 6	1.2 to 76
ABM 5	25% MMA + 25% ODMA + 25% EHA + 25% MAA	75 ± 8	11 to 69
CBM 16	2% CS + 2% PVA + 1% CMC + 2% Gelatin + 2% PEG 300 + 0.2% Glyoxal	41 ± 7	31 to 36

[c] In the UV radiation was used the range of transmittance values since the curve has a wide range of values, which would lead to the existence of standard deviations above the average.

In the visible range, the best membranes are ABM 4 and ABM 4.4 with an average transmittance of 81% and 80%, respectively, as presented by Table 3.5. For UV light, the smaller the transmission the better the protection of the eyes by the SCL. Then, it is appropriate that the transmittance in UV range is as low as possible. The membranes that best protects the eye from ultraviolet radiation are ABM 4.1 and ABM 4.4, both with less than 3% transmittance at 200 nm.

It is noted that the ABM 5 in ATS increased 2 – 2.5% in size, unlike all the other membranes. It means that there is a greater amount of water in its polymeric matrix, influencing the transparency of the membrane. On the other hand, it is thicker than the others due to its high swelling capacity. As such, a comparison with the other membranes is not straightforward.

Regarding the CBM 16, the results point to the low suitability of the material obtained as SCL. Its low transmittance of visible light should be related to its yellowish tint, which implies that it absorbs light in the blue/violet region. As well as ABM 5, CBM 16 is also a hydrogel, having water in the polymeric matrix influencing the transparency.

3.5.4 FT-IR/ATR characterization

As described in Chapter 1 (Section 1.13.4), the FT-IR/ATR technique allows to identify the chemical groups present in each sample. It can monitor the success of the reaction. The assignments of the main bands in all these spectra can be found on Table 3.6.

Results and Discussion

Table 3.6 - Characteristic IR Absorption wavenumbers of the functional groups from the two main polymers used in this work.

Membranes	Functional group	Type of vibration	Characteristic wavenumber (cm^{-1})	References
Acrylic-based	Alkane C-H	Stretch	2850 - 3000	[76]
	Ester C=O	Stretch	1735 - 1750	[77]
	Alkene C=C	Stretch	1620 - 1680	[76]
	Alkane -C-H	Bending	1350 - 1480	[76]
	Alcohol C-O	Stretch	1050 - 1150	[76]
	Aliphatic amine -N(CH$_3$)$_2$	Bending	2800- 2830	[78]
Chitosan-based	O-H	Stretch	3300 - 2500	[76]
	C-H	Stretch	2850 - 3000	[76]
	Amine N-H (I)	Bending	1600 - 1650	[77]
	Amide N-H (II)	Bending	1550 - 1640	[77]
	Amide N-H (III)	Bending	1200 - 1400	[77]
	C-O	Stretch	1050 - 1150	[77]
	Saccharide Structure	-	1112 - 1120	[77]

Figure 3-5 shows the IR spectrum of the acrylic-based membranes (ABM 4, ABM 4.1, ABM 4.2, ABM 4.4, ABM 5) and Figure 3-6 shows the IR spectrum of the chitosan-based membrane (ABM 16) and of the main reagents used (CS, Gelatin, PVA and PEG).
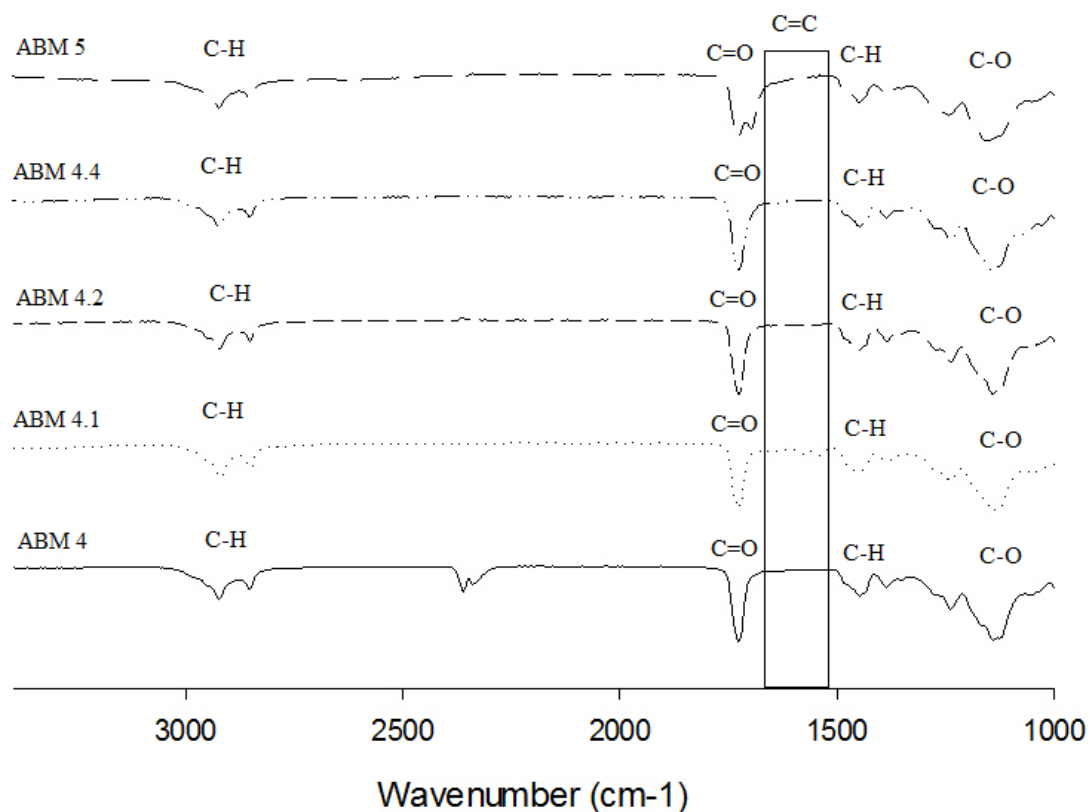
Figure 3-5 - FT-IR/ATR spectra of the Acrylic membranes studied.

The complete polymerization of the monomers was confirmed by IR spectroscopy as shown in Figure 3-5 by the total absence of the band due to the C=C group (1620 – 1680 cm^{-1} [76]). The IR spectra showed characteristic absorption bands at 2946 and 2870 cm^{-1}, attributed to aliphatic (C-H) stretching (2850 - 3000 cm^{-1} [76]). This is mainly due to the ODMA copolymer that has long aliphatic chains. The band at 1724 cm^{-1} is attributed to C=O stretching, which corresponds to the ester groups (1735 - 1750 cm^{-1} [77]). The peak present in the rage 2300-2400 cm^{-1} of ABM 4 is due to atmospheric CO_2. From the analysis of the Figure 3-5, it can also be concluded that no membrane has a peak which would distinguish it from the others. It would be expected, in the membranes modified with DMAEMA, the appearance of the functional group –$N(CH_3)_2$ (2800- 2830 cm^{-1}[78]). This band is near the C-H (2850 - 3000 cm^{-1} [76]) which is one possible reason for not being clearly visible.
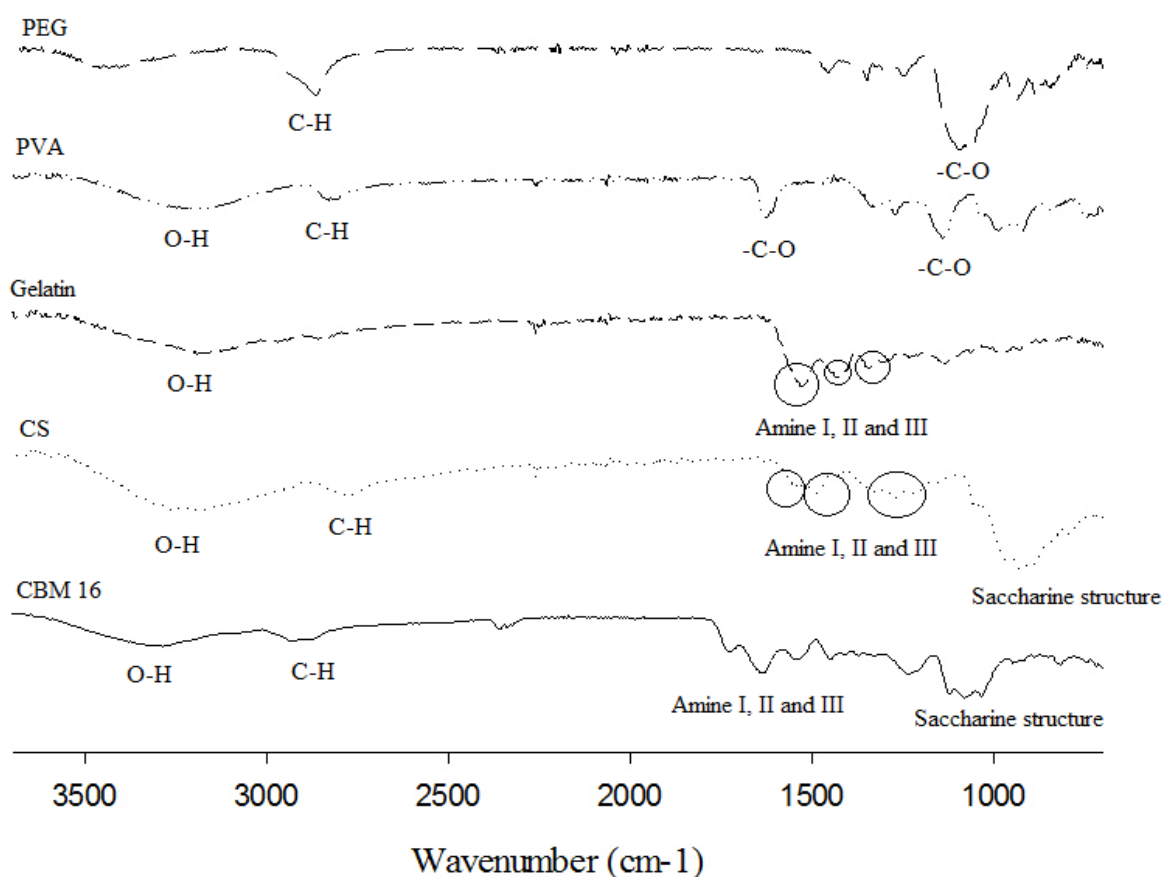
Figure 3-6 - FT-IR/ATR spectra of the Chitosan membrane studied.

As shown in Figure 3-6 and as expected, the chitosan-gelatin membranes have some characteristic bands in IR spectrum associated with chitosan and gelatin. The gelatin and chitosan spectrum demonstrates a band in the range of 3000 and 3500 cm^{-1}, attributed to OH vibrations (3300 - 2500 cm^{-1} [76]). It shows also characteristic absorption peaks relative to amide I, amide II and amide III. Amide I corresponds to C=O and NH vibrations of the amide group and amide II and III to NH and C-N vibrations. The amide I band of the chitosan spectrum shows the presence of C=O, indicating the presence of CH$_3$-COO groups. It was previously reported [78] that during the deacetylation of chitin (Figure 1-5) the intensity of the amide I gradually decreases while the intensity of amide II increases, indicating the substitution of NH$_2$ on the CH$_3$-C=O groups. The chitosan spectrum shows a characteristic saccharide band in the range 800-1000 cm^{-1} (1112 - 1120 cm^{-1} [77]).

The spectrum of the membrane with chitosan and gelatin shows differences in the position of all the individual bands relatively to isolated CS and gelatin spectrum, as can be seen in Table 3.7. Staroszczyk *et al.* [79] reported that it indicates interaction between both components of the membrane.

Table 3.7 - Characteristic groups and respective wavenumbers of CBM 16, Chitosan and gelatin.

Spectrum	Band position (cm^{-1})				
	OH	Amide I	Amide II	Amide III	Saccharide
CBM 16	3312	1738	1637	1541	1122, 1077, 1027
CS	3204	1560	1484	1325	976, 925, 881
Gelatin	3186	1529	1427	1338	-
References	[76]	[77]	[77]	[77]	[77]

3.6   Kinetic study of drug released from the controlled release systems

3.6.1   Drug absorption spectrum

To ensure that the maximum absorbance of MFX found in the literature matches the maximum absorbance of the MFX available in the laboratory, an absorbance spectrum of MFX was obtained (Figure 3-7). The obtained maximum of the peak (290 nm) was according to literature. It was the wavelength used to quantify MFX in the

samples taken from the release medium, employing a calibration curve (Figure A-1, Appendix A).
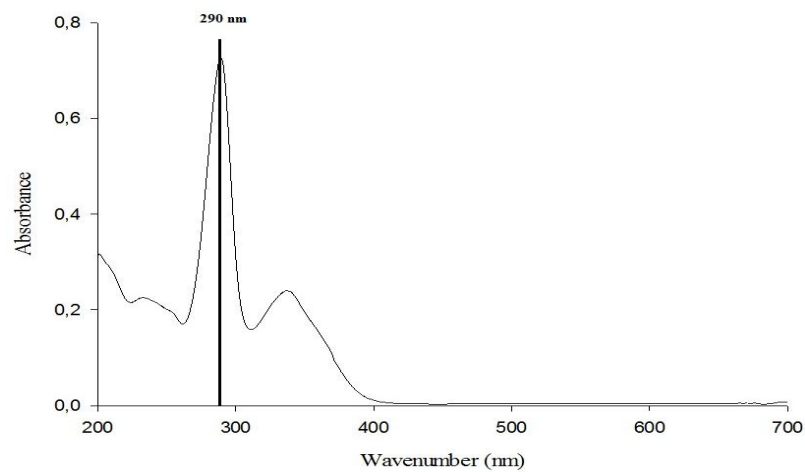
Figure 3-7 - MFX absorbance spectrum at a concentration of 8 μg/mL in ATS.

3.6.2 Drug release profiles

Figure 3-8 shows the variation of the released amount of MFX over time for CBM 16 - O, which had MFX incorporated by occlusion.
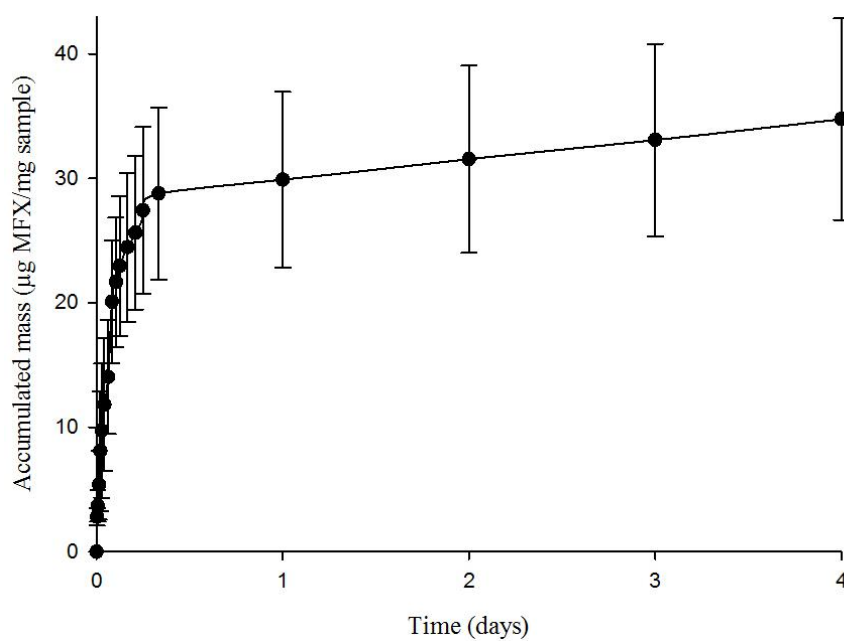
Figure 3-8 - Amount of MFX released over time in ATS at 37 °C for CBM 16 – O (error bars: standard deviation, $n = 3$).

It can be seen that the system releases MFX for 8 h and, after that, there seems to happen a very slow drug release. However, this is not clear due to the high variability from sample to sample, reflected in the large error bars.

Figure 3-9 shows the released amount of MFX over time for ABM 4 - O and ABM 5 - O.

Figure 3-9 - Amount of MFX released over time in ATS at 37 °C for ABM 4 – O and ABM 5 - O (error bars: standard deviation, $n = 3$).

Assuming that the MFX was uniformly distributed in the membrane, it is possible to conclude that the CBM 16 – O is the membrane that releases greater amount of drug, but it releases it quickly. This probably happens due to the plasticizer used. In chitosan membrane, it was used an external plasticizer. The addition of an external plasticizer increases the free volume of the polymeric matrix, since it inserts in between the polymer chains. This will enhance the output of MFX, stabilizing more quickly. ABM 4 - O and ABM 5 - O membranes have a similar release profile. This fact was expected since the difference between them is the presence of MAA whose consequence is to swell the

membrane: the membrane containing MAA (ABM 5 - O) releases more MFX. Analyzing the Figure 3-9, it is possible to conclude that the release ends in both membranes at day 3. However, the release profiles of these membranes are very irregular. ABM 4 - O and ABM 5 - O released a lower amount of drug relatively to CBM 16 - O. Since the acrylate-based membranes used internal plasticizers (ODMA and EHA), which are comonomers, their side-chains are present in between the main polymer chains, providing flexibility, but reducing the free volume. Thus, the drug in the ABM 4 - O and ABM 5 - O is released in smaller amounts for a longer time.

Membrane ABM 4 - O became completely opaque and white after the release. Probably, MFX precipitated in the polymer matrix. As the matrix is hydrophobic (Table 3.3), it hardly absorbs water, holding the drug therein. In the ABM 5 membrane this did not happen; this membrane increased about $3\times$ in size when in the ATS solution, allowing the MFX release.

In order to evaluate the influence of the drug impregnation method, membranes were also loaded by soaking. It is shown in the Figure 3-10 the released amount of MFX over time for CBM 16 - S, ABM 4 - S and ABM 5 - S for drug loading by soaking.
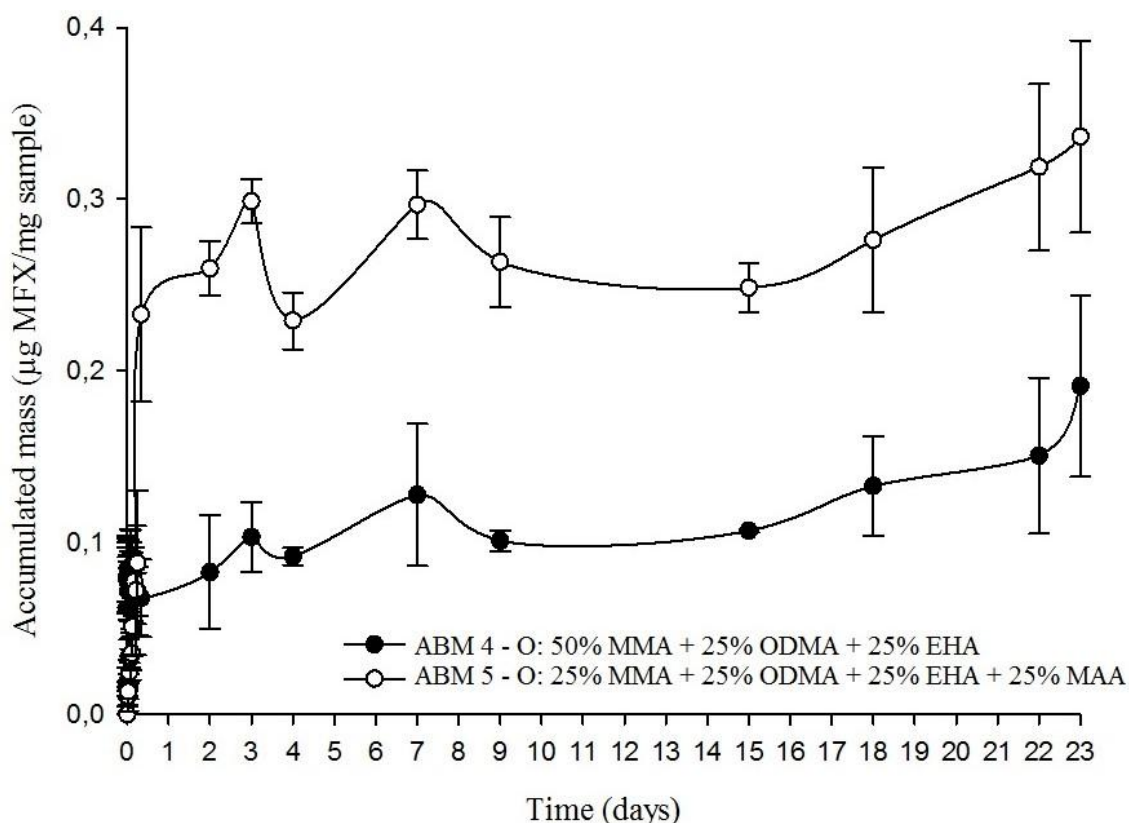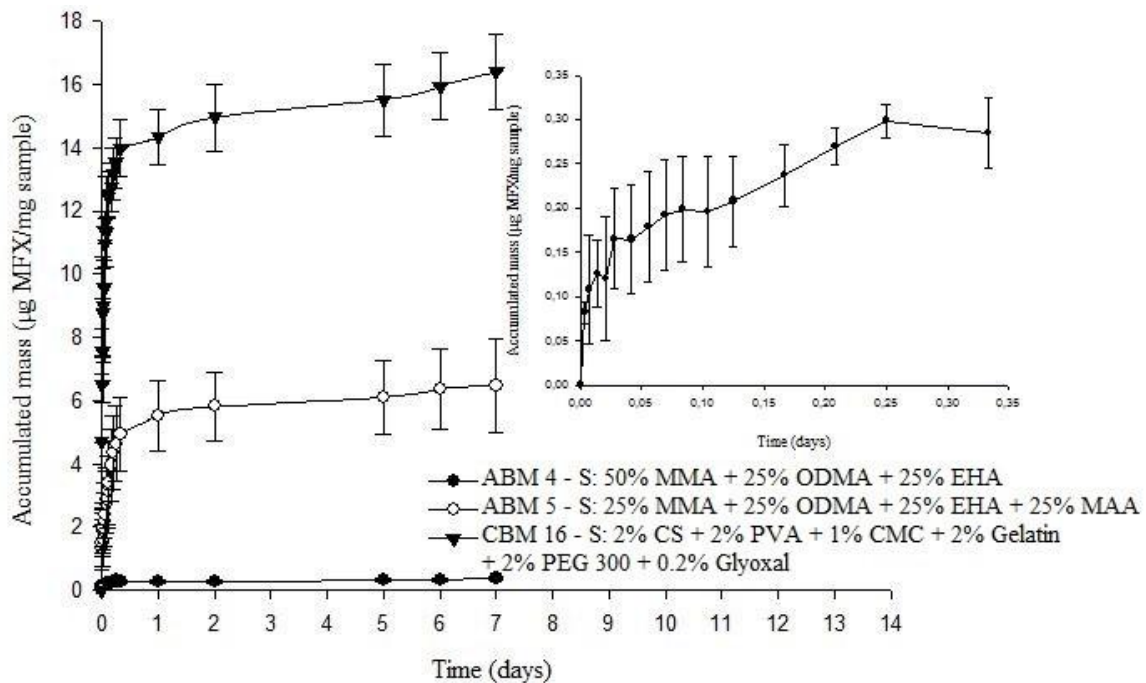

Figure 3-10 - Amount of MFX released over time in ATS at 37 °C for ABM 4 –S, ABM 5 – S and CBM 16 – S (error bars: standard deviation, $n = 3$). Insert: magnification of the release profile of ABM 4 membrane in the first 8 h.

As shown in the Figure 3-10, the release of membranes loaded by soaking begins to stabilize after a few hours. Quick release of drugs loaded in SCLs is typical of SCLs loaded by soaking and it is one of the major obstacles in the preparation of drug release systems based in SCLs [22]. ABM 4 - S stabilizes after 6 hours and ABM 5 - S and CBM 16 - S becomes progressively slower after 1 day and 8 hours, respectively.

CBM 16 - S is the membrane that releases greater amount of MFX, as was concluded before with drug loading by occlusion (Figure 3-9). This is probably because, when the drug is loaded by soaking, the drug is limited by the equilibrium solubility of the drug in the membrane matrix. The drug is hydrophilic and the chitosan-based membrane is more hydrophilic than acrylate-based membranes (as can be seen in the swelling study, Section 3.5.1, Table 3.3), then the drug enters more easily in the chitosan-based membrane. There is also the possibility of being associated with the plasticizer used, as was referred before in the release by occlusion.

Although the greater amount of MFX was released by CBM 16 – O in relation to CBM 16 - S, in ABM membranes this did not occur simply because the soaking method used employed 5 times more drug than the occlusion method and these membranes have low free volume, increasing the MFX concentration on the surface of the membranes. For time release, the occlusion method is clearly better. Only the chitosan-based membrane had the same release time in both methods.

To perform the study of the influence of the surface modification by grafting, ABM 4 was modified in three different ways: (i) ABM 4 + HEMA coating irradiated with 25 kGy (ABM 4.1), (ii) ABM 4 + DMAEMA coating irradiated with 25 kGy (ABM 4.2) and (iii) ABM 4 + DMAEMA coating irradiated with 15 kGy (ABM 4.4), with MFX loaded by soaking in all cases. Additionally, a membrane was grafted in the same way as ABM 4.4, but with MFX present in the grafting solution (ABM 4.3) and, additionally, this ABM 4.3 membrane was reloaded with MFX by soaking (called ABM 4.3 with recharging). Figure 3-12 shows the release profiles of the original membrane, ABM 4 and the profiles of the membranes with the modified surface, all loaded by soaking.
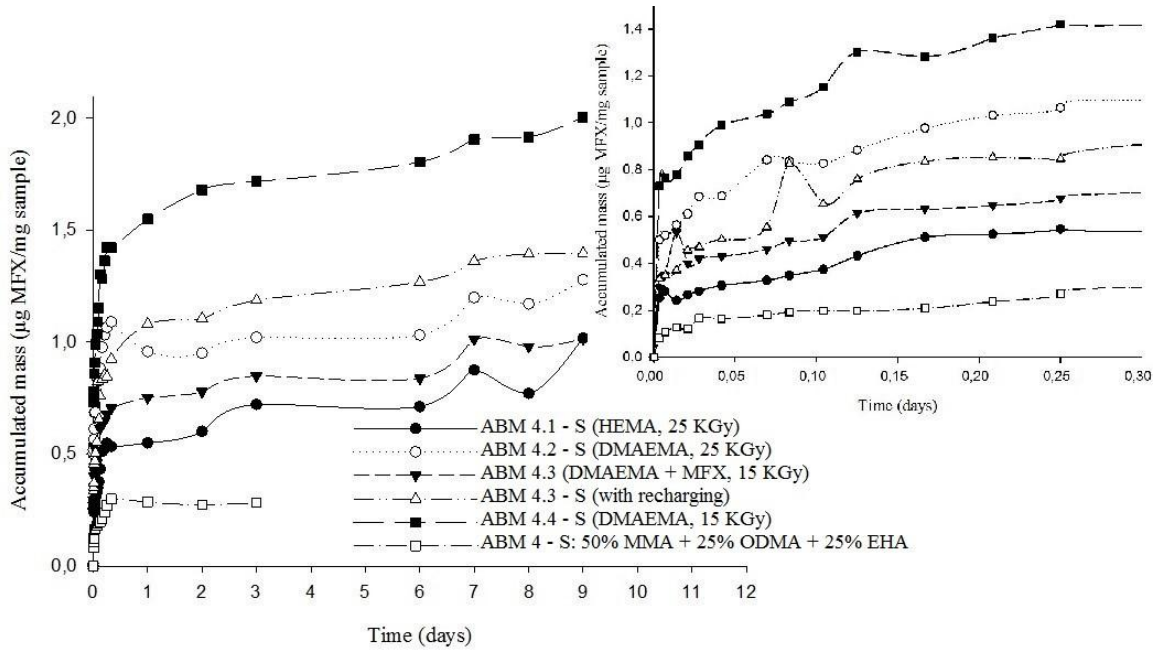
Figure 3-11 - Amount of MFX released over time in ATS at 37 °C for acrylate-based membranes modified by gamma radiation grafting with DMAEMA (25KGy and 15 KGy), DMAEMA with MFX (15 KGy) with and without recharging and HEMA (25 KGy). Drug loaded by soaking (error bar: standard deviation, $n = 1$).
Insert: magnification of the release profile of the membranes in the first 8 h.

As shown in the Figure 3-11, all membranes with a modified surface had higher amount of drug released from the membrane relatively to the membrane without modification, although these results are based in single membranes, not in triplicates, due to lack of samples. It can be concluded that the modification was successful, that the modification does not prevent the drug from entering the membrane and that the grafted layer can accommodate extra drug. The membrane which allowed the lowest MFX entry/release was ABM 4.1 - S, grafted with HEMA, and all the membranes grafted with DMAEMA released higher amounts of MFX. As concluded in the Section 3.5.1 by contact angle studies, membranes grafter with DMAEMA (ABM 4.4 and ABM 4.2) are the most hydrophilic, followed by ABM 4.1, grafted with HEMA. This difference may explain the fact that membranes modified with DMAEMA release more drug than when modified with HEMA. ABM 4 – S is the one that releases less MFX perhaps due the absence of a modified surface which, as we have seen, has the capacity to hold drug. It is also noted that the ABM 4.2 - S, grafted with DMAEMA and irradiated for longer (25 KGy), releases less than ABM 4.4 - S, which was grafted with the same monomer but irradiated during a shorter period of time (15 KGy). This fact is probably due to the greater grafting at the surface, which causes the drug to have greater difficulty in crossing the modified surface of ABM 4.2. As expected, membrane ABM 4.3 with recharging,

which was grafted in the presence of MFX (occlusion) and recharged afterwards by soaking in an MFX solution, had higher drug release than the non-charged membrane (ABM 4.3; Figure 3-11).

Relatively to the time at which the drug release system attains equilibrium with the surrounding medium and the drug release stops, the membranes that have greater drug release duration than the membrane without modification are ABM 4.4, with 2 days, becoming progressively slower with the time, ABM 4.3 which releases MFX during 1 day, and ABM 4.1 and ABM 4.2, both with 8 hours. Only ABM 4.2 has no advantage over the unmodified membrane ABM 4 – S (with 6 hours), releasing for 5 hours, which leads again to believe that excessive grafting does not allow the drug to cross the membrane. Note that it is not clear when it reaches a plateau (and release stops) because the analysis was done only on a single sample and the release profile is irregular.

3.6.3   Kinetic study of the release of MFX

In this section, mathematical models were used to analyse the kinetics of drug release from the membranes. To do so, the following models were selected: Korsmeyer-Peppas, Higuchi, zero order and first order models (Section 1.10). The results of the fitting of these models to the obtained data can be seen in Figure -1 to Figure B- (Appendix B). The quality of the adjustment of the model to the experimental points was assessed through the value of R^2, the coefficient of determination. Models which showed R^2 values ≥ 0.95 were considered as fitting the data (see Section 1.10). The R^2 values obtained for the fitting of the different models to the data from the different membranes can be seen in Table 3.8.

Results and Discussion

Table 3.8 - Correlation coefficients, R^2, obtained by linearization of mathematical models for the release profile MFX.

Membrane	Composition	Model			
		Korsmeyer - Peppas	Higuchi	Ordem zero	Primeira ordem
ABM 4 - O	50% MMA + 25% ODMA + 25% EHA	0.05	0.17	0.12	0.30
ABM 5 - O	25% MMA + 25% ODMA + 25% EHA + 25% MAA	0.68	0.88	0.90	0.63
CBM 16 - O	2% CS + 2% PVA + 1% CMC + 2% Gelatin + 2% PEG 300 + 0.2% Glyoxal	0.99	0.98	0.78	0.60
ABM 4 - S	50% MMA + 25% ODMA + 25% EHA	0.96	0.88	0.80	0.79
ABM 4.1 - S	ABM 4 + HEMA coating irradiated with 25 kGy	0.85	0.63	0.78	0.94
ABM 4.2 - S	ABM 4 + DMAEMA coating irradiated with 25 kGy	0.93	0.82	0.66	0.86
ABM 4.3 - S	ABM 4 + DMAEMA + MFX coating irradiated with 25 kGy	0.57	0.58	0.61	0.72
ABM 4.3 - S with recharge	ABM 4 + DMAEMA + MFX coating irradiated with 25 kGy	0.90	0.89	0.70	0.73
ABM 4.4 - S	ABM 4 + DMAEMA coating irradiated with 15 kGy	0.94	0.72	0.37	0.44
ABM 5 -S	25% MMA + 25% ODMA + 25% EHA + 25% MAA	0.95	0.94	0.89	0.90
CBM 16 - S	2% CS + 2% PVA + 1% CMC + 2% Gelatin + 2% PEG 300 + 0.2% Glyoxal	0.96	0.91	0.68	0.57

For CBM 16 – O, both Korsmeyer- Peppas and Higuchi methods fulfilled the requirement of $R^2 \geq 0.95$, being the Korsmeyer- Peppas the one that best fits. Many of the membranes have not reached the limit required in the models studied and then there is no model that fits to the release profile.

For membranes for which the Korsmeyer-Peppas model fit the data, the type of diffusion mechanism is evaluated through the slope obtained by linear regression of the graph obtained employing the Korsmeyer-Peppas model. Table 3.9 summarizes the results obtained.

Table 3.9 - Values of the parameter n and transport mechanism obtained by Korsmeyer-Peppas model in the membranes prepared by occlusion and soaking, which R^2 has accepted a setting defined criteria.

Membrane	Composition	n value	Transport mechanism
CBM 16 - O	2% CS + 2% PVA + 1% CMC + 2% Gelatin + 2% PEG 300 + 0.2% Glyoxal	0.61	Anomalous transport
ABM 4 - S	50% MMA + 25% ODMA + 25% EHA	0.05	Quasi-Fickian diffusion
ABM 5 - S	25% MMA + 25% ODMA + 25% EHA + 25% MAA	0.25	Quasi-Fickian diffusion
CBM 16 – S	2% CS + 2% PVA + 1% CMC + 2% Gelatin + 2% PEG 300 + 0.2% Glyoxal	0.28	Quasi-Fickian diffusion

Results and Discussion

From the *n* value, it can be concluded that CBM 16-O membrane shows anomalous transport. It means that the drug diffusion rate and the rate of relaxation of the polymer chains of the matrix are similar. Thus, the drug transport kinetics results from a combination of these two mechanisms. For the remaining membranes, transport is quasi-Fickian, implying that the drug diffusion rate is much lower than the polymer matrix relaxation rate. In this case, the loading methods can't be related since only CBM 16 – O can be distinguished from the others. From the Korsmeyer-Peppas model, it can be calculated the apparent diffusion coefficient (Equation 2) for each membrane, through the release constant (*k*). The results are shown in Table 3.10. The diffusion coefficient is designated as 'apparent', since the mechanism that controls the release of drug is not pure Fickian diffusion.

Table 3.10 - Apparent diffusion coefficient ($D_{apparent}$) and release constant (*k*) obtained through the Korsmeyer-Peppas model.

Membrana	Composição	k (s^{-1})	l (mm)	$D_{apparent}$ (m^2/s)
CBM 16 - O	2% CS + 2% PVA + 1% CMC + 2% Gelatin + 2% PEG 300 + 0.2% Glyoxal	2.7×10^{-5}	0.84	1.0×10^{-16}
ABM 4 - S	50% MMA + 25% ODMA + 25% EHA	1.2×10^{-5}	0.50	7.3×10^{-18}
ABM 5 - S	25% MMA + 25% ODMA + 25% EHA + 25% MAA	1.5×10^{-5}	0.50	1.1×10^{-17}
CBM 16 - S	2% CS + 2% PVA + 1% CMC + 2% Gelatin + 2% PEG 300 + 0.2% Glyoxal	1.8×10^{-5}	0.82	4.1×10^{-17}

As expected, the apparent diffusion coefficient for the CBM 16 - S is greater than for ABM 4 - S and the ABM 5 - S since, in both cases, membrane CBM 16 releases larger amount of drug. As mentioned in Section 3.6.2, this fact is due to the plasticizer used which suggests that the free volume in the chitosan membranes is greater than in the acrylate membranes. Relatively to the drug loading methods, CBM 16 - O have a greater $D_{apparent}$ than with the drug loaded by soaking, probably due to the fact that soaking is limited by the equilibrium solubility of the drug in the membrane matrix.

3.6.4 Cytotoxicity evaluation

Figure 3-12 shows the photomicrographs of cells grown in direct contact with the most promising membranes developed − ABM 5 and ABM 5 containing MFX loaded by occlusion − for 1 and 3. In the positive control (k+), no cell adhesion or proliferation was observed, indicating that cells could be killed with a cytotoxic substance (ethanol). Dead cells with their typical spherical shape can be observed in (Figure 3-12, (k+)). Cells cultured in the absence of any sample were used as negative control (Figure 3-12, (k⁻)). Cell viability in the presence of the membranes was then evaluated employing the MTS assay (Figure 3-12).
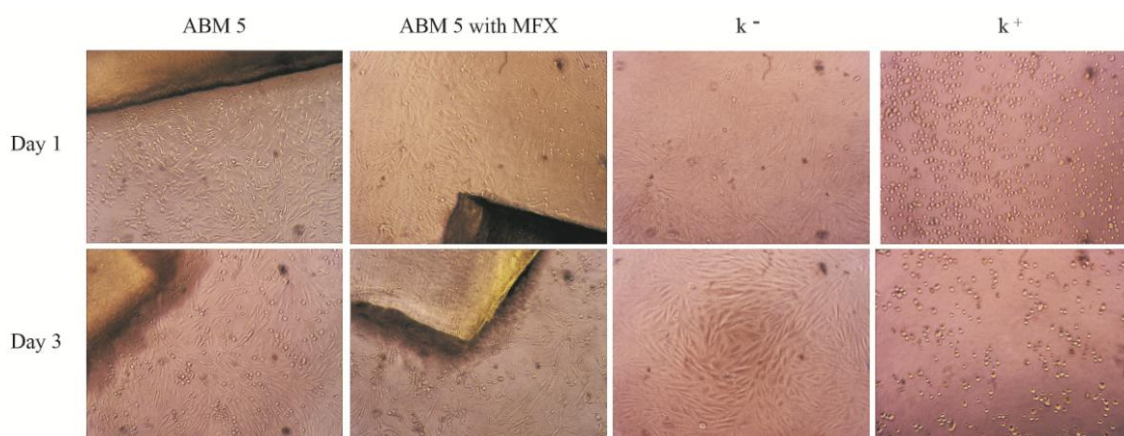

Figure 3-12 - Microscopic photographs of CEC in the presence of ABM 5 and ABM 5 with MFX with negative (k⁻) and positive (k⁺) control for day 1 and 3.

Comparing the membranes with the negative control (k⁻), which is the total of viable cells (100%), it appears that the unloaded membrane and membrane loaded with MFX are not cytotoxic until day 3, since all have less than 30% of cell viability reduction, although the unloaded membrane is close to this threshold value (Table 3.11).

Table 3.11 - Evaluation of the cellular activity reduction after day 1 and 3 for ABM 5 and ABM 5 with MFX.

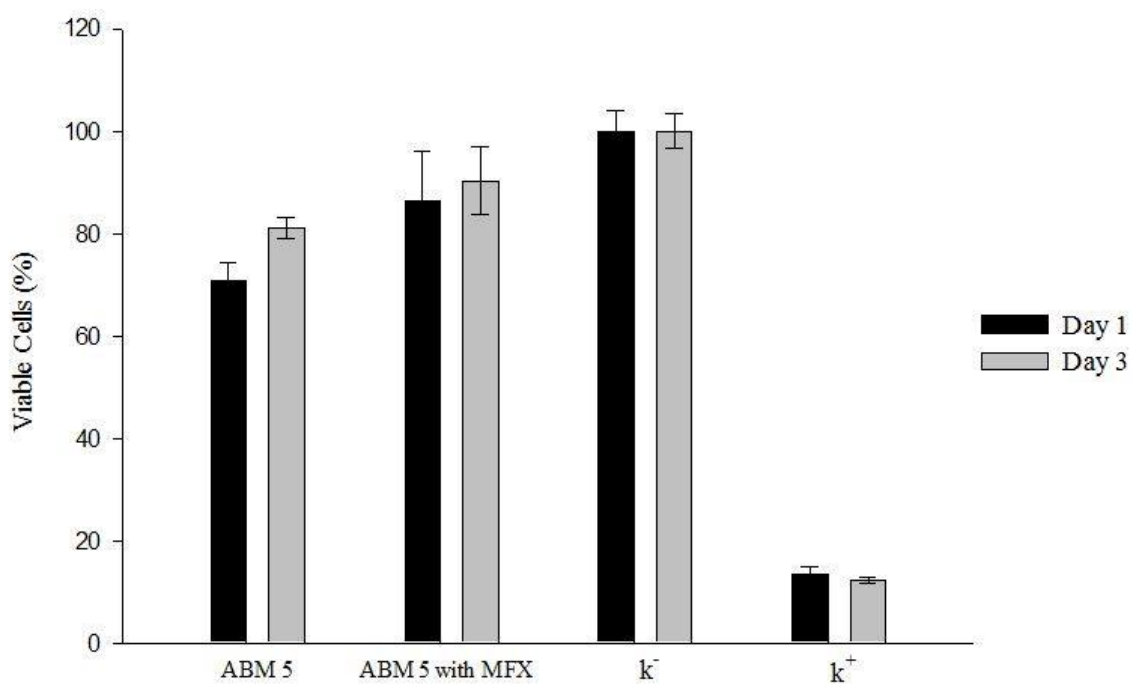| Membranes	Cell activity reduction (%)	
	Day 1	Day 3
ABM 5	29 ± 4	13 ± 10
ABM 5 with MFX	19 ± 2	10 ± 7

Figure 3-13 - Evaluation of the cellular activity after day 1 and 3 for ABM 5 and ABM 5 with MFX with negative (k⁻)
and positive (k⁺) control (error: standard deviation; $n = 5$)

By analysis of the Figure 3-13, relatively to the cellular viability of the ABM 5 there is a decrease in cytotoxicity from day 1 to day 3. The reason for the increase of the cell viability with time of contact with the cells is unclear. In the ABM membrane 5 – O, the difference is not significant due to the variability associated with each membrane. For k-, there was no difference between day 1 and 3.

4   Conclusions and Future Perspectives

In this thesis, in order to obtain a controlled drug release system which delivers a drug for an extended period of time, to be used as contact lens, different membrane formulations were prepared, based on chitosan (16) and polyacrylates (5). In the chitosan-based membranes, it was studied the effect of using linear and brancher PLA, Brij 35, TEC, PEG 300, gelatin and glyoxal. It was found that, with the branched PLA, it was obtained a membrane which tears easily; with linear PLA a very opaque membrane was obtained. With the addition of TEC and Brij®35, opaque and brittle membranes were obtained. It was also found that the addition of gelatin in combination with PEG 300, it is obtained a transparent membrane with good malleability. The addition of glyoxal has prevented the dissolution of the membranes when placed in water, as occurred with the membranes without glyoxal. In acrylate based membranes, the effect of including ODMA, EHA, HEMA and MAA as comonomers of MMA was studied. It was concluded that addition of HEMA gives rise to very rigid membranes; EHA and ODMA make the membrane more pliable as well as the addition of MAA. Thus, the best membranes for characterization studies and drug incorporation were the following: CBM 16 (2% CS + 2% PVA + 1% CMC 2% Gelatin 2% PEG-300 + 0.2% Glyoxal), ABM 4 (50% MMA + 25% + 25% ODMA EHA) and ABM 5 (25% ODMA% MMA + 25% + 25% + 25 EHA MAA).

It was also studied the modification of the surface of the ABM 4 by gamma radiation grafting with HEMA, employing an irradiation dose of 25 kGy (ABM 4.1) and with DMAEMA, irradiated with 25 kGy (ABM 4.2) and 15 kGy (ABM 4.4). The characterization of membranes by swelling revealed that ABM 5 and CBM 16 are indicated for use as contact lenses since it was obtained values similar to the commercial SCLs. The contact angle characterization allowed to conclude that all the membranes can be used as SCLs for the same reason. Regarding the transmittance of the membranes, the ABM 4.4 showed better UV protection and higher transmittance in the visible range.

Regarding the drug release, it was found that in both drug-loading methods, chitosan-based membranes released a greater amount of drug than acrylate based membranes, although for a shorter period of time. The ABM 5 – O was the membrane with longer release duration.

Mathematical models were employed to analyze the release kinetics and to identify the model that best fitted the release profiles. The model that best fitted most of the release profiles was the Korsmeyer-Peppas model, allowing to infer that the drug release mechanism was anomalous in the case of CBM 16 – O and quasi-Fickian diffusion for ABM 4 – S, ABM 5 – S and CBM 16 – S.

The cytotoxicity of the best membrane (ABM 5) unloaded and loaded with MFX was studied employing cells endothelial cells. It was concluded that this drug release system does not affect significantly cell viability at least until the third day, when drug release has stopped.

In view of all these results, it is concluded that none of the prepared membranes showed a long release of MFX, which was required for the intended application (prophylaxis of pre- and post-operative ocular infection). It should be noted that as these are new formulations, never employed for SCLs, there are variables that should be studied separately, such as the thickness of the membranes and the crosslinking degree.

As a suggestion for future work, in order to increase the drug time release, a membrane with drug incorporated by occlusion could have a surface treatment with nanoparticles with drug incorporated within the membrane matrix in order to prolong drug release. There is also the possibility to try other formulations, in view to other applications. Chitosan-based membranes could be optimized to another application, such as facemasks with drug release or other substances useful for the skin. For characterization of membranes, there are other important properties that should be considered such as refractive index, glass transition temperature and its oxygen transmissivity. It could also be done a biocompatibility test *in vivo* to assess effects on blood and inflammatory or allergic reactions. It could be also analyzed the efficiency of impregnation methods, determining the drug mass contained in the membranes so as to be able to compare them and proceed to release studies with drug ratios according to a therapy (moxifloxacin or other drug interest) more strictly.

Bibliography

[1] C. Bourlais, L. Acar, H. Zia, P. Sado, T. Needham and R. Leverge, "Ophthalmic Drug Delivery Systems Recent Advances," *Progress in Retinal and Eye Research,* vol. 17, pp. 33-58, 1998.

[2] C Alvarez-Lorenzo, F. Yañez, R. Barreiro-Iglesias, A. Concheiro, "Imprinted soft contact lenses as norfloxacin delivery systems," *Journal of Controlled Release,* vol. 113, pp. 236-244, 2006.

[3] R. Galante, P. Paradiso, G. Moutinho, A. Fernandes, J. Mata, R. Colaço, B. Saramago, A. Serro, "Libertação de Levofloxacina a Partir de Um Hidrogel à Base de PHEMA: Uma Contribuição para o Desenvolvimento de Lentes de Contacto Terapêuticas Contendo Fármacos," *Revista da Sociedade Portuguesa de Oftalmologia,* vol. 36, pp. 237-244, 2012.

[4] J. Coelho, P. Ferreira, P. Alves, R. Cordeiro, A. Fonseca, J. Góis, and M. Gil, "Drug delivery systems: Advanced technologies potentially applicable in personalized treatments," *The EPMA Journal,* vol. 1, pp. 164-209, 2010.

[5] "Guillaumon.com," Cirurgia Refrativa, [Online]. Available: http://www.guillaumon.com/557.html. [Accessed 23 March 2016].

[6] "probecure.com," MOST STANDARD AND COMMON LASER SURGERIES TO TREAT GLAUCOMA, 26 November 2014. [Online]. Available: http://probecure.com/b/most-standard-and-common-laser-surgeries-to-treat-glaucoma/. [Accessed 10 March 2016].

[7] "The free Dictionary," [Online]. Available: http://medical-dictionary.thefreedictionary.com/lacrimal+apparatus. [Accessed 12 March 2016].

[8] Chauhan, D. Gulsen and Anuj, "Ophthalmic Drug Delivery through Contact Lenses," *Investigative Ophthalmology & Visual Science,* vol. 45, pp. 2342-2347, 2004.

[9] Ahmed, Chethana SR and M. Gulzar, "Hydrogel Contact Lense for Extended Delivery of an Anti-Biotic in Combination with Anti-Inflammatory Drug for Ophthalmic Application," *Asian Journal of Biomedical and Pharmaceutical Sciences,* vol. 5, pp. 16-21, 2015.

[10] Mukherji, K. Sengupta and Ranabir, "Essentials of Ocular Pharmacology and Therapeutics," New Delhi, BI Publications Pvt Ltd, pp. 9-12, 2006.

[11] I. K. Reddy, in *Ocular Therapeutics and Drug Delivery*, Lancaster, Technomic Publishing Company, Inc., pp. 6-8, 1996.

[12] D. S. Patel, MEDeuronet, 23 September 2015. [Online]. Available: http://www.medeuronet.com/medeuronet/ocular-drug-delivery-in-search-of-the-holy-grail/. [Accessed 16 March 2016].

[13] Liechty WB, Kryscio DR, Slaughter BV, Peppas NA, "Polymers for drug delivery systems.," *Annual Review of Chemical and Biomolecular Engineering,* vol. 1, pp. 149-173, 2010.

[14] K. K. Jain, "Drug Delivery Systems," in *Drug Delivery Systems - An Overview*, Basel, Humana Press, pp. 1-50, 2008.

[15] Heller, Jorge. Drug Delivery Systems. In B. Ratner, A. Hoffman, F. Schoen, J. Lemons, editors, *Biomaterials Science,* An Introduction to Materials in Medicine, Chapter 7.8, p. 347. Academic Press, California, 1996.

[16] P. Coimbra, *Preparação e caracterização de sistemas de libertação controlada de fármacos com base em polimeros de origem natural,* Coimbra: Universidade de Coimbra, 2010.

[17] A. Ribeiro, A. Figueiras, F. Veiga, "Improvements in Topical Ocular Drug Delivery Systems: Hydrogels and," *Journal of Pharmacy & Pharmaceutical Sciences,* vol. 18, pp. 683-695, 2015.

[18] S. Xin-Yuan, T. Tian-Wei, "New Contact Lens Based on Chitosan/Gelatin Composites," *SAGE jourlnals,* vol. 19, pp. 467-479, 2004.

[19] L. Xinming, C. Yingde, A. Lloyd, S. Mikhalovsky, S. Sandeman, C. Howel, L. Liewen, "Polymeric hydrogels for novel contact lens-based ophthalmic drug," Elsevier Ltd, 2008.

[20] A. Hui, "Contact lenses for drug delivery – overview and recent developments," 29 June 2012. [Online]. Available: http://contactlensupdate.com/2012/06/29/contact-lenses-for-drug-delivery-overview-and-recent-developments/. [Accessed 19 July 2016].

[21] M. Abelson, MD, CM, FRCSC, FARVO, and J. McLaughlin, MD, Andover, Mass, "Attempts to engineer contact lenses that also elute therapeutic drugs face hurdles in both the world of lenses and of drugs. - See more at: http://www.reviewofophthalmology.com/content/t/contact_lenses/c/52895/#sthash.9l8DO6cu.dpuf," *Review of ophthalmology,* 2015.

[22] Gulsen, Derya; Chauhan, Anuj, "Ophthalmic Drug Delivery through Contact Lenses," *Investigative Ophthalmology & Visual Science,* vol. 45, pp. 2342-7, 2004.

[23] F. Rouxinol, *Preparação de nanopartículas para sistemas de libertação controlada de substâncias activas usadas no tratamento de doenças oftalmológicas,* Coimbra: University of Coimbra, 2009.

[24] S. Lin, L. Bowman, S. Chandrasekaran, T. Harvey, "Surface treatment of soft contact lenses". USA Patent 4,687,816, 18 Aug 1987.

[25] A. Hasan, L. Pandey, "Review: Polymers, Surface-Modified Polymers, and Self Assembled Monolayers as surface-Modifying Agents for Biomaterials," *Polymer-Plastics Technology and Engineering,* vol. 54, pp. 1358-1378, 2015.

[26] A. Hoffman, "SURFACE MODIFICATION OF POLYMERS: Physical, Chemical, Mechanical and Biological Methods," *Macromolecular Symposia,* vol. 101, pp. 443-454, 1996.

[27] M. Lira, *Uso de lentes de contacto : deteriorização das suas propriedades e alterações fisiológicas associadas,* Tese de Doutormento em ciências: RepositóriUM, 2007.

[28] "WebMD," [Online]. Available: http://www.webmd.com/drugs/2/drug-17874/moxifloxacin-oral/details. [Accessed 9 March 2016].

[29] Callegan MC, Ramirez R, Kane ST, Cochran DC, Jensen H., "Antibacterial activity of the fourth-generation fluoroquinolones gatifloxacin and moxifloxacin against ocular pathogens.," Adv. Ther., vol. 20, pp. 246-252, 2003.

[30] S. Matthew, "Complicated skin and soft tissue infection," *Journal of Antimicrobial Chemotherapy,* vol. 65, pp. 35-44, 2010.

[31] "Santa Clara Biotechnology," [Online]. Available: https://www.scbt.com/pt/datasheet-205758-moxifloxacin-hydrochloride.html. [Accessed 17 July 2016].

[32] P. Djurdjevica, A. Cirica, A. Djurdjevicb, M. Stankovc, "Optimization of separation and determination of moxifloxacin and its related substances by RP-HPLC," *Journal of Pharmaceutical and Biomedical Analysis,* vol. 50, pp. 117-126, 2009.

[33] D. Miller, "Review of moxifloxacin hydrochloride ophthalmic solution in the treatment of bacterial eye infections," *Clinical Ophthalmology,* vol. 2, pp. 77-91, 2008.

[34] Shashank N, B. Sogali, Thakur, "Formulation and evolution of pH triggered in situ ophthalmic gel of moxifloxacin hydrochloride," *International Journal of Pharmacy and Pharmaceutical Sciences,* vol. 4, pp. 452-459, 2012.

[35] P. Dandagi, A. Belekar, V. Mastiholimath, A. Gadad, V. Sontake, and P. Salian, "An Improvement of the Efficacy of Moxifloxacin HCl for the Treatment of Bacterial Keratitis by the Formulation of Ocular Mucoadhesive Microspheres," *Scientia Pharmaceutica,* vol. 81, pp. 259-280, 2013.

[36] "emc," Alcon Laboratories (U.K) Limited, 18 August 2014. [Online]. Available: https://www.medicines.org.uk/emc/medicine/23828. [Accessed 11 April 2016].

[37] "INFARMED," 13 August 2009. [Online]. Available: http://pdg.estiga.com/moxifloxacina-para-infeccoes-oculares. [Accessed 12 March 2016].

[38] NPCS Board of Consultants & Engineers, in *Water Soluble Polymers*, Delhi, Asia Pacific Business Press Inc., pp. 172-180, 2009.

[39] J. Pecora, "The Mechanics of Gelatin and the DCG Process," [Online]. Available: http://holowiki.org/wiki/File:Gelatin1.gif. [Accessed 30 June 2016].

[40] P. Wojciechowska, "The Effect of Concentration and Type of Plasticizer on the Mechanical Properties of Cellulose Acetate Butyrate Organic-Inorganic Hybrids," in *Recent Advances in Plasticizers*, Poznań, InTech, pp. 141-164, 2012.

[41] N. Cao, X. Yang, Y. Fu, "Effects of various plasticizers on mechanical and water vapor barrier properties of gelatin films," *Food Hydrocolloids,* vol. 23, pp. 729-735, 2009.

[42] A. Carreira, P. Ferreira, T. Correia, P. Coutinho, I. Correia, "New drug-eluting to be applied as bandages after keratoprosthesis implantation," *International Journal of Pharmaceutics,* vol. 477, pp. 218-226, 2014.

[43] C. Andreuccetti, R. Carvalho, C. Grosso, "Effect of hydrophobic plasticizers on functional properties of gelatin-based films," *Food Research International,* vol. 42, p. 1113–1121, 2009.

[44] K. Tomihata, Y. Ikada, "Cross-Linking of Gelatin with Carbodiimides," *Mary Ann Liebert, Inc., publishers,* vol. 2, pp. 307-313, 2007.

[45] L. Xu, Yun-An Huang, Qiu-Jin Zhu and C. Ye, "Chitosan in Molecularly-Imprinted Polymers: Current and Future Prospects," *International Journal of Molecular Sciences,* vol. 16, p. 18328–347, 2015.

[46] C. Cammarata, M. Hughes, and C. Ofner, "Carbodiimide Induced Cross-linking, Ligand Additior, and degradation in gelatin," *Molecular Farmaceutics,* vol. 12, pp. 783-793, 2015.

[47] Q. Yang, F. Dou, B. Liang, and Q. Shen, "Studies of cross-linking reaction on chitosan fiber with glyoxal," *Carbohydr. Polym.,* vol. 59, pp. 205-210, 2005.

[48] "The Chemical Company," October 2015. [Online]. Available: http://www.spezialmonomere.basf.com/portal/streamer?fid=235706. [Accessed 18 May 2016].

[49] B. Koiry and N. Singha, "Copper mediated controlled radical copolymerization of styrene and 2-ethylhexyl acrylate and determination of their reactivity ratios," *Front. Chem.,* vol. 2, pp. 2-91, 2014.

[50] "The Chemistry of Contact Lenses," Compound interest, 13 October 2015. [Online]. Available: http://www.compoundchem.com/2015/10/13/contactlenses/. [Accessed 5 May 2016].

[51] C Maldonado-Codina, N. Efron, "Hydrogel Lenses – Materials and Manufacture: A Review," *Optometry in Practice,* vol. 4, pp. 101-115, 2003.

[52] L. Meisberger, R. Keller, and R. Shalek, "The Effective Attenuation in Water of the Gamma Rays of Gold 198, Iridium 192, Cesium 137, Radium 226, and Cobalt 60," *Radiology,* vol. 90, p. 953, May 1968.

[53] A. Chmielewski, "GAMMA IRRADIATORS FOR RADIATION PROCESSING," in *Trends in Radiation Sterilization of Health Care Products*, Vienna, 2008 .

[54] J. Crank, in *The Mathematics of Diffusion*, Bristol, Oxford University Press, 1975.

[55] P. Ritger and N. Peppas, "A single equation for description of solute release II. Fickian and anomalous release from swellable devices.," *J. Control. Release,* vol. 5, pp. 37-42, 1987.

[56] C. Lopes, J. Lobo, and P. Costa, "Formas farmaceuticas de liberação modificada: polímeros hidrofílicos.," *Rev. Bras. Ciências Farm.,* vol. 41, pp. 143-154, 2005.

[57] N. Peppas and L. Brannon-Peppas, "Water diffusion and sorption in amorphous macromolecular systems and foods," *J. Food Eng.,* vol. 22, pp. 189-210, 1994.

[58] S. Dash, P. Murthy, L. Nath, and P. Chowdhurry, "Kinetic modeling on drug release from controlled drug delivery systems," *Acta Pol. Pharm.,* vol. 67, pp. 217-223, 2010.

[59] Y. Fu and W. Kao, "Drug Release Kinetics and Transport Mechanisms of Non-degradable and Degradable Polymeric Delivery Systems," *Expert Opin Drug Deliv.,* vol. 7, pp. 429-444, 2010.

[60] P. Costa, J. Lobo, "Modeling and comparison of dissolution profiles," *European Journal of Pharmaceutical Sciences,* vol. 13, p. 123–133, 2001.

[61] P. Stoica, "Model-order selection: a review of information criterion rules," *IEEE Signala Process. Mag.,* vol. 21, pp. 36-47, 2004.

[62] M. Alvesa, P. Almeida, H. Polonini, N. Raposo, A Ferreira, M. Brandão, "Green tea in transdermal formulation: HPLC method for quality control and in vitro," *Quim. Nova,* vol. 37, pp. 728-735, 2014.

[63] "Columbia University," GO ASK ALICE, 2 July 2015. [Online]. Available: http://goaskalice.columbia.edu/answered-questions/contact-lenses-which-type-better. [Accessed 1 May 2016].

[64] S. McArthur, K. McLean, H. John and H. Griesser, "XPS and surface MALDI-MS characterisation of worn HEMA-based contact lenses," *Biomaterials,* vol. 22, pp. 3295-3304, May 2001.

[65] R. Grant, "Developments in Contact Lens Surfaces," Contact Lens Spectrum, 2010.

[66] Krasowska M, Zawala J, Malysa K., "Air at hydrophobic surfaces and kinetics of three phase contact formation.," *Advances in Colloid and Interface Science,* Vols. 147-148, pp. 155-169, 2008.

[67] JC, "Methods for Wettability Determination on Hydrogels," KRÜSS, Hamburg, 2006.

[68] M. Read, P. Morgan and C. Maldonado-Codina, "Measurement Errors Related to Contact Angle Analysis ofHydrogel and Silicone Hydrogel Contact Lenses," *Journal of Biomedical Materials Research,* vol. 91B, pp. 662-668, 2009.

[69] Carole Maldonado-Codina, Philip B. Morgan, "In vitro water wettability of silicone hydrogel contact lenses determined using the sessile drop and captive bubble techniques," *Journal of Biomedical Materials Research,* vol. 83A, pp. 496-502, 2007.

[70] M. Harris, R. Chin, D. Lee, M. Tarot and C. Dobkins, "Comparison of two hydrogel formulations for drug release in ophthalmic lenses," *Wiley Online Library,* vol. 102, pp. 1170-80, 2014.

[71] "Toxikon," Advancing your innovation, [Online]. Available: http://www.toxikon.com/resources/biocompatibility_2011.cfm. [Accessed 31 July 2016].

[72] IHS, "ISO 10993-5," International Organization for Standardization, Switzerland, 2009.

[73] A. Vieira, P. Ferreira, J. Coelho, H. Gil, "Photocrosslinkable starch-based polymers for ophthalmologic drug delivery," *International Journal of Biological Macromolecules,* vol. 43, pp. 325-332, 2008.

[74] F. Taktak, M. Yildiz, H. Sert, C. Soykan, "A Novel Triple-Responsive Hydrogels Based on 2-(Dimethylamino) Ethyl Methacrylate by Copolymerization With 2-(N-morpholino) Ethyl Methacrylate," *ournal of Macromolecular Science Part A,* vol. 52, pp. 39-46, 2015.

[75] Sung-Joo Hwang, N. Baek, H. Park, K. Park, "Hydrogels in Cancer Drug Delivery Systems," in *Cancer Drug Discovery and Development*, New Jersey, Humana Press, pp. 97-115, 2004.

[76] Silverstein, R.M.; Bassler, G.C.; and Morrill, T.C, Spectrometric Identification of Organic Compounds, 4th ed. New York: John Wiley and Sons, 1981.

[77] V. Uversky, E. Permiakov, Methods in Protein Structure and Stability Analysis: Vibrational spectroscopy, New York, 2007.

[78] G. Socrates, "Alkane Group Residues: C-H Group," in *Infrared and Raman Characteristic Group Frequencies*, The University of West London, 2001, p. 56.

[79] H. Staroszczyk, K. Sztuka, J. Wolska, A. Wojtasz-Pająk, I. Kołodziejska, "Interactions of fish gelatin and chitosan in uncrosslinked and crosslinked with EDC films: FT-IR study," *Spectrochimica Acta Part A: Molecular Spectroscopy,* vol. 117, pp. 707-712, 2014.

Appendix

Appendix A - MFX calibration curve

Figure A-1 shows the MFX calibration curve obtained by fitting the experimental data points to a quadratic equation.
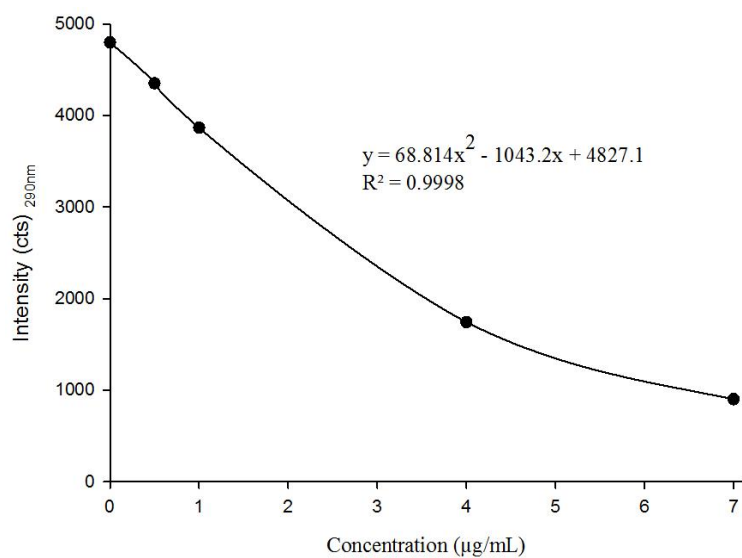

$$y = 68.814x^2 - 1043.2x + 4827.1$$
$$R^2 = 0.9998$$

Figure A-1 - Calibration curve MFX in ATS.

Appendix B - Drug release profile fitting to mathematical models.

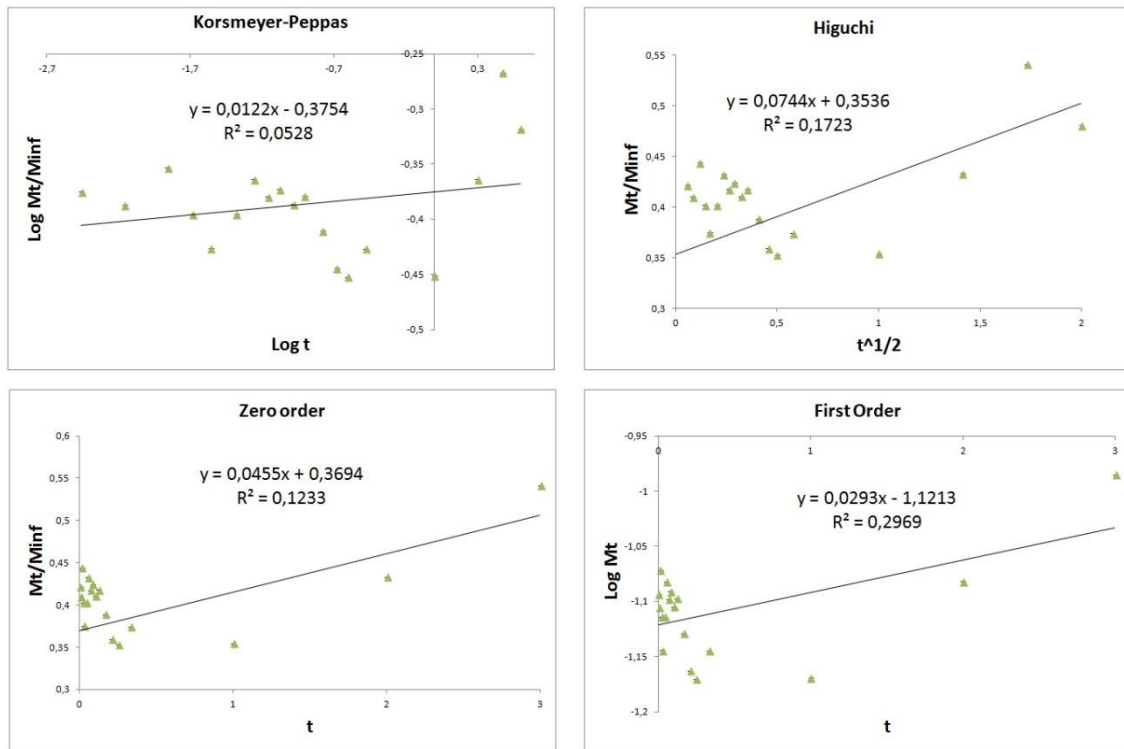Figure B-1 to Figure B-11 shows the release profiles for each membrane, with drug impregnated by occlusion and soaking, for Korsmeyer-Peppas, Higuchi, zero order and first order models.

Figure B-1- Graphical representation of models Korsmeyer-Peppas, Higuchi, zero order and first order for ABM 4 - O (50% MMA + 25% ODMA + 25% EHA).
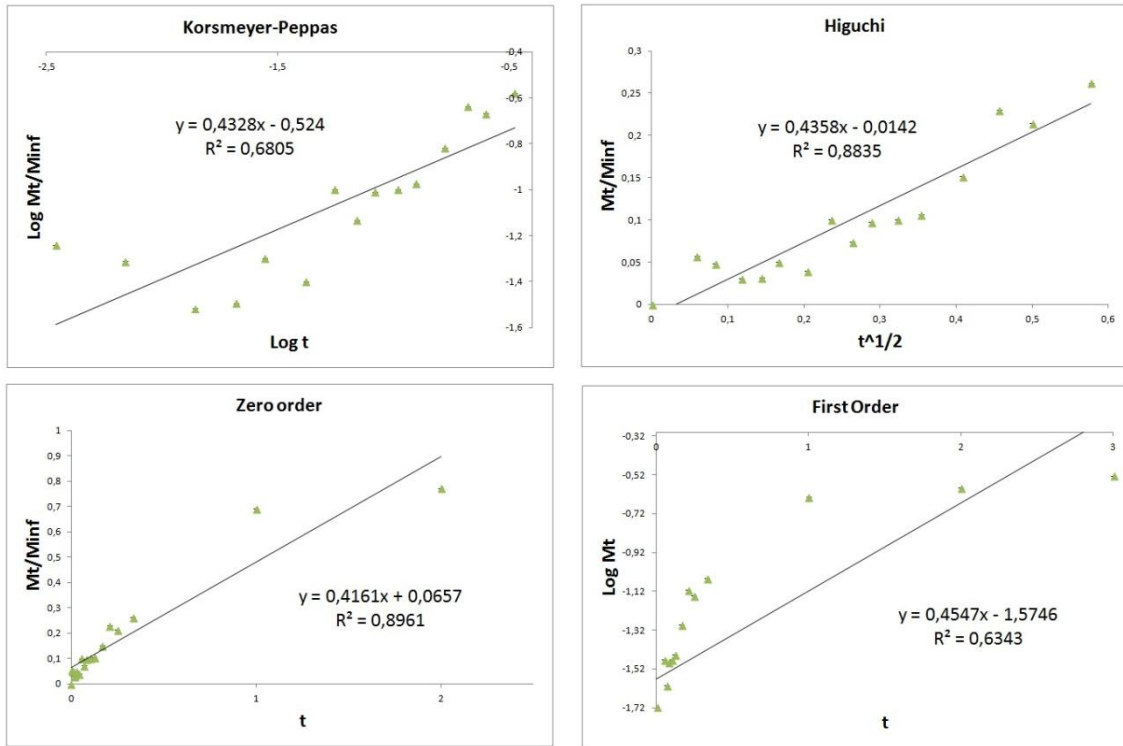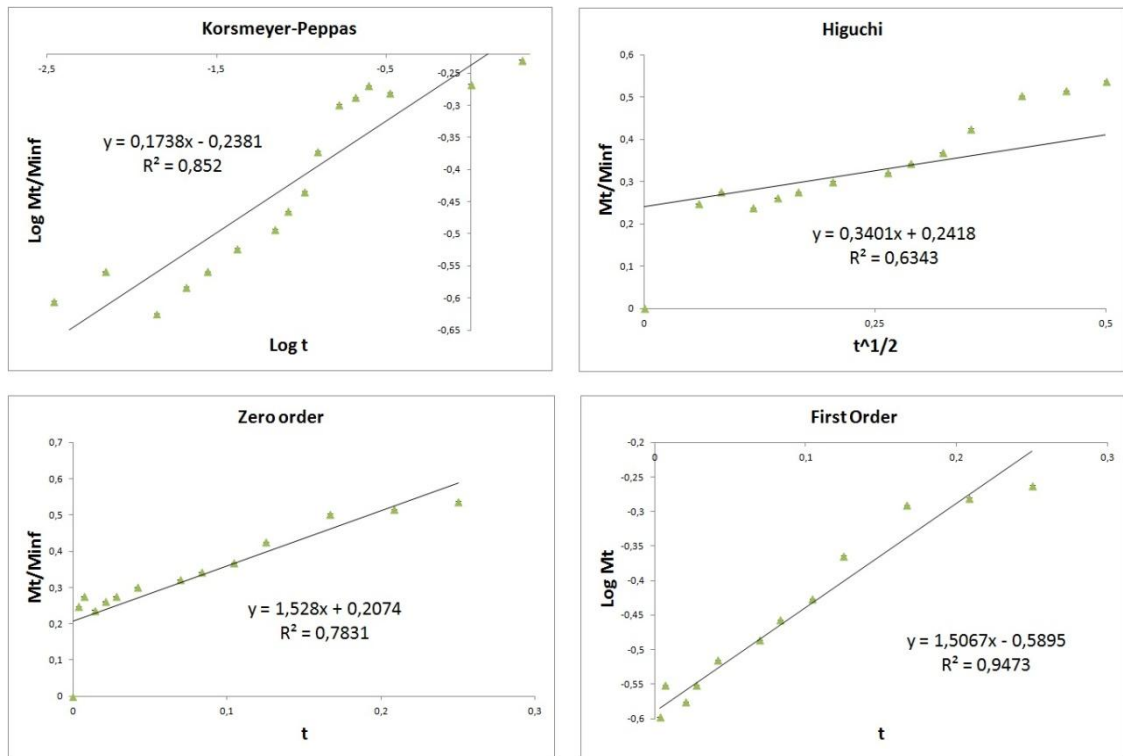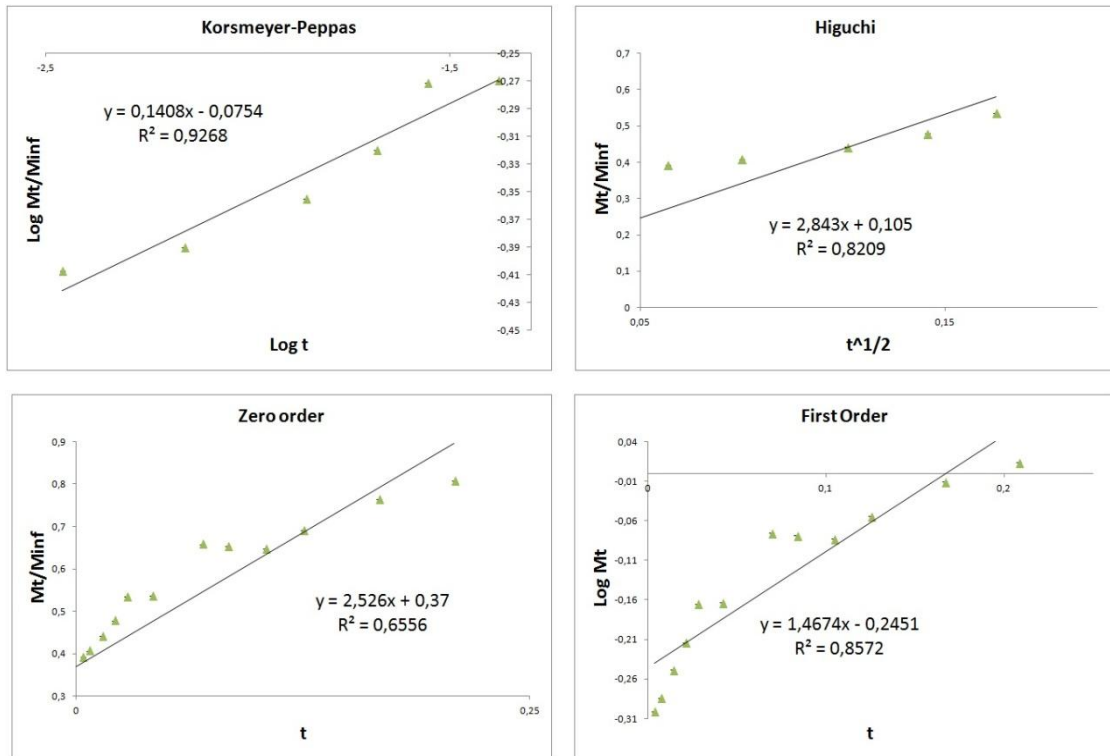
Figure B-2 - Graphical representation of models Korsmeyer-Peppas, Higuchi, zero order and first order for ABM 5 - O (25% MMA + 25% ODMA + 25% EHA + 25% MAA).
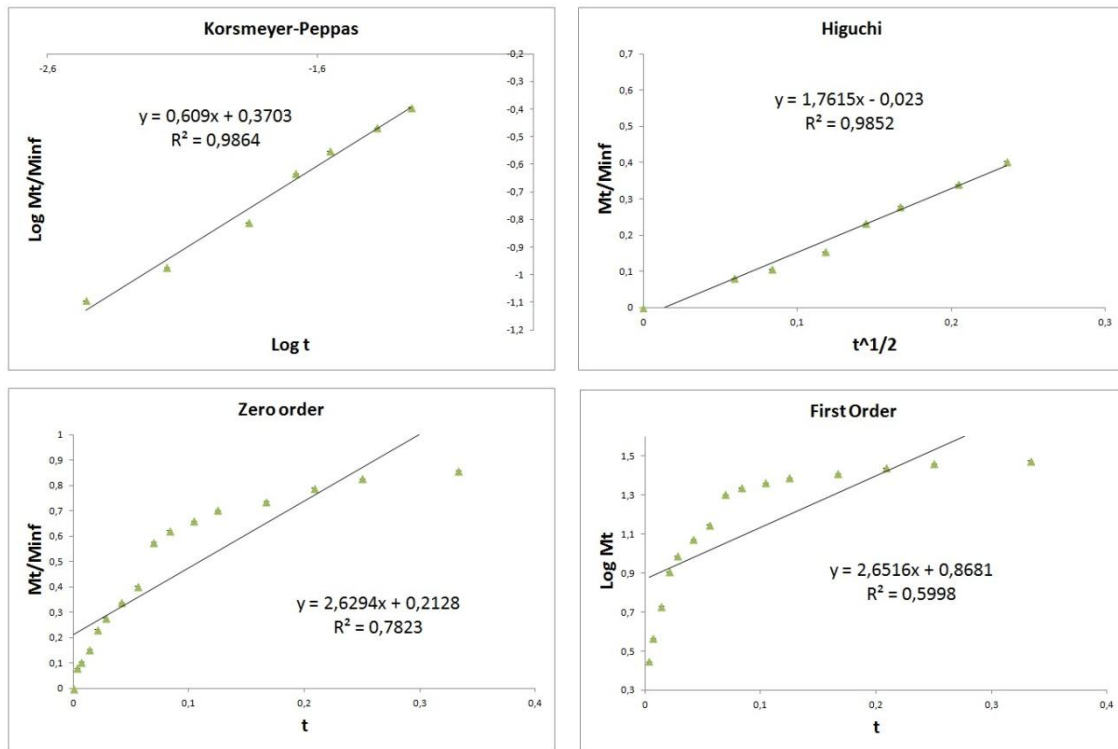
Figure B-3 - Graphical representation of models Korsmeyer-Peppas, Higuchi, zero order and first order for CBM 16 – O (2% CS + 2% PVA + 1% CMC + 2% Gelatin + 2% PEG 300 + 0.2% Glyoxal).
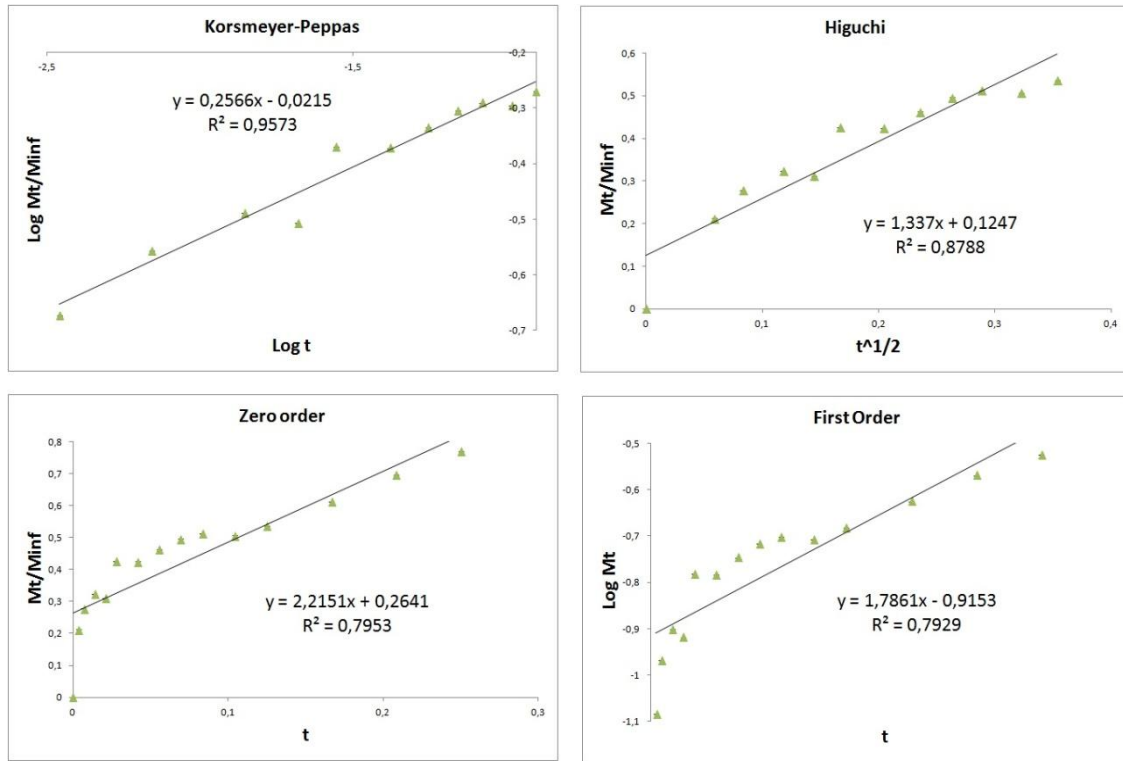
Figure B-4 - Graphical representation of models Korsmeyer-Peppas, Higuchi, zero order and first order for ABM 4 – S (50% MMA + 25% ODMA + 25% EHA).

Figure B-5 - Graphical representation of models Korsmeyer-Peppas, Higuchi, zero order and first order for ABM 4.1 - S (ABM 4 + HEMA coating irradiated with 25 kGy).
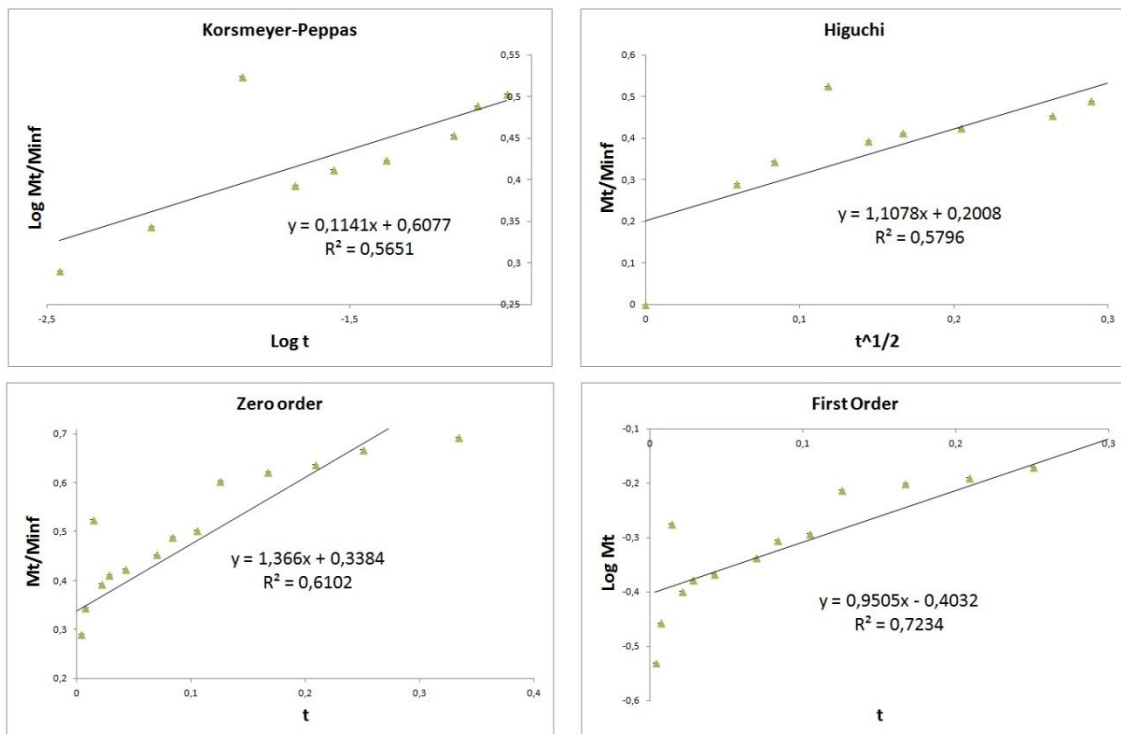
Figure B-6 - Graphical representation of models Korsmeyer-Peppas, Higuchi, zero order and first order for ABM 4.2 - S (ABM 4 + DMAEMA coating irradiated with 25 kGy).

Figure B-7 - Graphical representation of models Korsmeyer-Peppas, Higuchi, zero order and first order for ABM 4.3 (ABM 4 + DMAEMA + MFX coating irradiated with 25 kGy).
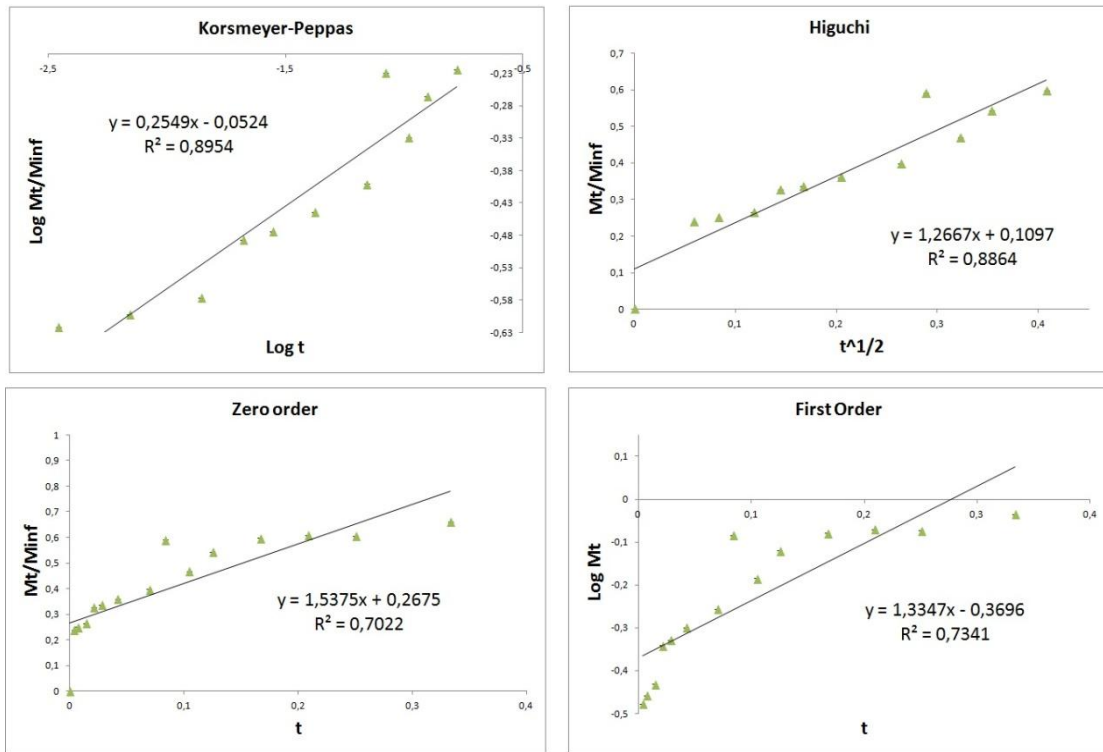
Figure B-8 - Graphical representation of models Korsmeyer-Peppas, Higuchi, zero order and first order for ABM 4.3 - S (with recharge) (ABM 4 + DMAEMA + MFX coating irradiated with 25 kGy).
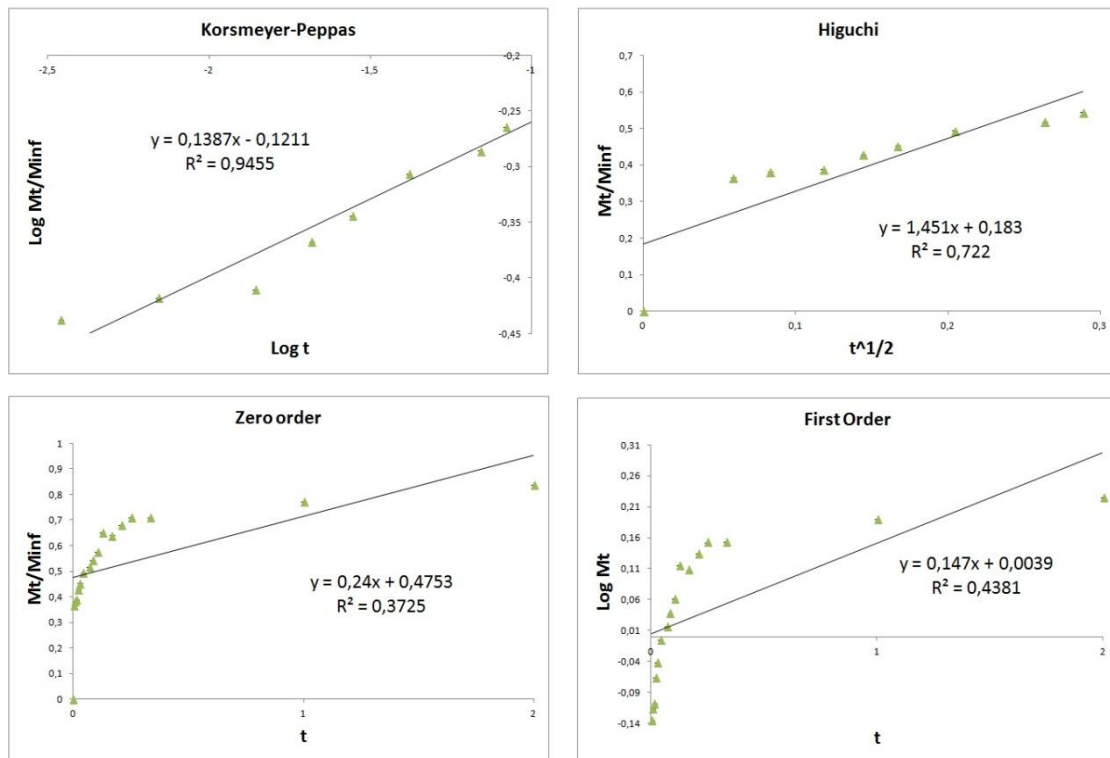

Figure B-9 - Graphical representation of models Korsmeyer-Peppas, Higuchi, zero order and first order for ABM 4.4 - S (ABM 4 + DMAEMA coating irradiated with 15 kGy).
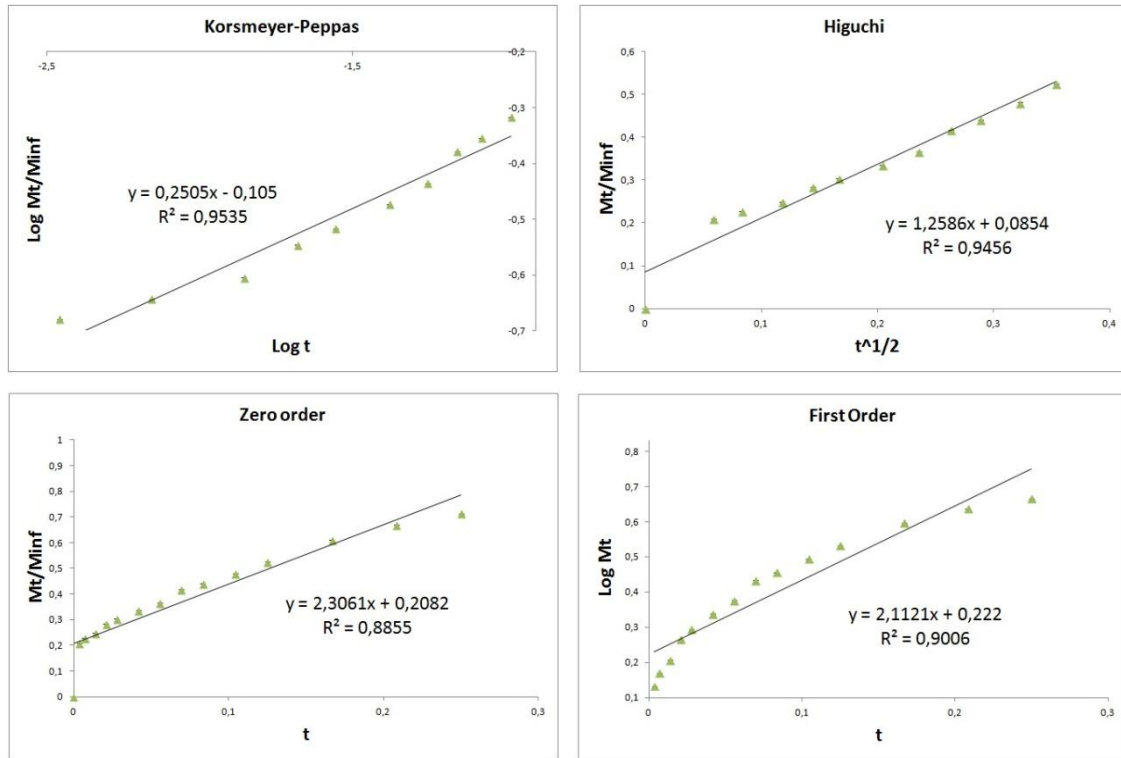
Figure B-10 - Graphical representation of models Korsmeyer-Peppas, Higuchi, zero order and first order for ABM 5 - S (25% MMA + 25% ODMA + 25% EHA + 25% MAA).
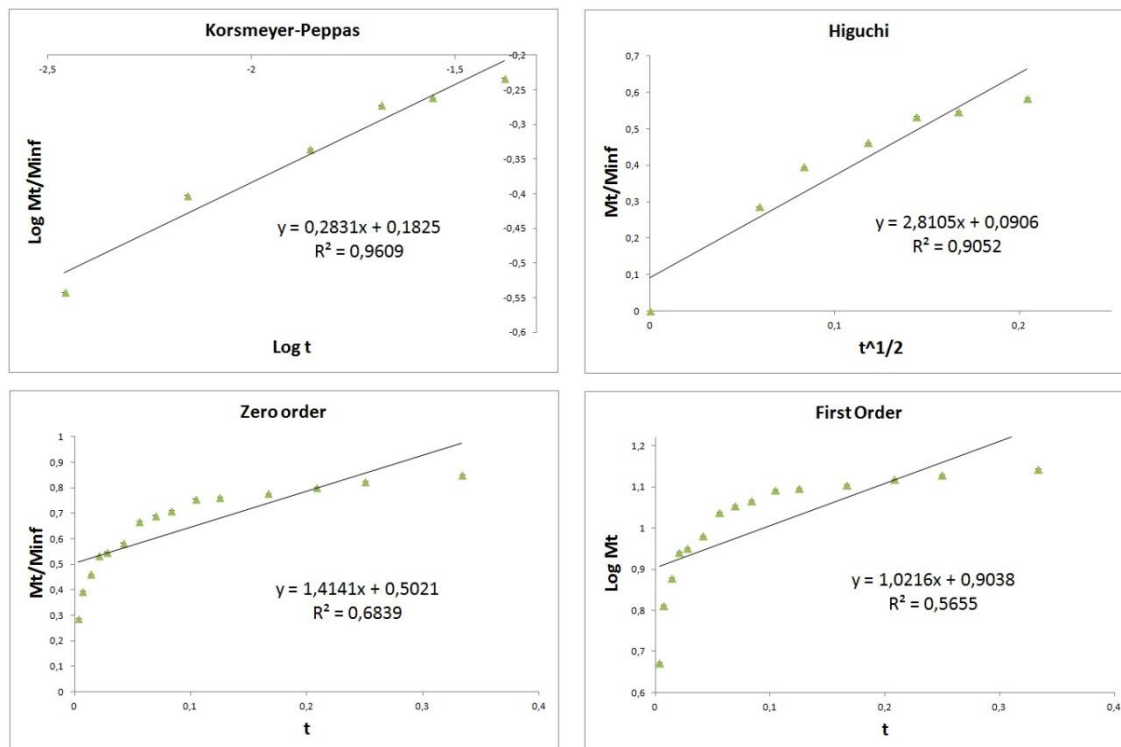

Figure B-11 - Graphical representation of models Korsmeyer-Peppas, Higuchi, zero order and first order for CBM 16 - S (2% CS + 2% PVA + 1% CMC + 2% Gelatin + 2% PEG 300 + 0.2% Glyoxal).